Contributions à la physique statistique des systèmes à longue portée : relaxation collisionnelle, systèmes analogues

Mémoire présenté par

Bruno Marcos

Laboratoire de Mathématiques J.A. Dieudonné

presentée en vue d'obtenir

l'Habilitation à diriger les recherches de l'Université Côte d'Azur

Discipline : Physique

Soutenue le 19 janvier 2024

devant un jury composé de :

Alberto Bramati	Professeur, Sorbonne Université	Examinateur
Francisco J. Cao-García	Professeur, Universidad Complutense	Examinateur
Didier Clamond	Professeur, Université Côte d'Azur	Examinateur
Yves Elskens	Professeur, Aix-Marseille Université	Rapporteur
Christophe Pichon	Directeur de Recherche, IAP	Rapporteur
Simona Rota Nodari	Professeure, Université Côte d'Azur	Examinatrice
Stefano Ruffo	Professeur, SISSA	Rapporteur

Contributions to statistical physics of long-range interacting systems: collisional relaxation, analogue systems

Bruno Marcos

Laboratoire de Mathématiques J.A. Dieudonné

Habilitation Thesis

in Physics

defended on 19th January 2024

jury members:

Alberto Bramati	Professor, Sorbonne Université	Examinateur
Francisco J. Cao-García	Professor, Universidad Complutense	Examinateur
Didier Clamond	Professeur, Université Côte d'Azur	Examinateur
Yves Elskens	Professor, Aix-Marseille Université	Rapporteur
Christophe Pichon	Senior Researcher, IAP	Rapporteur
Simona Rota Nodari	Professor, Université Côte d'Azur	Examinatrice
Stefano Ruffo	Professor, SISSA	Rapporteur

Résumé en français

Les systèmes de particules ayant des interactions à longue portée présentent deux phases dans leur évolution : premièrement, la formation d'états quasi-stationnaires, tels que les galaxies, dans le cadre d'un processus appelé « relaxation violente », et deuxièmement, une relaxation beaucoup plus lente vers l'équilibre thermique, dans un processus appelé « relaxation collisionnelle ». Dans la nature, la plupart de ces systèmes correspondent à des systèmes gravitationnels, dans lesquels il n'est pas possible d'observer leur dynamique, car ils se produisent sur des échelles de temps de l'ordre de millions d'années au moins. Pour pouvoir observer de tels phénomènes, on peut utiliser des systèmes analogues en laboratoire, c'est-à-dire des systèmes qui sont régis par les mêmes équations que le système original. Cette Habilitation à Diriger des Recherches couvre des contributions sur deux sujets : des résultats sur la relaxation collisionnelle, et des résultats théoriques et expérimentaux sur des systèmes gravitationnels analogues.

Relaxation collisionnelle

L'approximation de Chandrasekhar modélise la relaxation collisionnelle dans les systèmes auto-gravitants comme une succession de collisions binaires indépendantes. Pour la généraliser aux interactions en loi de puissance, nous étendons la formule de la diffusion de Rutherford, sous forme de séries en loi de puissance. Ensuite, nous généralisons l'approximation de Chandrasekhar aux interactions en loi de puissance, en montrant qu'elle est valable pour une large gamme d'interactions, depuis celles où les collisions sont dominées par le plus petit facteur d'impact jusqu'à celles où elle sont dominées par un grand facteur d'impact. De plus, cette approche permet d'introduire une nouvelle classification de la portée des interactions, qui prend en compte les propriétés dynamiques du système, au lieu de ses propriétés thermodynamiques. Afin de tester plus précisément la validité de l'approximation de Chandrasekhar, nous avons pu monter qu'il est possible de décrire correctement la relaxation collisionnelle dans la gravité en deux dimensions à l'aide d'un modèle minimal basé sur cette approximation. Puis, en utilisant une approche qui prend en compte les résonances et les effets collectifs, nous présentons des calculs exacts des coefficients de diffusion pour des distributions spatialement inhomogènes dans un modèle simple. Enfin, l'existence de modes de Goldstone classiques est étudiée, qui apparaissent lorsqu'un état stationnaire rompt spontanément une symétrie continue de l'Hamiltonien.

Systèmes analogues coulombiens et gravitationnels

Nous nous concentrons premièrement sur les systèmes atomiques froids (mais classiques) dans des pièges optiques. Ces systèmes peuvent être analogues à des systèmes gravitationnels (attractifs) ou coulombiens (répulsifs), en contact avec un bain thermique et en présence de friction. Nous présentons un modèle simple qui décrit le mode de respiration dans ces systèmes. Dans ce type de système, des forces non potentielles peuvent apparaître ; nous décrirons théoriquement et numériquement les transitions de phase hors-équilibre. Nous décrivons ensuite l'observation expérimentale d'un système unidimensionnel analogue à un système auto-gravitant à équilibre thermodynamique. Enfin, nous présenterons quelques conclusions de la mesure expérimentale de la longueur de corrélation (longueur de Debye). Nous nous concentrons deuxièmement sur des systèmes non linéaires à focalisation thermique. Ces milieux sont des analogues presque parfaits de systèmes auto-gravitants bidimensionnels, depuis le régime quantique jusqu´au régime semi-classique. Ils sont parfaitement adaptés à l'observation de phénomènes tels que relaxation violente. Tout d'abord, nous présentons des résultats sur les méthodes numériques pour décrire ces systèmes. Ensuite, à l'aide d'un système expérimental proche de la limite semi-classique, nous décrivons l'observation, pour la première fois, du processus de relaxation violente et de la formation d'une galaxie analogue.

Abstract

Systems of particles with long-range interactions present two phases in their evolution: first, the formation of Quasi-Stationary states (such as galaxies) in a process called *violent relaxation* and, second, a much slower relaxation towards thermal equilibrium, in a process called *collisional relaxation*. In nature, most of these systems correspond to gravitational ones, in which it is not possible to observe their *dynamics*, because they occur on time scales of, at least, the order of millions of years. To be able to *observe* such phenomena, we may use *analogue systems* in the laboratory, i.e., systems which are governed by the same equations. This Habilitation covers contributions on two subjects: results on the *collisional relaxation* process, and theoretical and experimental results on analogue gravitational systems.

Collisional relaxation

The Chandrasekhar approximation models the collisional relaxation in self-gravitating systems as a succession of binary collisions. To generalize it for power-law interactions, we extend the formula of Rutherford scattering, obtaining full infinite power series. Then, we generalize the Chandrasekhar approximation to interactions with power-law interactions, determining that it is valid along a wide range of interactions, from those in which collisions are dominated by small impact factor to those in which they are dominated by large ones. In addition, this approach allows to introduce a novel classification of the range of interactions, which considers the *dynamical* properties of the system, instead of its *thermodynamical* properties. To test further the validity of the Chandrasekhar approximation, we have been able to describe correctly collisional relaxation in two-dimensional gravity using a Chandrasekhar-based minimal model. Then, using an approach which considers resonances and collective effects, we present exact calculations of the diffusion coefficients for spatially inhomogeneous distributions in a simple model. Finally, the existence of classical Goldstone modes is studied, which appear when a stationary state spontaneously breaks a continuous symmetry of the Hamiltonian.

Analogue gravitational and coulomb systems

We focus first on cold (but classical) atomic systems trapped in magneto-optic traps (MOTs). These systems can be analogue of gravitational (attractive) or coulomb (repulsive) systems, in contact with a heat bath and in presence of friction. We present

a simple model which describes the breathing mode in systems of trapped interacting particles. In this kind of system, non-potential forces may appear; we will describe theoretically and numerically non-equilibrium phase transition in such a system. We then describe the experimental observation of a one-dimensional gravitational-like system of particles in thermodynamical equilibrium. Finally, we will present some conclusions in the experimental measurement of the correlation (Debye) length.

We focus then on thermally focusing non-linear mediums. These mediums mimic quasi-perfectly two-dimensional self-gravitating systems, from the deep quantum regime to the semi-classical one. They are perfectly suited to observing phenomena such as *violent relaxation*. First, we present results about numerical methods to describe these systems. Second, using an experimental system tuned close to the semi-classical limit, we describe the observation, for the first time, of the violent relaxation process and the subsequent formation of an analogue galaxy.

Acknowledgments

I am grateful to Yves Elskens, Christophe Pichon and Stefano Ruffo to have accepted to review this manuscript. I warmly thank Alberto Bramati, Francisco J. Cao-García, Didier Clamond and Simona Rota Nodari to have accepted to be a member of the committee.

I can only be extremely grateful to all my collaborators, which have made this work possible. I would like to make a special mention to Fernanda Benetti and Martino Lovisetto, with whom I had the opportunity to advise their PhD work.

I am indebted to all the colleagues of the Laboratoire Dieudonné, and specially the administrative staff, who create a great and stimulating working environment every day. I would like to thank also Francisco Cao and Juan Parrondo who kindly hosted me at the Physics Department of the Universidad Complutense in which part of this manuscript has been written.

Many thanks to my colleagues Afeintou Sangam and Dario Vincenzi who have been a great support during the process of writing this Habilitation.

I am extremely grateful to Irene, who not only supported me unconditionally all these years, but also knew how to listen to me through the best and worst scientific moments.

Contents

Presentation

My research work has been focused on the study of the statistical physics of long-range interacting systems. In this manuscript I will cover two lines of research: the study of collisional relaxation in long-range systems, and the theoretical and experimental study of analogue long-range systems. On these subjects I have supervised two PhD. students. First, Fernanda Benetti, who was doing her PhD in Porto Alegre, spent her last year of PhD in Nice working independently of her advisors. We studied the collisional relaxation in the inhomogenous Hamiltonian Mean Field model, paper [V] (see the list at the end of this section). Second, Martino Lovisetto, who did his PhD under my co-supervision with Didier Clamond. We studied from one side numerical methods to solve the Schrödinger equation [XV,XVI], and from the other side theory and experiment to observe violent relaxation in a non-linear optical system [XIV].

This dissertation covers topics of statistical physics, astrophysics, cold atoms and non-linear optics. The minimal concepts of each field are introduced in order to make it self-consistent. In chapter 1 appears a general introduction to the statistical physics of long-range system, focused on the topics that will be developed in this dissertation. In chapter 2 can be found the contributions related to the collisional relaxation in long-range systems. In chapter 3, after an introduction on analogue long-range systems in cold atoms and non-linear optics, appear the contributions on this topic. The full publication list appears in the Appendix A at the end of the manuscript by chronological order. The papers whose material has been used to write this manuscript are listed below, in the order of citation in this manuscript (not chronologically). They are cited in the manuscript with the roman number of the list. These papers can be found in a different volume than this manuscript (to avoid unnecessary printing when printing the main manuscript).

Papers treated in the dissertation

Collisional relaxation

I *"Series expansions of the deflection angle in the scattering problem for power-law potentials"*, D. Chiron and B. Marcos, J. Math. Phys. **60**, 052901 (2019).

II *"Quasi-stationary states and the range of pair interactions"*, A. Gabrielli, M. Joyce, B. Marcos, Phys. Rev. Lett, 105, 210602 (2010).

III *"Formation and relaxation of quasi-stationary states in particle systems with power law interactions"*, B. Marcos, A. Gabrielli and M. Joyce, Phys. Rev. E **96**, 032102 (2017).

IV *"A dynamical classification of the range of pair interactions"*, A. Gabrielli, M. Joyce, B. Marcos, F. Sicard, J. Stat. Phys., **141**, 970 (2010).

V *"Collisional relaxation of two-dimensional self-gravitating systems"*, B. Marcos, Physical Review. E, **88**, 032112 (2013).

VI *"Collisional relaxation in the inhomogeneous Hamiltonian-Mean-Field model: diffusion coefficients"*, F. Benetti et B. Marcos, Phys. Rev. E **95**, 022111 (2017).

VII *"Classical Goldstone modes in Long-Range Interacting Systems"*, T. M. Rocha Filho and B. Marcos, Phys. Rev. E **102**, 032122 (2020).

Analogue long-range systems

VIII *"Breathing mode for systems of interacting particles"*, A. Olivetti, J. Barré, B. Marcos, F. Bouchet, R. Kaiser, Phys. Rev. Lett. 103, 224301 (2009) .

IX *"Breathing Dynamics for Systems of Interacting Particles in the Microcanonical and Canonical Descriptions"*, A. Olivetti, J. Barré, B. Marcos, F. Bouchet and R. Kaiser, Transp. Theo. and Stat. Phys. 39, 524 (2010).

X *"Symmetry Breaking in d-Dimensional Self-Gravitating Systems"*, R. Pakter, B. Marcos, Y. Levin, Physical Review Letters **111**, 230603 (2013).

XI *"Nonequilibrium Phase Transition with Gravitational-like Interaction in a Cloud of Cold Atoms"*, J. Barré, B. Marcos D. Wilkowski, Physical Review Letters, **112**, 133001 (2014).

XII *"Long-range one-dimensional gravitational-like interaction in a neutral atomic cold gas"*, M. Chalony, J. Barré, B. Marcos A. Olivetti,D. Wilkowski, **87**, 013401 (2013).

XIII *"Towards a measurement of the Debye length in very large Magneto-Optical traps"*, J. Barré, R. Kaiser, G. Labeyrie, B. Marcos and D. Metivier, Phys. Rev. A **100**, 013624 (2019).

XIV *"Experimental observation of violent relaxation and the formation of out-of-equilibrium quasi-stationary states"*, M. Lovisetto, M.C. Braidotti, R. Prizia, C. Michel, D. Clamond, M. Bellec, E.M. Wright, B. Marcos and D. Faccio, `arXiv:2205.10948`.

XV *"Integrating factor techniques applied to the Schrödinger-like quations. Comparison with Split-Step methods"*, M. Lovisetto, D. Clamond, B. Marcos, `hal-03483942`.

XVI *"Optimized integrating factor technique for Schrödinger-like equations"*, M. Lovisetto, D. Clamond, B. Marcos, Applied Numerical Mathematics, **178**, 329 (2022).

1. Long-range interacting systems

Long-range interacting systems are defined mathematically, for a system of particles interacting with a two-body potential $u(r)$, embedded in a d-dimensional space, by the relation [1]

$$\lim_{R\to\infty}\int_{\epsilon}^{R} \mathrm{d}^d r\, u(r) \to \infty, \tag{1.1}$$

where ϵ is a regularization to prevent eventual singularities at small distances. In other words, the integral (1.1) diverges because of the large distances. The consequences of this

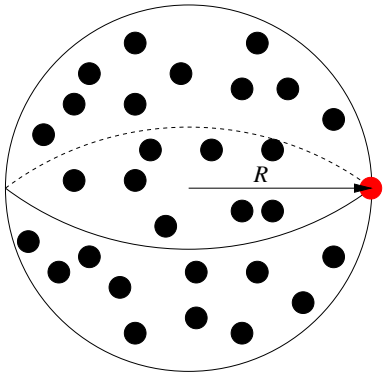

Figure 1.1 – System of particles randomly distributed in a d-dimensional sphere of radius R.

condition can be understood intuitively by considering a system of particles randomly distributed in a d-dimensional sphere (which would correspond to a galaxy halo or a globular cluster in $d = 3$), see Fig. 1.1. Let us consider the (red) particle, located at a distance R from the center, and compute the ratio of the contribution of the potential $\phi_{\rm nn}$ caused by the nearest neighbor to the (mean-field) contribution of the potential $\phi_{\rm mf}$ caused by all the other particles. We will assume that the interacting potential is

$$u(r) = \frac{g}{r^\gamma}, \tag{1.2}$$

where $r = |\mathbf{r}|$ is the distance between the particles and g the coupling constant. Using, e.g., Gauss theorem, we get

$$\phi_{\mathrm{mf}} \sim \frac{gN}{R^\gamma}. \tag{1.3}$$

The potential due to the nearest neighbor is

$$\phi_{\mathrm{nn}} \sim \frac{g}{d_{\mathrm{nn}}^\gamma} \sim \frac{gN^{\gamma/d}}{R^\gamma}, \tag{1.4}$$

where N is the number of particles. The last equality comes from the nearest-neighbor typical distance $d_{\mathrm{nn}} \sim N^{-1/d}R$. Therefore, we have

$$\frac{\phi_{\mathrm{nn}}}{\phi_{\mathrm{mf}}} \sim N^{\gamma/d-1}. \tag{1.5}$$

We observe two different possible behaviors of the scaling (1.5) for the $N \gg 1$ limit: if $\gamma > d$, the nearest-neighbor contribution of the potential dominates over the mean field potential, whereas for $\gamma < d$, the mean field potential dominates over the nearest-neighbor one, and indeed in the $N \to \infty$ limit the mean field becomes *exact*. In this limit the finite N effects are completely suppressed; the *granularity* of the system disappears. It is possible to verify that the distinction between these behaviors of the potential corresponds to the classification given in Eq. (1.1): replacing $u(r)$ by (1.2) in Eq. (1.1), we get

$$\lim_{R\to\infty} \int_\epsilon^R \mathrm{d}^d r \, \frac{g}{r^\gamma} \sim \lim_{R\to\infty} gR^{d-\gamma}. \tag{1.6}$$

The integral diverges (converges) for $\gamma < d$ ($\gamma > d$). The fact that the mean-field potential dominates has consequences on the dynamics of the system: starting from some initial condition, the long-range system does not evolve directly towards Maxwell-Boltzmann equilibrium but remains trapped in a succession of quasi-stationary states (hereafter QSS). The reason is that the relaxation towards Maxwell-Boltzmann equilibrium is due to finite N effects. Because granularity is suppressed increasing N, this implies that the time that the system remains trapped in a quasi-stationary state can be very large, and indeed infinite in the limit $N \to \infty$. We will come back later on the relaxation mechanism towards Maxwell-Boltzmann equilibrium, called *collisional relaxation*. We will focus now on the *collisionless relaxation*, the mechanism responsible for the formation of the quasi-stationary state.

1.1 Collisionless relaxation

This mechanism can be divided into two processes: *mixing* and *violent relaxation* [2]. Mixing is caused by the evolution of the density distribution in the mean-field potential, which "mixes" the phase-space while conserving the distribution of energy density. Violent relaxation consists in the evolution of the distribution of energy because of oscillations of the potential. Mixing alone can give rise to a quasi-stationary state, but violent relaxation makes the process much more efficient.

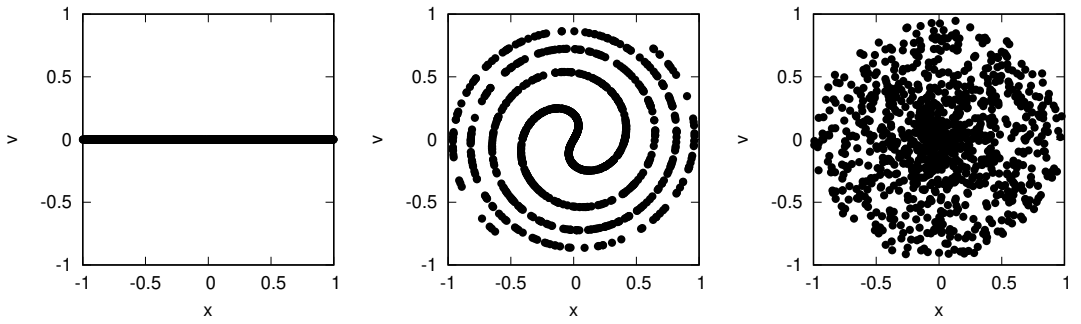

Figure 1.2 – Evolution of the phase-space of the system (1.9) for $N = 10^4$ particles. From left to right, $t = 0$, $t = 200$ and $t = 10000$.

In the $N \to \infty$ limit, the system can be described by the one-point probability density function $f(\mathbf{x}, \mathbf{v}, t)$, where f corresponds to the probability of finding a particle at the position $\mathbf{x}$ with velocity $\mathbf{v}$ at time t. Two-point probability density function vanishes because correlation between particles also vanishes in this limit, as it can be intuited by the analysis presented in the previous section. The evolution of f follows an *incompressible* dynamics in phase-space, i.e.,

$$\frac{df}{dt} = 0. \tag{1.7}$$

Applying the chain rule to (1.7) we get

$$\frac{df}{dt} = \frac{\partial f}{\partial t} + \dot{\mathbf{x}} \cdot \frac{\partial f}{\partial \mathbf{x}} + \dot{\mathbf{v}} \frac{\partial f}{\partial \mathbf{v}} = \frac{\partial f}{\partial t} + \mathbf{v} \cdot \frac{\partial f}{\partial \mathbf{x}} + \frac{\mathbf{F}[f]}{m} \cdot \frac{\partial f}{\partial \mathbf{v}} = 0, \tag{1.8}$$

where the "dot" denotes derivative with respect to time, $\mathbf{F}(\mathbf{x}, t)$ is the force at the position x at time t and m the mass of the particles. Equation (1.8) is the Vlasov equation. Despite its apparent simplicity, it is a very difficult equation to solve because the force $\mathbf{F}$ is a functional of the probability density function f. This is therefore, in general, a highly non-linear equation.

It is possible to visualize the mixing mechanism in a very simple model of independent one-dimensional pendula. The equation of motion for each particle is

$$\ddot{x}_i = -\sin(x_i). \tag{1.9}$$

We choose as initial condition the particles uniformly distributed along the x axis, with $|x| \leq 1$, and with zero initial velocities. The evolution is represented in Fig. 1.2. We show a typical "filamentation" of phase-space, which leads to a macroscopically stationary state. It is worth noting that the entropy, defined as

$$S(t) = -\int \mathrm{d}\,\mathbf{x}\,\mathrm{d}\,\mathbf{v}\, f(\mathbf{x}, \mathbf{v}, t) \ln f(\mathbf{x}, \mathbf{v}, t) \tag{1.10}$$

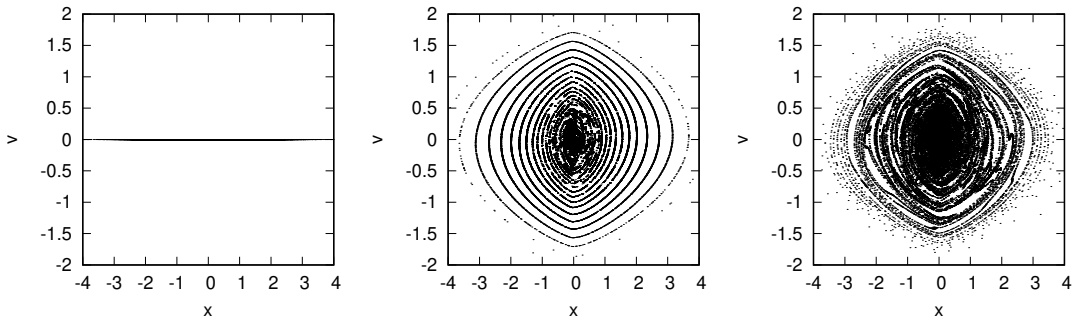

Figure 1.3 – Evolution of the phase-space of the system (1.11) for $N = 10^5$ particles. From left to right, $t = 0$, $t = 10$ and $t = 40$.

does not evolve during the evolution because the system is collisionless, i.e., it obeys the evolution equation (1.8). It is possible to define a "coarse-grained" entropy, using a definition similar to (1.10), but using a coarse grained distribution function of f, which leads to an increment of entropy during evolution (see Lynden-Bell [3]).

In addition to mixing, violent relaxation is present when the mean-field potential evolves with time. This occurs generically when the system evolution is driven by a potential (and a force) generated self-consistently by the particle distribution. Particles exchange energy, and consequently the energy distribution evolves. In Fig. 1.3 we give an example of the evolution of phase space of a one-dimensional gravitational system of particles, which follows the equation of motion:

$$\ddot{x}_i = -\frac{1}{N}\sum_{j\neq i} \mathrm{sign}(x_j - x_i). \tag{1.11}$$

We have chosen as initial condition in positions a Gaussian distribution of variance unity and zero initial velocities. We observe a characteristic filamentation followed, once the quasi-stationary state is reached, by a complex phase-space structure.

It is very difficult to compute analytically the evolution of Vlasov equation (1.8), and it is indeed very difficult to determine the properties (i.e. f) of the QSS. Despite a very beautiful attempt by Lynden-Bell [3] there is no theory which predicts the one-point distribution function of the quasi-stationary state. The reason is that it is neither possible to compute analytically the evolution of Vlasov equation nor even the one-point density function of the stationary state. The only hope is to build a statistical theory (as Equilibrium Statistical Physics), which takes into account the incompressible evolution of f through Vlasov equation. This is what Lynden-Bell did. Unfortunately, his theory does not give correct results in general because the system is in general not *ergodic*, i.e., it does not explore the whole phase space [4]. In some toy models, in which it does, the theory is successful (e.g. [5, 6]). Other attempts have been done, such as the *core-halo model*, which gives correct results in some cases [7, 8], or models with fitted parameters [9, 10], but neither of these models can be considered as a general theory.

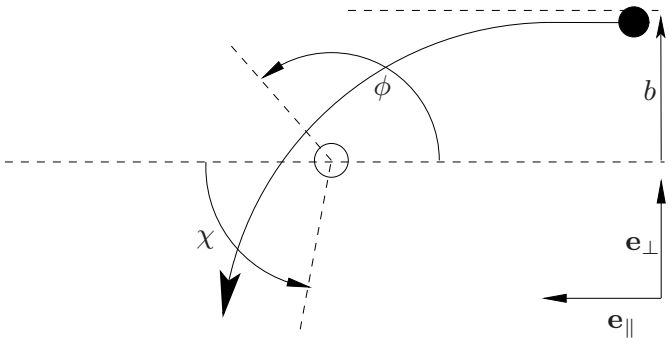

Figure 1.4 – Trajectory of a particle in a two body collision in the center of mass frame, with definition of the relevant quantities (see text).

1.2 Collisional relaxation

A system of particles relaxes towards Maxwell-Boltzmann equilibrium because of *collisions* between particles[1]. The first estimation of the relaxation time was done by Chandrasekhar in 1941 [12], showing that galaxies have not collisionally relaxed (they are in the QSS), and globular cluster have partially relaxed.

1.2.1 Chandrasekhar approach

The approach of Chandrasekhar consists in estimating the relaxation rate calculating the change of velocity of the particles because of successive collisions between them. The system has relaxed when the cumulative change of velocity is of the order of the velocity itself. The first step in the calculation consists in calculating the angle of deflection between two isolated particles. In the center of mass frame, the collision occurs as depicted in Fig. 1.4, in which appears the definition of the impact factor b, the angle of closest approach ϕ and the angle of deflection $\chi = 2\phi - \pi$. To define the angles with the usual mathematical signs, the incident particle comes from $+\infty$. This picture assumes that the two particles are far away from each other for $t \to -\infty$ and for $t \to +\infty$. The angle ϕ can be calculated, as a function of the impact factor b, using the classical formula [13]

$$\phi(b) = \int_{r_{min}}^{\infty} \frac{(b/r^2)\,\mathrm{d}\,r}{\sqrt{1-(b/r)^2-2u(r)/(mV^2)}}, \tag{1.12}$$

where V is the norm of the asymptotic relative velocity of the particles (which is a conserved quantity), m is the reduced mass and $u(r)$ is given by Eq. (1.2) with $\gamma = 1$ and $g < 0$. The quantity r_{min} is the largest positive root of the denominator. We

1. We will use here the term "collisions", a term borrowed from short-range systems, in which "collisions" are localized in space and time [11]. In the general context of long-range systems it would be more appropriate to call them "finite-N effects" or "granularity".

introduce the characteristic scale

$$b_0 = \frac{2|g|}{mV^2}. \tag{1.13}$$

Assuming that the system is in a QSS, there is a relationship between kinetic and potential energy, called the *virial* relation, which states that [2]

$$2K + \gamma U = 0, \tag{1.14}$$

where K and U are the kinetic and potential energy respectively. This relation implies that $K \sim mNV^2$ and the potential $U \sim gN^2/R$. Therefore, using Eqs. (1.13) and (1.14) we infer that

$$b_0 \sim \frac{R}{N}. \tag{1.15}$$

We see that for $N \gg 1$, b_0 is much smaller the R. We will use this result later. Performing the change of variable $r = r_{min}/x$ in Eq. (1.12), we obtain

$$\phi(b/b_0) = \frac{b}{r_{min}} \int_0^1 \frac{\mathrm{d}\, x}{\sqrt{1 - (bx/r_{min})^2 + (b_0 x/r_{min})}}. \tag{1.16}$$

We observe that ϕ depends only on the ratio b/b_0.

Computing the integral (1.16) we get

$$\phi(b/b_0) = \pi - \arctan\left(\frac{2b}{b_0}\right). \tag{1.17}$$

We decompose the relative change in velocity as $\Delta\mathbf{V}$ as

$$\Delta\mathbf{V} = \Delta V_\perp \mathbf{e}_\perp + \Delta V_\parallel \mathbf{e}_\parallel, \tag{1.18}$$

where $\mathbf{e}_\parallel$ is a unit vector defined parallel to the initial axis of motion, and $\mathbf{e}_\perp$ a unit vector orthogonal to it, in the plane of the motion. It follows that

$$\frac{\Delta V_\perp}{V} = -\sin(\chi) = -\frac{4b/b_0}{4(b/b_0)^2 + 1} \tag{1.19a}$$

$$\frac{\Delta V_\parallel}{V} = 1 - \cos(\chi) = \frac{2}{4(b/b_0)^2 + 1}. \tag{1.19b}$$

To estimate the accumulated effect of two body collisions on a particle as it crosses the whole system, we estimate first the number of encounters per unit of time with impact parameter b. In doing so we make the following approximations:

1. the system is treated as a homogeneous random distribution of particles in a sphere of radius R,
2. the initial squared relative velocity of colliding particles is given by the variance of the particle velocities in the system.

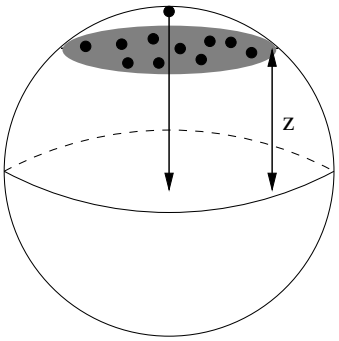

Figure 1.5 – The system is approximated as a perfectly spherical distribution of particles with radius R.

Each particle is then assumed to perform a simple homogeneous random walk in velocity space, with zero mean change in velocity (because the deflections due to each encounter have no preferred direction), and a positive mean squared velocity which we determine below. We assume therefore that successive collisions are uncorrelated.

As illustrated schematically in Fig. (1.5), we now divide the system in disks of thickness dz, and write the average number of encounters with impact parameter between b and $b + db$ of a particle crossing this disk as

$$\delta n = \frac{3N}{R^3} b \, db \, dz. \tag{1.20}$$

Multiplying Eq. (1.20) by the square of Eq. (1.19), and integrating from $z = 0$ to $z = R$ and from $b = 0$ to $b = \sqrt{R^2 - z^2}$, we then estimate the average change of the velocity *during one crossing* of the system, for the perpendicular and parallel components of the velocity respectively:

$$\frac{\langle \Delta V_{\perp,\parallel}^2 \rangle}{V^2} = \frac{3N}{R^3} \int_0^R \mathrm{d}\, b \, b \sqrt{R^2 - b^2} \, \left(\frac{\Delta V_{\perp,\parallel}}{V} \right)^2. \tag{1.21}$$

Using Eqs.(1.19), and using the fact that $b_0 \ll R$, we obtain

$$\frac{\langle \Delta V_{\perp}^2 \rangle}{V^2} = 3N \left(\frac{b_0}{R} \right)^2 \ln \left(\frac{R}{b_0} \right) \tag{1.22a}$$

$$\frac{\langle \Delta V_{\parallel}^2 \rangle}{V^2} = \frac{3}{2} N \left(\frac{b_0}{R} \right)^2, \tag{1.22b}$$

for each crossing of the system. The quantity

$$\Lambda = \frac{R}{b_0}. \tag{1.23}$$

is called the *Coulomb logarithm*. Using Eq. (1.15), we observe, as anticipated above, that for sufficiently large N, the average change in the longitudinal velocity is much smaller than the change in the normal one, i.e., $\langle \Delta V_{\parallel}^2 \rangle \ll \langle \Delta V_{\perp}^2 \rangle$.

We define the relaxation rate Γ as the inverse of the time scale at which the normalized average change in velocity squared due to collisions is equal to one, i.e., the time needed to randomize the velocities, $\langle \Delta V_{\perp}^2 \rangle \sim V^2$. Calling τ_{dyn} the typical time a particle needs to cross the system (which coincides with the collisionless typical time), we get from Eqs. (1.15) and (1.22a) for the collisional relaxation rate Γ:

$$\Gamma \tau_{dyn} \sim \frac{\ln N}{N}. \tag{1.24}$$

We observe that as we approach the mean field limit (i.e. N increases), the relaxation rate decreases. This is due to the fact that the granularity ("collisions") are responsible of the relaxation.

1.2.2 Rigorous approach: spatially homogeneous systems

The approach of Chandrasekhar, albeit being very successful to describe the collisional relaxation process (as we will see in next chapter), it is not a rigorous theory for collisional relaxation, because

i it has been derived for spatially homogeneous systems and

ii it neglects "collective effects", which are the reaction of the mean field potential to the finite N perturbations.

Moreover, the largest impact factor is unknown, and in practice, it is a free parameter in the model, which enters in the calculations in the Coulomb logarithm (1.23). Finally, collisions are treated as independent, and it is well known (see [14]) that this is a justified approximation only when the time-correlation scale of the noise caused by the finite-N fluctuations is much smaller than the characteristic orbital period of a particle. This is not the case in our system, as the noise is generated by (the finite-N) particles, and therefore the two timescales have the same order of magnitude.

In this section we will outline the derivation of the kinetic equations describing the collisional relaxation dynamics for a *spatially homogeneous* system. Then, we will give a sketch of the derivation for the technically more complex *spatially inhomogenous system*. The derivation is based in the quasi-linear approximation [15, 16], and we will follow closely the derivation given in [17]. We will use the discrete distribution function $f_d(\mathbf{x}, \mathbf{v}, t) = \sum_i \delta(\mathbf{x} - \mathbf{x}_i)\delta(\mathbf{v} - \mathbf{v}_i)$, where i is the index corresponding to particle i, which obeys the Klimontovich equation, which has the same form than the Vlasov equation, replacing f by f_d in Eq. (1.8). This is an exact equation, equivalent to the Liouville one. The one-point distribution function f can be obtained averaging f_d over realizations, i.e., $f(\mathbf{x}, \mathbf{v}, t) = \langle f_d(\mathbf{x}, \mathbf{v}, t) \rangle$, giving a smooth distribution. As we are dealing with a spatially homogeneous distribution, we have that $f = f(\mathbf{v}, t)$. We write $f_d = f + \delta f$, where δf are the finite-N fluctuations. Substituting this decomposition in Eq. (1.8) (replacing first f

by f_d), keeping only linear terms in f and δf and averaging over initial conditions, we get the following pair of equations:

$$\frac{\partial f}{\partial t} = \frac{\partial}{\partial \mathbf{v}} \cdot \langle \delta f \frac{\partial \delta\phi}{\partial \mathbf{r}} \rangle, \tag{1.25a}$$

$$\frac{\partial \delta f}{\partial t} + \mathbf{v} \cdot \frac{\partial \delta f}{\partial \mathbf{r}} - \frac{\partial \delta\phi}{\partial \mathbf{r}} \cdot \frac{\partial f}{\partial \mathbf{v}} = 0. \tag{1.25b}$$

The fluctuations of the potential are defined as

$$\delta\phi(\mathbf{r}, t) = \int \mathrm{d}\,\mathbf{r}' d\mathbf{v}' u(|\mathbf{r} - \mathbf{r}'|) \delta f(\mathbf{r}', \mathbf{v}', t). \tag{1.26}$$

In order to get an equation for the evolution of f, our goal is to compute the r.h.s of Eq. (1.25a), solving Eq. (1.25b) to get δf and $\delta\phi$. To solve the latter equation it is convenient to use the Fourier-Laplace transform, defined for the generic function $g(\mathbf{r}, \mathbf{v}, t)$ as

$$\widetilde{g}(\mathbf{k}, \mathbf{v}, \omega) = \frac{1}{(2\pi)^d} \int \mathrm{d}\,\mathbf{r} \int_0^\infty \mathrm{d}\,t\, e^{-\mathrm{i}(\mathbf{k}\cdot\mathbf{r} - \omega t)} g(\mathbf{r}, \mathbf{v}, t), \tag{1.27}$$

and the Fourier transform, defined as

$$\widehat{g}(\mathbf{k}, \mathbf{v}, t) = \frac{1}{(2\pi)^d} \int \mathrm{d}\,\mathbf{r}\, e^{-\mathrm{i}\mathbf{k}\cdot\mathbf{r}} g(\mathbf{r}, \mathbf{v}, t). \tag{1.28}$$

Taking the Fourier-Laplace transform of equation (1.25b), we have

$$\widehat{\delta f}(\mathbf{k}, \mathbf{v}, 0) - \mathrm{i}(\mathbf{k}\cdot\mathbf{v} - \omega)\, \widetilde{\delta f}(\mathbf{k}, \mathbf{v}, \omega) + \mathrm{i}\mathbf{k} \cdot \frac{\partial f}{\partial \mathbf{v}}\, \widetilde{\delta\phi}(\mathbf{k}, \omega) = 0. \tag{1.29}$$

From the above equation, we can isolate $\widetilde{\delta f}$ and thus find an expression relating the fluctuations of the distribution function and the fluctuations of the potential and the initial condition,

$$\widetilde{\delta f}(\mathbf{k}, \mathbf{v}, \omega) = \underbrace{\frac{\mathbf{k} \cdot \frac{\partial f}{\partial \mathbf{v}} \widetilde{\delta\phi}(\mathbf{k}, \omega)}{\mathbf{k}\cdot\mathbf{v} - \omega}}_{\substack{\text{collective} \\ \text{effects}}} + \underbrace{\frac{\widehat{\delta f}(\mathbf{k}, \mathbf{v}, 0)}{\mathrm{i}(\mathbf{k}\cdot\mathbf{v} - \omega)}}_{\substack{\text{initial} \\ \text{fluctuations}}}. \tag{1.30}$$

The first term on the r.h.s. of Eq. (1.30) corresponds to *collective effects*, which are the global response of the system to fluctuations, and the second term corresponds to contribution of the initial fluctuations. The next step in the derivation consists in expressing the Fourier transform of the fluctuation of the potential $\widetilde{\delta\phi}(\mathbf{k}, \omega)$ as a function of the fluctuation $\widetilde{\delta f}(\mathbf{k}, w)$. To do so, we integrate equation (1.30) over $\mathbf{v}$, and using the Fourier transform of equation (1.26), we get

$$\widetilde{\delta\phi}(\mathbf{k}, \omega) = (2\pi)^d \hat{u}(\mathbf{k}) \int_{-\infty}^{\infty} \mathrm{d}\,\mathbf{v} \widetilde{\delta f}(\mathbf{k}, \mathbf{v}, \omega) = (2\pi)^d \frac{\hat{u}(\mathbf{k})}{\epsilon(\mathbf{k}, \omega)} \int_{-\infty}^{\infty} \mathrm{d}\,\mathbf{v} \frac{\widehat{\delta f}(\mathbf{k}, \mathbf{v}, 0)}{i(\mathbf{k}\cdot\mathbf{v} - \omega)}, \tag{1.31}$$

where we have defined the plasma response dielectric function

$$\epsilon(\mathbf{k},\omega) = 1 - (2\pi)^d \hat{u}(\mathbf{k}) \int \mathrm{d}\,\mathbf{v} \frac{\mathbf{k}\cdot\partial f(\mathbf{v})/\partial \mathbf{v}}{\mathbf{k}\cdot\mathbf{v}-\omega}. \tag{1.32}$$

We should take care performing the integral of Eq. (1.32) as the denominator is zero for $\mathbf{k}\cdot\mathbf{v} = \omega$. This implies that there is a discontinuity when ω crosses the real axis. To determine which part of the complex ω half-plane is the physical one (i.e. $\mathrm{Im}(\omega > 0)$ or $\mathrm{Im}(\omega < 0)$), we take into account that a next step in the derivation consists, in order to obtain physical quantities, in computing an inverse Laplace transform using the Bromwich formula [18]:

$$\delta f(k,v,t) = \frac{1}{2\pi \mathrm{i}} \int_{-\infty+\mathrm{i}\sigma}^{-\infty+\mathrm{i}\sigma} \mathrm{d}\,\omega\, e^{-\mathrm{i}\omega t} \widetilde{\delta f}(k,v,\omega), \tag{1.33}$$

with $\sigma > 0$. Looking at the integration path of integral (1.33), we conclude that the upper half-plane is therefore the physical one, and we must therefore analytically continue the lower one by deforming the integration path below the poles of the denominator of (1.32), the contribution of the poles being computed simply using the residue theorem. Therefore, the integrals of the form

$$\int \mathrm{d}\,z \frac{g(z)}{z-\omega} \tag{1.34}$$

should be interpreted as Landau did in the context of Landau damping in plasmas [19, 20]:

$$\int \mathrm{d}\,z \frac{g(z)}{z-\omega} = \begin{cases} \int_{-\infty}^{\infty} \mathrm{d}\,x \frac{g(x)}{x-\omega} & \mathrm{Im}(\omega) > 0 \\ \mathcal{P}\int_{-\infty}^{\infty} \mathrm{d}\,x \frac{g(x)}{x-\omega} + \mathrm{i}\pi g(\omega) & \mathrm{Im}(\omega) = 0 \\ \mathcal{P}\int_{-\infty}^{\infty} \mathrm{d}\,x \frac{g(x)}{x-\omega} + \mathrm{i}2\pi g(\omega) & \mathrm{Im}(\omega) < 0, \end{cases} \tag{1.35}$$

where $\mathcal{P}$ means principal value.

We can compute now the r.h.s. of Eq. (1.25a) using the Bromwich inverse Laplace formula (1.33):

$$\left\langle \delta f \frac{\partial \delta\phi}{\partial \mathbf{r}} \right\rangle = \frac{1}{(2\pi)^2} \int_{-\infty}^{\infty} \mathrm{d}\,\mathbf{k}\,\mathrm{d}\,\mathbf{k}' \int_{\mathcal{C}} \mathrm{d}\,\omega\,\mathrm{d}\,\omega'\, i\mathbf{k}' e^{i\mathbf{k}\cdot\mathbf{r}-\omega t} e^{i\mathbf{k}'\cdot\mathbf{r}-\omega' t} \left\langle \widetilde{\delta f}(\mathbf{k},\mathbf{v},\omega)\widetilde{\delta\phi}(\mathbf{k}',\omega') \right\rangle, \tag{1.36}$$

where $\mathcal{C}$ is a contour which must pass *above* all the poles of the integrand. Using Eqs. (1.30) and (1.31), and assuming that there are not correlations between particles at $t = 0$, we can write the r.h.s. of Eq. (1.36) as a function of the interacting potential, the dielectric function and the velocity distribution [17].

A last step is necessary in the derivation: if the force is long-range, we expect the timescale of fluctuations τ_{fluctu} to be much larger than the typical time of evolution τ_{coll} of f. In this case we are not interested in all the functional dependence of (1.36) with time, but its asymptotic behavior for $\tau_{fluctu} \ll t \ll \tau_{coll}$. We can therefore take the limit $t \to \infty$ in our equation. Technically, this is equivalent to consider only the poles in the

real axis, which corresponds to the undamped modes, and not those in the negative ω axis, which corresponds to damped modes. This procedure is called *Markovianization*, because we transform the kinetic equation in a Markovian one, i.e., in an equation which does not depend on the past. Technically we transform an integro-differential equation in a differential one, which simplifies enormously the solving of the equation (see e.g. [11] for a pedagogical discussion of the Markovianization process).

Performing algebra which does not carry additional hypothesis (see e.g. [17, 21]) we get finally the equation:

$$\frac{\partial f}{\partial t} = \pi(2\pi)^d m \frac{\partial}{\partial v_i} \int \mathrm{d}\,\mathbf{k}\,\mathrm{d}\,\mathbf{v}' k_i k_j \frac{\hat{u}(\mathbf{k})^2}{|\epsilon(\mathbf{k}, \mathbf{k}\cdot\mathbf{v})|^2} \delta\big[\mathbf{k}\cdot(\mathbf{v}-\mathbf{v}')\big] \left(\frac{\partial}{\partial v_j} - \frac{\partial}{\partial v'_j} \right) f(\mathbf{v}, t) f(\mathbf{v}', t). \tag{1.37}$$

Equation (1.37), through the term $\delta[\mathbf{k}\cdot(\mathbf{v}-\mathbf{v}')]$ shows that contributions to collisional relaxation is produced by particles which are *in resonance*. When collective effects are neglected, i.e., the first term of equation (1.30) is neglected, this implies that $\epsilon(\mathbf{k}, \omega) = 1$.

From Eq. (1.37) it is possible to write a Fokker-Planck equation for the evolution of the probability density function $P(\mathbf{v}, t)$ of a test particle. Replacing $f(\mathbf{v}, t)$ by $P(\mathbf{v}, t)$ in Eq. (1.37), we get

$$\frac{\partial P}{\partial t} = -\frac{\partial}{\partial v_i}(P A_i) + \frac{1}{2}\frac{\partial^2}{\partial v_i \partial v_j}(D_{ij} P), \tag{1.38}$$

where we have defined the diffusion coefficients

$$D_{ij}(\mathbf{v}, t) = \pi(2\pi)^d m \int \mathrm{d}\,\mathbf{k}\,\mathrm{d}\,\mathbf{v}' k_i k_j \frac{\hat{u}(\mathbf{k})^2}{|\epsilon(\mathbf{k}, \mathbf{k}\cdot\mathbf{v})|^2} \delta\big[\mathbf{k}\cdot(\mathbf{v}-\mathbf{v}')\big] f(\mathbf{v}', t) \tag{1.39a}$$

$$A_i(\mathbf{v}, t) = \pi(2\pi)^d m \int \mathrm{d}\,\mathbf{k}\,\mathrm{d}\,\mathbf{v}' k_i k_j f(\mathbf{v}', t) \left(\frac{\partial}{\partial v_j} - \frac{\partial}{\partial v'_j} \right) \frac{\hat{u}(\mathbf{k})^2}{|\epsilon(\mathbf{k}, \mathbf{k}\cdot\mathbf{v})|^2} \delta\big[\mathbf{k}\cdot(\mathbf{v}-\mathbf{v}')\big]. \tag{1.39b}$$

In the limit without collective effects (i.e. $\epsilon(\mathbf{k}, \omega) = 1$) the computation of the diffusion coefficients using Eqs. (1.39) or using the formalism given in Subsect. 1.2.1 are equivalent (see. e.g. [22] for the derivation using Eqs. (1.39) and [23] for the one using the Chandrasekhar approach).

1.2.3 Rigorous approach: inhomogenous systems

In the case of spatially inhomogenous systems, it is necessary to work with dynamical variables which are constant in the unperturbed system. For this reason, we will use angle-actions variables $(\mathbf{w}, \mathbf{J})$ corresponding to the mean-field potential. Using these variables, particles described by the mean-field Hamiltonian $\mathcal{H}$ keep their action $\mathbf{J}$ constant during the dynamics, and their angle evolves with time with the trivial equation $\mathbf{w} = \mathbf{\Omega}(\mathbf{J})t + \mathbf{w}_0$ where $\mathbf{w}_0$ is the angle at $t = 0$ and $\mathbf{\Omega}(\mathbf{J}) = \partial\mathcal{H}/\partial\mathbf{J}$ is the angular frequency. The system thus becomes "homogeneous" in the new coordinates [24]. Obviously, the complexity of the dynamics is hidden in the change of variables. Using the

same procedure than the one used to compute Eq. (1.25), we obtain the same structure of the equations in angle-action variables:

$$\frac{\partial \overline{f}}{\partial t} = \frac{\partial}{\partial \mathbf{J}} \cdot \left\langle \overline{\delta f \frac{\partial \delta\phi}{\partial \mathbf{w}}} \right\rangle, \tag{1.40a}$$

$$\frac{\partial \overline{\delta f}}{\partial t} + \mathbf{\Omega}(\mathbf{J}) \cdot \frac{\partial \overline{\delta f}}{\partial \mathbf{w}} - \overline{\frac{\partial \delta\phi}{\partial \mathbf{w}} \cdot \frac{\partial f}{\partial \mathbf{J}}} = 0, \tag{1.40b}$$

where $\overline{A}$ represents the angle-averaging of A, which corresponds to a canonical transformation which removes the fast variables (see e.g. [25]). From now on we will simplify notations and we will replace $\overline{A}$ by simply A. The price to pay to have the simple equations (1.40) is that we have to express the r.h.s. of Eq. (1.40a) and the last term of the l.h.s. of Eq. (1.40b) in angle-action variables. This can be technically very difficult.

In order to obtain a kinetic equation from (1.40) there is a crucial step which consists in choosing a bi-orthogonal basis $\{\rho_\alpha, \Phi_\alpha\}$ (introduced by Kalnajs in 1976 [26]), which satisfies

$$\int u(|\mathbf{r}-\mathbf{r}'|)\rho_\alpha(\mathbf{r}')\,\mathrm{d}\,\mathbf{r}' = \Phi_\alpha \tag{1.41}$$

$$\int \rho_\alpha(\mathbf{r})\Phi^\star_{\alpha'}(\mathbf{r})\,\mathrm{d}\,\mathbf{r} = -\delta_{\alpha,\alpha'}. \tag{1.42}$$

The coefficients of the density fluctuations $\delta\rho(\mathbf{r},t)$ and potential $\delta\phi(\mathbf{r},t)$ in the basis of ρ_α and $\{\Phi_\alpha\}$ respectively, are the same

$$\delta\rho(\mathbf{r},t) = \sum_\alpha A_\alpha(t)\rho_\alpha(\mathbf{r}) \tag{1.43a}$$

$$\delta\phi(\mathbf{r},t) = \sum_\alpha A_\alpha(t)\Phi_\alpha(\mathbf{r}). \tag{1.43b}$$

Using this basis, the derivation of the kinetic equation follows step-by-step the one of the homogeneous case. The result is [27, 28]

$$\frac{\partial f}{\partial t} = \pi(2\pi)^d m \frac{\partial}{\partial \mathbf{J}} \cdot \sum_{\mathbf{k},\mathbf{k}'} \int d\mathbf{J}'\mathbf{k} \frac{\delta[\mathbf{k}\cdot\mathbf{\Omega}(\mathbf{J}) - \mathbf{k}'\cdot\mathbf{\Omega}(\mathbf{J}')]}{|D_{\mathbf{k},\mathbf{k}'}(\mathbf{J},\mathbf{J}',\mathbf{k}\cdot\mathbf{\Omega}(\mathbf{J}))|^2} \left(\mathbf{k}\cdot\frac{\partial}{\partial \mathbf{J}} - \mathbf{k}'\cdot\frac{\partial}{\partial \mathbf{J}'}\right) f(\mathbf{J},t) f(\mathbf{J}',t) \tag{1.44}$$

where

$$\frac{1}{D_{\mathbf{k},\mathbf{k}'}(\mathbf{J},\mathbf{J}',\omega)} = \sum_{\alpha,\alpha'} \hat{\Phi}_\alpha(\mathbf{k},\mathbf{J})(\epsilon^{-1})_{\alpha,\alpha'}(\omega)\hat{\Phi}^\star_{\alpha'}(\mathbf{k}',\mathbf{J}'), \tag{1.45}$$

and $\hat{\Phi}_\alpha$ are the Fourier transforms of the potential in the bi-orthogonal representation with respect to the angles, i.e.,

$$\hat{\Phi}_\alpha(\mathbf{k},\mathbf{J}) = \frac{1}{(2\pi)^d} \int \mathrm{d}\,\mathbf{w} e^{-i\mathbf{k}\cdot\mathbf{w}} \Phi_\alpha(\mathbf{w},\mathbf{J}), \tag{1.46}$$

and $\epsilon_{\alpha\alpha'}(\omega)$ is the dielectric tensor

$$\epsilon_{\alpha\alpha'}(\omega) = \delta_{\alpha\alpha'} + (2\pi)^d \sum_{\mathbf{k}} \int d\mathbf{J} \frac{\mathbf{k}\cdot\partial f/\partial \mathbf{J}}{\mathbf{k}\cdot\mathbf{\Omega}(\mathbf{J}) - \omega} \hat{\Phi}^{\star}_{\alpha}(\mathbf{k},\mathbf{J})\hat{\Phi}_{\alpha'}(\mathbf{k},\mathbf{J}), \tag{1.47}$$

where the Landau prescription (1.35) has to be used to define the integral. We observe that Eq. (1.44) has exactly the same structure as the homogeneous case Eq. (1.37). Following exactly the same procedure, it is therefore possible to write an associated Fokker-Planck equation

$$\frac{\partial f}{\partial t} = \sum_{i,j=1}^{d} \frac{\partial^2}{\partial J_i \partial J_j} D^{ij}_{dif}(\mathbf{J},t) f(\mathbf{J},t) - \frac{\partial}{\partial \mathbf{J}} \cdot \mathbf{D}_{fr}(\mathbf{J},t) f(\mathbf{J},t) \tag{1.48}$$

with diffusion coefficients

$$D^{ij}_{dif}(\mathbf{J},t) = \pi(2\pi)^d m \sum_{\mathbf{k},\mathbf{k}'} \int \mathrm{d}\,\mathbf{J}' \frac{k_i k_j}{|D_{\mathbf{k},\mathbf{k}'}(\mathbf{J},\mathbf{J}',\mathbf{k}'\cdot\mathbf{\Omega}(\mathbf{J}'))|^2} \delta[\mathbf{k}\cdot\mathbf{\Omega}(\mathbf{J}) - \mathbf{k}'\cdot\mathbf{\Omega}(\mathbf{J}')] f(\mathbf{J}',t) \tag{1.49a}$$

$$\mathbf{D}_{fr}(\mathbf{J},t) = \pi(2\pi)^d m \sum_{\mathbf{k},\mathbf{k}'} \int \mathrm{d}\,\mathbf{J}' f(\mathbf{J}',t)\,\mathbf{k} \left(\mathbf{k}\frac{\partial}{\partial \mathbf{J}} - \mathbf{k}'\frac{\partial}{\partial \mathbf{J}'}\right) \frac{\delta[\mathbf{k}\cdot\mathbf{\Omega}(\mathbf{J}) - \mathbf{k}'\cdot\mathbf{\Omega}(\mathbf{J}')]}{|D_{\mathbf{k},\mathbf{k}'}(\mathbf{J},\mathbf{J}',\mathbf{k}'\cdot\mathbf{\Omega}(\mathbf{J}'))|^2}. \tag{1.49b}$$

2. Collisional relaxation

My first interest in this topic came with the question about the proper definition of "long-range system" when dynamics is taken into account. As written in Eq. (1.1), the "usual" definition of a long-range interacting system consists in stating that the interacting potential is non integrable, because of the large scales. The consequences of this have been illustrated in Sect. 1, showing that the potential of a particle is dominated by contribution of the whole distribution of particles rather than the nearest neighbors. This definition is of course very reasonable, but we know that in classical mechanics the physics is governed by *forces* and not by *potentials*. Equilibrium statistical mechanics deals only with energies, and hence the important quantity is the potential rather than the force. However, when *dynamics* enters into the game, what is important is the *force*. Consequently, is the classification based on property (1.1) *always* relevant?

As a starting point we should define what we call a "long-range interacting system". Of course, many definitions are possible. For example, a definition which would lead to definition (1.1) would be the existence of unusual behavior of the system in thermal equilibrium: non-concavity of the entropy, inequivalence of ensembles, negative specific heat etc (see e.g. [29]). If we look however at the *out-of-equilibrium* behavior of the system, e.g., the existence of quasi-stationary states, we will be led to a different classification of interactions. The key point consists in studying the lifetime of quasi-stationary states (QSS) as a function on the number of particles: we will define a system as *long-range* if this lifetime increases increasing N, and short-range if it decreases increasing N, going eventually to zero in the limit $N \to \infty$. It is possible to estimate the duration of the QSS generalizing the Chandrasekhar estimate (1.24) for a system of particles with an interacting potential

$$u(r) = \frac{g}{r^\gamma}, \tag{2.1}$$

where $g < 0$ and $\gamma > 0$. The first step consists in generalizing the Rutherford scattering formula Eq. (2.5) for any $\gamma > 0$. In this case the problem does not admit an analytical solution (except for particular values of γ), and opens an interesting and challenging mathematical problem, described in the subsequent section.

2.1 Generalization of the Rutherford formula

Paper [I].

The Rutherford scattering formula has been a crucial to determine experimentally, in 1911, that the atoms are made by a central nucleus where all the charge of (positive) sign is accumulated in a very small region, surrounded by the (negative) electrons orbiting around the nucleus. In order to arrive to this conclusion Rutherford needed a formula which gives the angle of deflection of a charged particle (in this case an α particle) with another charged "particle", the nucleus. In this section we are going to generalize the formula derived in Sect. 1.2.1 for power-law potentials Eq. (2.1), for repulsive or attractive interactions, which can eventually be regularized at small scales. The formula for the angle $\phi(b)$ now reads:

$$\phi(b) = \int_{r_{min}}^{\infty} \frac{(b/r^2)dr}{\sqrt{1-(b/r)^2 \mp (b_0/r)^\gamma}}, \tag{2.2}$$

where r_{min} is the largest root of the denominator. The "minus" sign in the denominator corresponds to a repulsive interaction while the "plus" sign to an attractive one, b is the impact factor and

$$b_0 = \left(\frac{2|g|}{mV^2}\right)^{1/\gamma}. \tag{2.3}$$

Performing the same change of variables $r = r_{min}/x$ than in Eq. (1.16) we obtain

$$\phi(b/b_0) = \frac{b}{r_{min}} \int_0^1 \frac{dx}{\sqrt{1-(bx/r_{min})^2 \mp (b_0 x/r_{min})^\gamma}}. \tag{2.4}$$

We observe that, also in this case, ϕ is a function of b/b_0.

The integral (2.4) cannot be in general solved analytically. We can look to the solution we know for $\gamma = 1$, treated in Sect. 1.2.1, in order to give us some insight of the properties of (2.4). In this case, it exists the following analytical solution of Eq. (2.4):

$$\phi(b/b_0) = \pi - \arctan\left(\frac{2b}{b_0}\right). \tag{2.5}$$

We observe that it is an analytical function of the variable b/b_0. It is simple to see that the solution (2.5) admits the following development in power series of b/b_0 for $\beta = b/b_0 \leq 1/2$

$$\phi(b/b_0) = \pi + \sum_{n=0}^{\infty} \frac{(-1)^{n+1}}{2n+1} \left(\frac{2b}{b_0}\right)^{2n+1}, \tag{2.6}$$

and for $\beta = b/b_0 \geq 1/2$

$$\phi(b/b_0) = \frac{\pi}{2} + \sum_{n=0}^{\infty} \frac{(-1)^{n}}{2n+1} \left(\frac{b_0}{2b}\right)^{2n+1}. \tag{2.7}$$

It is therefore possible to express the solution of the integral (2.4) in the form of a power series, for any value of b. It is however not simple to obtain such asymptotic series, for a general γ, from Eq. (2.4). The procedure to obtain such power series is the following:

1. identify the small parameter δ in which develop integral (2.4), adapted to the sign of the interaction and the regime considered.
2. Expand Eq. (2.4) in some (non-integer) powers of δ. In the most favorable cases it results a single sum of power series in δ. However, in the more complicated cases, it results in a double sum of powers of δ.
3. Express δ in power series of b/b_0, which is in all cases a simple task.
4. Sum the power series over one or two indices, in order to obtain a result in the desired form, i.e., a single sum of, in general, non integer powers of b/b_0.

In the literature was only known the expansion for *soft scattering*, i.e., $b/b_0 > \beta$ [30], for both attractive and repulsive interactions – which has simply a sign difference between them– for $\gamma > 2$. Using the uniqueness of power series expansions, we deduce that it is valid for any $\gamma > 0$. This expansion is in powers of $(b_0/b)^\gamma$, i.e,

$$\phi(b/b_0) = \sum_{n=0}^{\infty} a_n(\gamma)(b_0/b)^{\gamma n}, \tag{2.8}$$

where a_n are coefficients which depends on the particular value of γ and can be computed using Gamma functions (see [I] for all the expressions we will not explicit here).

In addition, we have found the power series expansion for the *hard scattering regime*, i.e., $b/b_0 < \beta$, where $\beta = (\gamma/2)^{1/\gamma}|1 - 2/\gamma|^{2-\gamma/2\gamma}$. In the repulsive case, the expansion is in odd powers of b/b_0, i.e.,

$$\phi(b/b_0) = \sum_{n=0}^{\infty} a_n(\gamma)(b/b_0)^{2n+1}, \tag{2.9}$$

where the coefficients a_n are different of those appearing in Eq. (2.8).

The attractive case is more complex. For $\gamma < 2$, the angle ϕ is always well defined (independently of the value of b/b_0), and it is possible to obtain a power expansion in b/b_0. It is however a much more involved calculation compared to the previous ones, because in the point 2. listed above, we obtain a *double* power series in δ instead of a single one as in the other cases. It is then necessary to convert a sum over three indices (two for the development in powers of δ, and the other one for the expression of δ in powers of b/b_0) in a single sum. Finally, the result can be expressed in the form of the sum of two series in different powers of b/b_0:

$$\phi(b/b_0) = \sum_{n=0}^{\infty} \left\{ a_n(\gamma)(b/b_0)^{\frac{2\gamma}{2-\gamma}n} + c_n(\gamma)(b/b_0)^{2n+1} \right\}, \tag{2.10}$$

which is valid for $\gamma \neq 2\frac{2k+1}{2\ell+1} \in]0, 2[$ for some k, $\ell \in \mathbb{N}$, e.g. $\gamma \neq 2/3$, $\gamma \neq 6/7$, etc. For these special values of γ, the series has a third term in powers of $(b/b_0)^{2q+1}\ln(b/b_0)$,

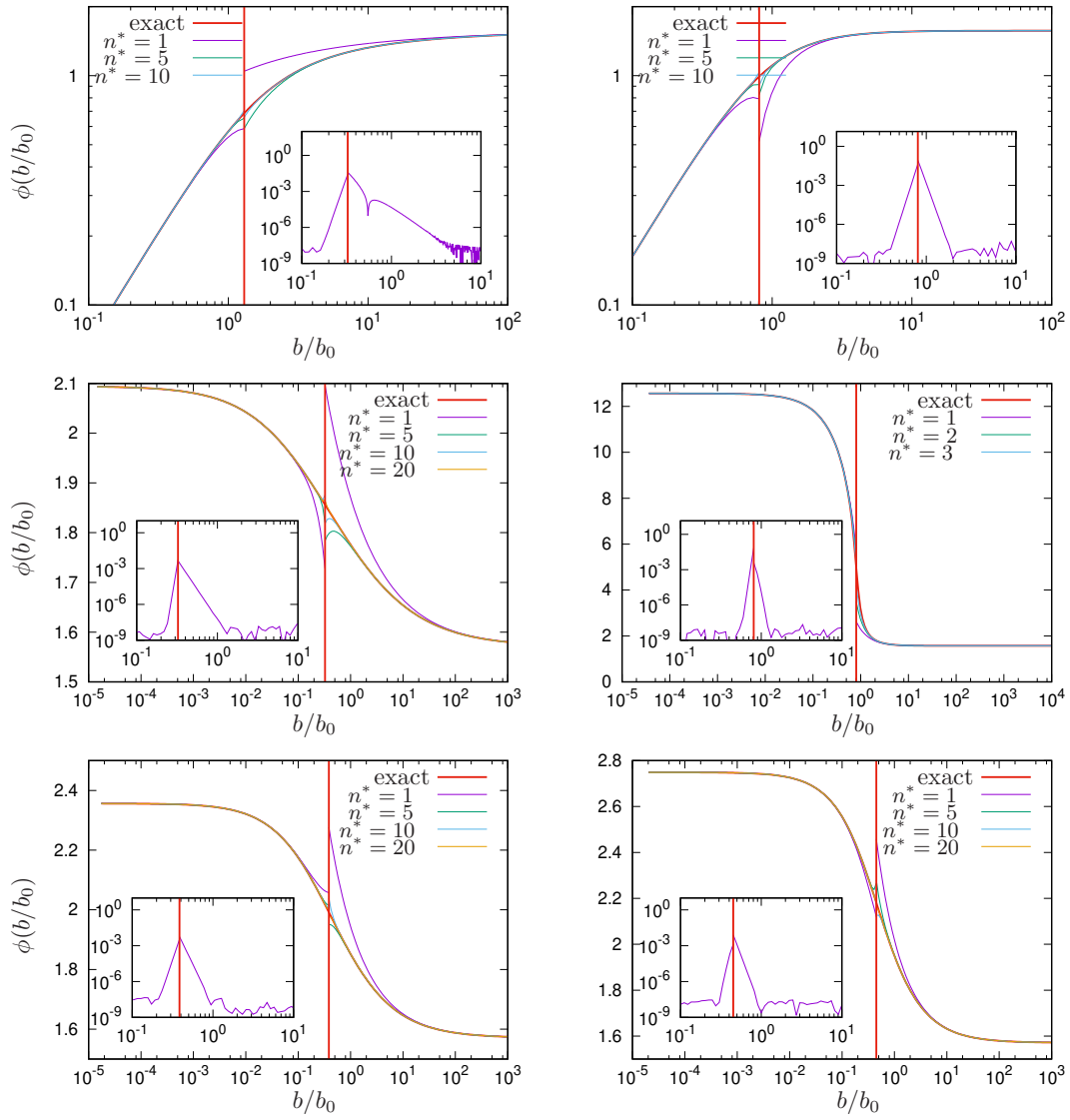

Figure 2.1 – Top: repulsive interaction, with $\gamma = 1/2$ (left) and $\gamma = 7/4$ (right). Middle: attractive interaction with the same values of γ. Bottom: two attractive cases in which logarithm corrections appear, with $\gamma = 2/3$ (left) and $\gamma = 6/7$ (right). The integer n^* corresponds to the number of terms summed in the first series, the number of terms summed in the second series is chosen such that the final exponents are as close as possible. Inset: relative error for maximal n^*.

$q \in \mathbb{N}$. The explicit full series can be found in [I]. In particular, we find in this case that

the leading coefficient in (2.10) is

$$a_0(\gamma) = \frac{\pi}{2-\gamma}. \tag{2.11}$$

We observe therefore that the particles can do an arbitrarily large number of loops as $\gamma \to 2$, which is called in the literature *orbiting* [31]. For $\gamma \geq 2$ (and $b/b \leq \beta$) the kinetic barrier (corresponding to the term $(b/r)^2$ in the denominator of Eq. (2.4)) cannot balance the attractive interaction, and particles crash in a finite time. In Fig. 2.1 we show the convergence of the series, for repulsive and attractive interactions, for cases in which the series is in power laws of b/b_0, and two cases in which logarithm corrections appear.

In addition, we are often interested in interactions which are regularized at small scales. This is typically the case in cosmological N-body simulations, in which the interaction is "softened" at small scales in order to suppress collisions (see e.g. [32]). We are therefore interested in the modifications of the results listed above when such as regularization is present in the potential. Two very used regularized potential in the literature are the Plummer one

$$v^{\mathrm{Pl}}(r,\epsilon) = \frac{g}{(r^2+\epsilon^2)^{\gamma/2}} \tag{2.12}$$

and the compact softening

$$v^{\mathrm{co}}(r,\epsilon) = \begin{cases} \frac{g}{r^\gamma} & \text{if } r \geqslant \epsilon \\ \frac{g}{\epsilon^\gamma}\mathrm{v}\left(r/\epsilon\right) & \text{if } 0 \leqslant r \leqslant \epsilon, \end{cases} \tag{2.13}$$

where $\mathrm{v}(x)$ is some smooth function with $\mathrm{v}(1) = 1$. As the computations are much more complex than in the unregularized case, we had no hope of obtaining the full series expansion. Instead, we computed the values of ϕ at first order in b, which was sufficient for our application needs. We will not list the general results here, they can be found in [I]. In Sect. 2.2 we will need the leading order of the deflection angle for attractive interactions and $\epsilon \geq b_0$, which reads, for the regularizations (2.12) and (2.13):

$$\chi = 2\phi - \pi \sim \begin{cases} \left(\frac{b_0}{\epsilon}\right)^\gamma \left(\frac{b}{\epsilon}\right) & \text{if } b \lesssim \epsilon \\ \left(\frac{b_0}{b}\right)^\gamma & \text{if } b \gtrsim \epsilon. \end{cases} \tag{2.14}$$

2.2 The range of interactions

Papers [II, III].

We can now generalize Eqs. (1.22a) for the the pure power-law potential (2.1) and dimension of space $d \geq 2$ [1]:

$$\frac{\langle \Delta V_{\perp,\parallel}^2 \rangle}{V^2} = \frac{B_b N}{R^d} \int_0^R \mathrm{d}\, b\, b^{d-2} \sqrt{R^2 - b^2} \left(\frac{\Delta V_{\perp,\parallel}}{V}\right)^2, \tag{2.15}$$

1. An analogous expression can be found for $d = 1$.

where B_d is a geometrical factor which depends on the dimension d. The behavior of the change of the relative velocity as a function of b_0/R depends on the convergence properties of the integral (2.15), which depends on the asymptotic behavior of the angle $\chi = 2\phi - \pi$, given in the previous section. In order to understand the behavior of the integrals, it is sufficient to know the leading orders of χ in b/b_0 for the hard and soft collision regimes.

For the hard collisions regime we have, for $b/b_0 < \beta$ (and $\gamma < 2$)

$$\chi(b/b_0) = \frac{\gamma\pi}{2-\gamma} + \mathcal{O}\left((b/b_0)^\alpha\right), \tag{2.16}$$

and hence using the definitions given in Eq. (1.19), $\Delta V_\perp/V$ and $\Delta V_\parallel/V$ do not depend on b/b_0 in this regime at leading order. For the soft collisions we have

$$\frac{\Delta V_\perp}{V} \sim \left(\frac{b_0}{b}\right)^\gamma + \mathcal{O}((b_0/b)^{2\gamma}) \tag{2.17a}$$

$$\frac{\Delta V_\parallel}{V} \sim \left(\frac{b_0}{b}\right)^{2\gamma} + \mathcal{O}((b_0/b)^{4\gamma}). \tag{2.17b}$$

At this point it is convenient to divide the integral (2.15) in two pieces, the first one corresponding to the hard collisions and the second one to the soft ones. Using that $R \gg b_0$, we have

$$\begin{aligned} \frac{\langle \Delta V_{\perp,\parallel}^2 \rangle}{V^2} &= \frac{B_b N}{R^{d-1}} \int_0^{b_0} \mathrm{d}\, b\, b^{d-2} \left(\frac{\Delta V_{\perp,\parallel}}{V}\right)^2 \\ &+ \frac{B_b N}{R^d} \int_{b_0}^{R} \mathrm{d}\, b\, b^{d-2} \sqrt{R^2 - b^2} \left(\frac{\Delta V_{\perp,\parallel}}{V}\right)^2. \end{aligned} \tag{2.18}$$

In the first integral $\Delta V_{\perp,\parallel}/V \sim 1$ and therefore its contribution is of order $\sim N(b_0/R)^{d-1}$, which corresponds to the scaling of a repulsive hard core (see e.g. [13]). The scaling of the second integral depends on the value of γ and the dimension d of space:

— if $0 < \gamma < (d-1)/2$, the integral (2.18) is dominated by the upper cutoff and therefore the change of the relative velocity is dominated by soft scattering, i.e., the second integral of Eq. (2.18) dominates over the first one:

$$\frac{\langle |\Delta \mathbf{V}|^2 \rangle}{|V^2|} \sim N \left(\frac{b_0}{R}\right)^{2\gamma}. \tag{2.19}$$

— If $\gamma = (d-1)/2$, the second integral of Eq. (2.18) dominates again over the first one, and logarithmic corrections appear, as in the gravitational case in $d = 3$:

$$\frac{\langle |\Delta \mathbf{V}|^2 \rangle}{|V^2|} \sim N \left(\frac{b_0}{R}\right)^{d-1} \ln\left(\frac{R}{b_0}\right). \tag{2.20}$$

— If $\gamma > (d-1)/2$, the integral is dominated by the lower cutoff. In this case the two integrals of Eq. (2.18) give contributions of the same order, and the system behaves as a system of repulsive hard spheres (see e.g. [11]), i.e.

$$\frac{\langle|\Delta\mathbf{V}|^2\rangle}{|V^2|} \sim N\left(\frac{b_0}{R}\right)^{d-1}. \tag{2.21}$$

To estimate the relaxation as a function of the number of particles N we use the virial theorem for power-law interactions (1.14), which permits to infer that

$$b_0 \sim RN^{-1/\gamma}. \tag{2.22}$$

Using Eqs.(2.19), (2.20) and (2.22), we get the relaxation rate as a function of γ:

$$\Gamma\,\tau_{dyn} \sim \begin{cases} N^{-1}, & 0 < \gamma < (d-1)/2 \\ N^{-1}\ln(N), & \gamma = (d-1)/2 \\ N^{-(d-1-\gamma)/\gamma}, & \gamma > (d-1)/2. \end{cases} \tag{2.23}$$

We observe, that in the limit $N \to \infty$, if $\gamma > d-1$, the relaxation rate tends to infinity, which indicates that the existence time of the QSS is negligible before the system reach thermal equilibrium. In this case, we propose to call these systems as *dynamically* short-range, because they behave as a short-range system. Note that in the range $d-1 < \gamma < d$, even if they are *dynamically* short-range, they behave as *thermodynamically* long-range, i.e., ensembles can be inequivalent, negative specific heat can appear, etc. (see e.g. [29]). For $\gamma < d-1$, in the limit $N \to \infty$, the relaxation rate tends to zero. In this limit, the system remains trapped in the QSS forever. We propose to call these systems as *dynamically long-range*.

It is difficult to integrate numerically systems of particles without regularizing the divergence of the potential at small scales. For this reason, we have introduced a softening ϵ in the potential in the simulations, of the type given in Eq. (2.12) or (2.13). Using the result (2.14) (valid for $\epsilon \geq b_0$), the scalings are modified as follows:

$$\Gamma\,\tau_{dyn} \sim \begin{cases} N^{-1}, & 0 < \gamma < (d-1)/2 \\ N^{-1}\ln(R/\epsilon), & \gamma = (d-1)/2 \\ N^{-1}(\epsilon/R)^{d-1-2\gamma}, & \gamma > (d-1)/2. \end{cases} \tag{2.24}$$

We have checked in [II,III] that the scalings (2.24) work extremely well, keeping N or ϵ constant. In Fig. 2.2 top, we show an example of an interaction of the class $\gamma < (d-1)/2$, in which we observe that the relaxation rate is independent of the softening length ϵ, and the scaling of a macroscopic quantity as the evolution of the kinetic energy follows the one predicted by Eq. (2.24). In the same figure, bottom, we plot $\Gamma\tau_{dyn}$ as a function of ϵ, or N, for $\gamma = 5/4$ and $\gamma = 3/2$. We observe that the relaxation rate follows the scaling given by Eq. (2.24). We may conclude, as these scalings are correct for interactions dominated by close or distant encounters, that the Chandrasekhar approximation may

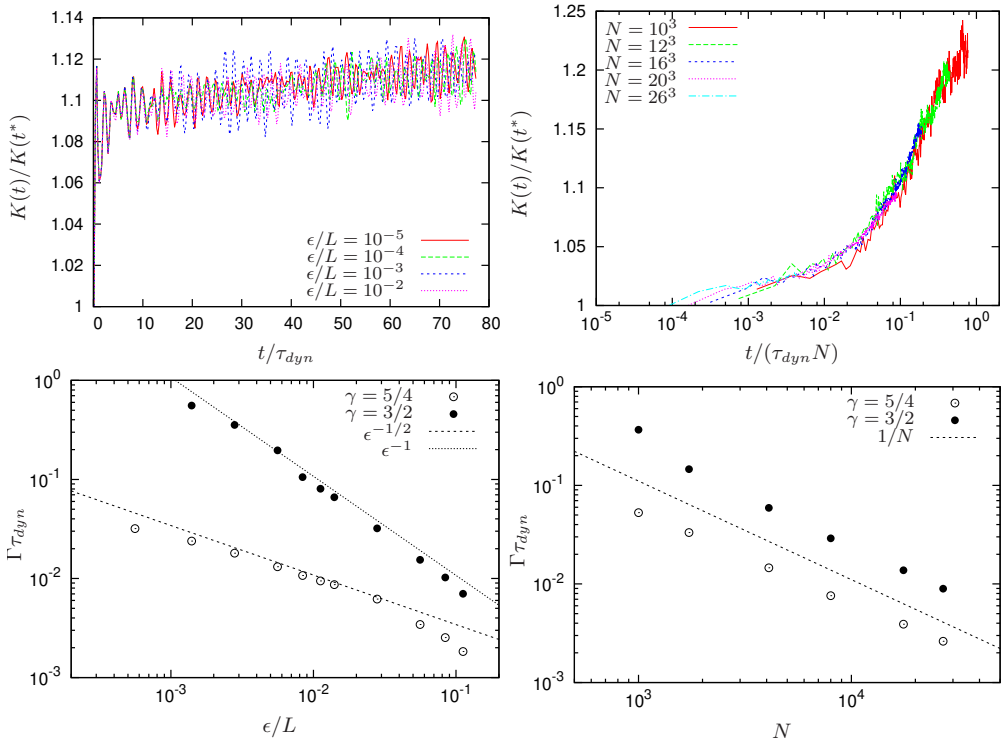

Figure 2.2 – Tests of scaling of measured relaxation rates. Top, interactions in the range $\gamma < (d-1)/2$. Evolution of the kinetic energy $K(t)$ normalized at the reference time t^*, for systems with $\gamma = 1/2$: left, for a range of different values of ϵ at fixed N, and right, for a range of N different number of particles at fixed ϵ. In the latter plot the time variable has been rescaled with N in line with the theoretically predicted scaling of Eq. (2.24). Bottom, interactions in the range $\gamma > (d-1)/2$: left, $\Gamma\tau_{dyn}$ as a function of ϵ, for the cases $\gamma = 5/4$ and $\gamma = 3/2$ in simulations, and, right, as a function of N for $\gamma = 5/4$ and $\gamma = 3/2$.

be valid for most of the collisions of pair of particles. We will discuss this point in the conclusions of the chapter.

In addition, using the scaling (2.24), we can give a conclusion about the maximum impact parameters that has to be used in the calculations. In our calculations we have taken the size of the system [2], but in the original paper of Chandrasekhar he has considered that the maximum impact parameter should be the distance of the nearest neighbor [12]. A subsequent controversy arose, with authors arguing to take the maximum impact parameter as the mean interparticle distance [33, 34, 35], whereas other authors claim

2. Choosing a fraction of the size of the system the scalings are unchanged, only the numerical prefactor is modified.

for the size of the system [36, 37, 38, 39]. Looking at the regime $\gamma < (d-1)/2$, if we assume that the maximum parameter scales with N as $b_{max} \sim RN^{-\alpha}$ (in the previous calculations we have chosen $\alpha = 0$), then the relaxation rate would be

$$\Gamma\tau_{dyn} \sim N^{\alpha(2\gamma-d+1)-1}. \tag{2.25}$$

In our simulations in $d = 3$ we obtain unambiguously a scaling $\Gamma\tau_{dyn} \sim N^{-1}$, in agreement with $\alpha = 0$. Moreover, in the gravitational case, it is possible to quantify the maximum impact factor by fitting the relaxation rate. We obtained

$$\Gamma\tau_{dyn} \sim N^{-1} \ln\left(\frac{R}{3\epsilon}\right), \tag{2.26}$$

which indicates, in our case that $b_{max} \simeq R/3$.

2.3 The range of interaction: a different approach

Paper [IV].

The classification of interactions presented in the previous section is based in studying how the system behaves when collisional relaxation is present. The question we ask here is if it is possible to arrive at the same classification of interactions from general properties of the force, and not looking to this particular mechanism. This classification would be therefore relevant in the mean field limit, i.e., the limit $N \to \infty$, relevant for the dynamics described by the Vlasov - Poisson equation (1.8).

This classification can be achieved studying the behavior of the probability distribution function $P(F)$ of the force field generated by an *infinite* distribution of matter. The approach was introduced by Chandrasekhar [40], in which he obtained, among other results, that the probability distribution function of the gravitational field corresponds to a Holtsmark distribution. In this context, we are interested on the (eventually divergent) properties of the force because of large scale properties of the system, so we will regularize the two-body force at small scales, when needed, to regularize divergent behaviors in which we are not interested [3]. This assumption implies that $P(F)$, when it exists, is a rapidly decaying function of F. Then, to study the well definiteness of the $P(F)$ it is sufficient to study one of its moments. A natural choice is to study the first non-zero one, the second moment $\langle \mathbf{F}^2 \rangle$.

First, we have to characterize the fluctuations of the density distribution. Assuming that the density consists in a homogeneous background plus fluctuations, i.e., $\rho(\mathbf{r}) =$

3. The Holtsmark distribution behaves as $P(F) \sim F^{-9/2}$ at large F. It is simple to see that this large F behavior, which leads to a divergent variance $\langle F^2 \rangle$ of the force, is caused by the small scale divergence of the two-body interacting force. The variance and all the higher moments are finite when regularizing the two-body force at small scales, see e.g. [41].

$\rho_0 + \delta\rho(\mathbf{r})$, fluctuations can be characterized by the *structure factor* $S(\mathbf{k})$ [4]

$$S(\mathbf{k}) = \lim_{V\to\infty} \frac{\left\langle |\widehat{\delta\rho}(\mathbf{k})|^2 \right\rangle}{\rho_0 V}, \tag{2.27}$$

definition which implies that

$$\lim_{k\to 0} k^d S(\mathbf{k}) = 0 \tag{2.28a}$$

$$\lim_{k\to\infty} S(\mathbf{k}) = 1. \tag{2.28b}$$

Assuming statistical homogeneity (i.e. $S(\mathbf{k}) = S(k)$), we can write that

$$\langle \mathbf{F}^2 \rangle = \frac{1}{2^{d-1}\pi^{d/2}\Gamma(d/2)} \int_0^\infty \mathrm{d}k\, k^{d-1} |\hat{f}_{\mathrm{int}}(k)|^2 S(k)\,, \tag{2.29}$$

where the interparticle force $\mathbf{f}(\mathbf{r})$ has be chosen to be central, i.e., $\mathbf{f}(\mathbf{r}) = f_{\mathrm{int}}(\mathbf{r})\mathbf{r}/r$, and

$$f_{\mathrm{int}}(\mathbf{r}) \sim \frac{g}{r^{\gamma+1}}, \tag{2.30}$$

for $r \to \infty$. Using the property of $S(k)$ (2.28a), we arrive to the same classification of interactions than in the previous section: it is simple to see that the integral converges, independently of $S(k)$ if $\gamma > d-1$, i.e., if the interparticle force (2.30) is absolutely integrable. If it is not absolutely integrable, its Fourier transform can be defined only in the sense of the distributions, and the integrals over space of $f(r)$ should be defined by a symmetric limiting procedure. The force should be calculated therefore as

$$\mathbf{F}(\mathbf{x}) = \lim_{\mu\to 0^+} \lim_{V\to\infty} \int_V \mathrm{d}^d x' \, \frac{\mathbf{x}-\mathbf{x}'}{|\mathbf{x}-\mathbf{x}'|} f_{\mathrm{int}}(|\mathbf{x}-\mathbf{x}'|) e^{-\mu|\mathbf{x}-\mathbf{x}'|} n(\mathbf{x}'). \tag{2.31}$$

Note that the two limits do not commute. This is equivalent to remove the $\mathbf{k} = \mathbf{0}$ vector in Fourier space, which is commonly called the "Jeans swindle" in the literature [42]. Assuming a small k (large r) behavior as $S(k) \sim k^n$ (e.g. in cosmology, the initial $S(k)$, called in this context *power spectrum*, is $S(k) \sim k$, see e.g. [43]) the integral (2.29) converges only for a sub-class (the full-class is given by conditions (2.28)) of stochastic processes such that $n > -d + 2(d-1-\gamma)$. Therefore, it seems that in three-dimensional gravity ($d = 3$, $\gamma = 1$), only the sub-class of processes with $n > -1$ gives a well defined dynamics. However, what matters is the well-definiteness of the *dynamics*, which in a spatially homogeneous distribution with fluctuations is however determined by the *differences of the forces* between two points, rather than the force itself, because there are no preferred points in the system. Performing the same analysis for such a quantity, we obtain that the PDF of the differences of the forces is absolutely convergent for $\gamma > d-2$. This result means that, in the infinite system limit, when $\gamma < d-2$, the

4. The structure factor is defined in a slightly different way in Sect. 3.4.2, in order to match with the definitions in the corresponding papers.

condition of large scale uniformity is violated immediately by the dynamical evolution. The reason is simply that in this case the *rate of growth of a perturbation at a given scale increases with the scale*. The gravitational case is the limiting (logarithmic) one ($\gamma = d - 2$), in which all the scales grow with the same rate; this is the well known behavior of the (same) linear amplification (of all the scales) of fluctuations in cosmology [44].

2.4 Relaxation in two-dimensional gravity

Paper [V].

One motivation to study collisional relaxation in two-dimensional gravity (i.e. $\gamma = 0$, which corresponds to a logarithmic interaction) was the striking relaxation rate $\Gamma\tau_{dyn} \sim N^{-1.35}$ observed in [45]. The authors, however, were not performing full numerical simulations, but quasi one-dimensional ones, in which they imposed radial symmetry for numerical speed-up. Performing full simulations, the relaxation resulted to be the one expected, predicted by the scaling (2.23).

It remains interesting to study this kind of system, which belongs to a different class than gravity in three dimensions, i.e., the relaxation process is dominated by collisions with the largest impact factors allowed in the system. We have modeled the long-time evolution of the system with the simplest Fokker - Planck equation (1.38) possible. We have assumed that the test particles, with velocity distribution $s(v)$, are evolving in a QSS with velocity distribution fixed, corresponding to the thermal equilibrium:

$$p(v) = \mathcal{C}e^{-\beta v^2}. \tag{2.32}$$

This is a much better approximation than in gravity in $d = 3$ dimensions, because in $d = 2$ dimensions, the virial theorem states that the total kinetic energy is constant during the collisional evolution of the system (see [45]), and then the first and second moments of the actual $p(v,t)$ of the system will be correctly described by Eq. (2.32) during the whole evolution of the system. We have then derived the diffusion coefficients in velocity space via the Rosenbluth potentials, in an analogous manner than in the three-dimensional case [46]. In this calculation, the "problem" of the Coulomb logarithm is even worse than in three-dimensional gravity: instead of having a divergence of the form

$$\int_{b_0}^{b_{max}} \frac{\mathrm{d}b}{b} = \ln\left(\frac{b_{max}}{b_0}\right), \tag{2.33}$$

the divergence is dominated by only the large scales, i.e., it is of the form

$$\int_{b_0}^{b_{max}} \mathrm{d}b \simeq b_{max}. \tag{2.34}$$

The effect of the maximum impact factor b_{max} (which is a free parameter in the Chandrasekhar approximation) is then enhanced compared with the gravitational case in $d = 3$

dimensions. For simplicity, we have chosen to work in velocity space instead than in angle-action variables, which introduce a systematic (but small) error in the diffusion coefficients, discussed in the paper [V].

With the approximations listed above, it is possible to write the following Fokker-Planck equation for the velocity distribution $s(v)$, expressed in polar coordinates

$$\frac{\partial s(v)}{\partial t} = C\left\{-\frac{\partial}{\partial v}\left[\left(q'(v)+\frac{p'(v)}{2v^2}\right)s(v)\right]+\frac{1}{2}\frac{\partial^2}{\partial v^2}\left[p''(v)s(v)\right]\right\}, \tag{2.35}$$

where $q(v)$ and $p(v)$ are the Rosenbluth potentials, and C a constant.

We simulated the evolution of the two classes of QSS: "compact" and "core-halo' (see [47] for their definition), from the formation of the QSS to thermal equilibrium, with an N-body code and Eq. (2.35), with the same initial condition. We choose the value of b_{max} in the computation of the Rosenbluth potentials imposing that the N-body system and the one described by Eq. (2.35) converges to thermal equilibrium at the same rate. The value of b_{max} appeared to be independent of the number of particles N but smaller than the size of the system. We will discuss this point in the conclusions of the chapter. Then, we looked at the evolution of the full velocity distribution, and it appeared that it was very well described by Eq. (2.35), see Fig. 2.3, despite all the approximations involved in the approach.

Surprised by the accuracy of the results, we have given in [V] some explanations why the Chandrasekhar approach gave good predictions in this case. We will discuss this point in the conclusions of the chapter.

2.5 Diffusion coefficients in the inhomogenous HMF model

Paper [VI].

The motivations of this work was to check that the kinetic equations derived a few years ago [27] were *(i)* correct and *(ii)* useful, i.e., it was possible to solve them at least in simple models. As a first step, we have chosen the Hamiltonian Mean Field Model (HMF) [48, 49], whose Hamiltonian is

$$H = \sum_{i=1}^{N}\frac{p^2}{2} - \frac{1}{2N}\sum_{i,j=1}^{N}\cos(\theta_i-\theta_j). \tag{2.36}$$

The mean field dynamics corresponds to a real pendulum. Its dynamics and thermodynamics have been widely studied, see e.g. [1, 50] for reviews. The phase-space is constituted by two distinct zones, separated by a *separatrix*. Particles inside the separatrix *oscillate*, whereas particles outside it *librate*. At thermal equilibrium it exhibits a second order phase transition at the inverse temperature $\beta = 2$. For $\beta < 2$, the system is spatially homogeneous, whereas for $\beta > 2$, it is spatially inhomogeneous [49]. In particular, the diffusion coefficients have been calculated for spatially homogeneous systems [51, 52].

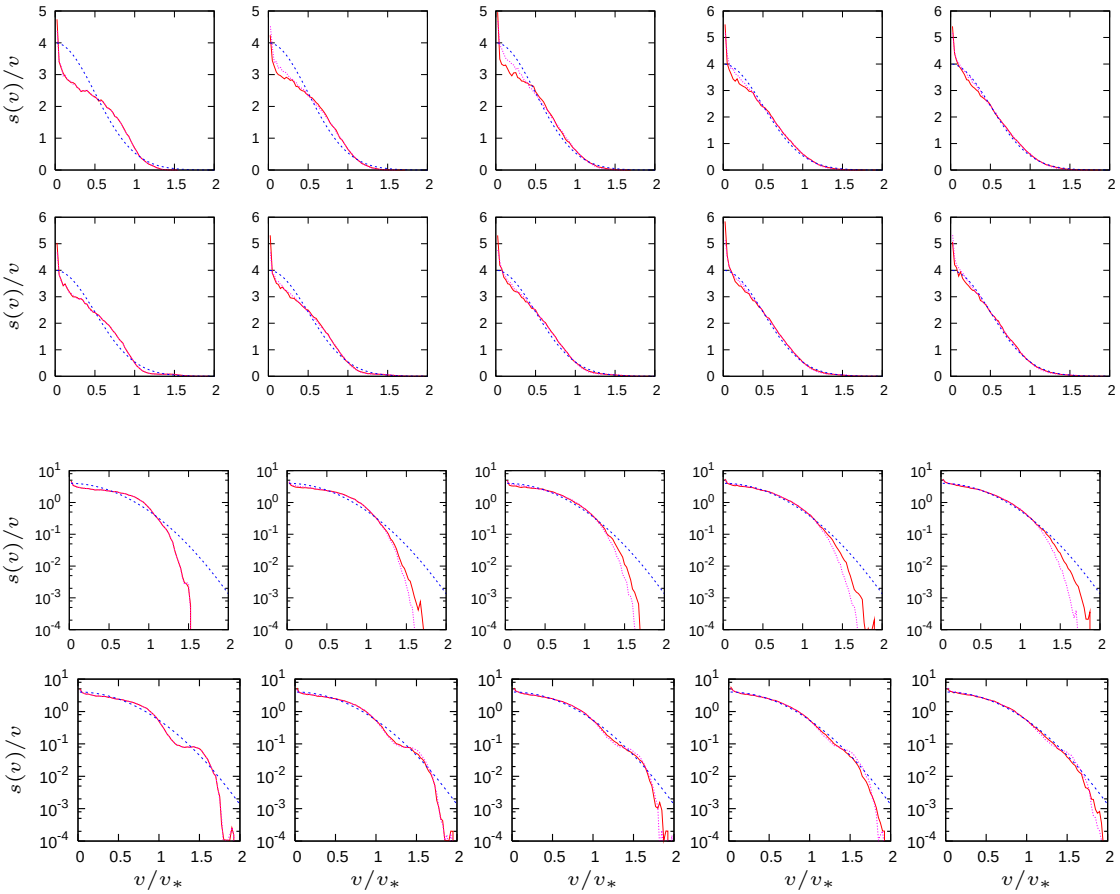

Figure 2.3 – First row of plots: evolution of the velocity pdf normalized to the characteristic velocity v^* for a compact QSS and increasing times from left to right. Second row of plots: evolution of the velocity pdf for a core-halo distribution and increasing times from left to right. The second block of plots are exactly the same but in log-linear scale. The plain red curve represents the simulations, the pink dotted one the theoretical prediction and the blue dashed curve the thermal equilibrium pdf.

The potential of the HMF corresponds to the first harmonic of the Fourier transform of any one-dimensional interaction. Consequently, any mean-field potential in this model can be characterized by only two real numbers. Then, the bi-orthonormal basis Eq. (1.41) has only two elements. In addition, their Fourier transforms with respect to the angles Eq. (1.46) can be computed analytically. We will denote them as the functions $c_n(\kappa)$ and $s_n(\kappa)$, where κ is defined as $\kappa = \sqrt{h/2M_0 + 1/2}$, where $M_0 = \sqrt{M_x^2 + M_y^2}$ is the total magnetization (for the explicit expressions of c_n and s_n see [VI]). This model is therefore ideal as a first step looking for an "exact" solution of kinetic equations of spatially inhomogeneous systems. All the terms in the kinetic equation can be computed

analytically, through Elliptic integrals, except the dielectric tensor

$$\epsilon_{ss}(\omega) = 1 + 2\pi \sum_{\ell=-\infty}^{\infty} \int \mathrm{d}\,\kappa \frac{g_\ell^{ss}(\kappa)}{\Omega(\kappa) - \omega/\ell}, \tag{2.37}$$

which has to be integrated numerically, using the Landau prescription Eq. (1.35). The diffusion coefficients are then expressed as a double sum over integers. The diffusion coefficient can be written as

$$D_{dif}(\kappa) = \frac{2\pi^2}{N} \sum_{n,n'=\infty}^{\infty} \sum_{\kappa^\star} \frac{n^2 |\partial J/\partial\kappa|_{\kappa^\star}}{|D_{nn'}(\kappa, \kappa^\star, n\Omega(\kappa))|^2} \frac{f(\kappa^\star, t)}{\left|n' \frac{\partial\Omega}{\partial\kappa'}\right|_{\kappa^\star}} \tag{2.38}$$

and the polarization coefficient as

$$D_{pol}(\kappa) = \frac{2\pi^2}{N} \sum_{n,n'=-\infty}^{\infty} \sum_{\kappa^\star} \frac{n\,n'}{|D_{nn'}(\kappa, \kappa^\star, n\Omega(\kappa))|^2} \frac{\partial f/\partial\kappa'|_{\kappa^\star}}{\left|n' \frac{\partial\Omega}{\partial\kappa'}\right|_{\kappa^\star}}. \tag{2.39}$$

where κ^* satisfies the condition $n\Omega(\kappa) = n'\Omega(\kappa^*)$, and

$$\frac{1}{D_{nn'}(\kappa, \kappa', \omega)} = \frac{c_n(\kappa) c_{n'}(\kappa')}{\epsilon_{cc}(\omega)} - \frac{s_n(\kappa) s_{n'}(\kappa')}{\epsilon_{ss}(\omega)}. \tag{2.40}$$

Using molecular dynamics simulations we compared the prediction of Eq. (2.38) with different QSS: a system at Maxwell-Boltzmann equilibrium in a range of temperatures from very inhomogenenous to close to homogeneity (see Fig. 2.4), and out of equilibrium but Vlasov-stable (i.e. stable QSS in the limit $N \to \infty$) of a core-halo form, and with and without collective effects ("Lenard-Balescu equation" or "Landau equation" respectively). In all the cases we find a very good agreement between theory and simulations, showing that the kinetic equations describe very well the evolution of the system. In addition, we show that it is possible to compute fully analytically (not reported here, see [VI]) the diffusion coefficients for highly magnetized states.

The approach we have used is not able to describe the diffusion coefficients very close to the separatrix, and in particular the flux of particles through it. This is due that near the separatrix the unperturbed frequencies $\Omega \to 0$, and therefore finite-N fluctuations are not small perturbation of the unperturbed Hamiltonian anymore (see e.g. [24]).

2.6 Goldstone modes in long-range systems

Paper [VII].

The motivation of this work comes from a simple observation: when a magnetized (i.e. inhomogeneous) configuration of the HMF model is at thermal equilibrium, *even if the total momentum of particles is exactly zero*, there is an evolution of the components of the magnetization M_x and M_y with time. This can be at first sight surprising, as

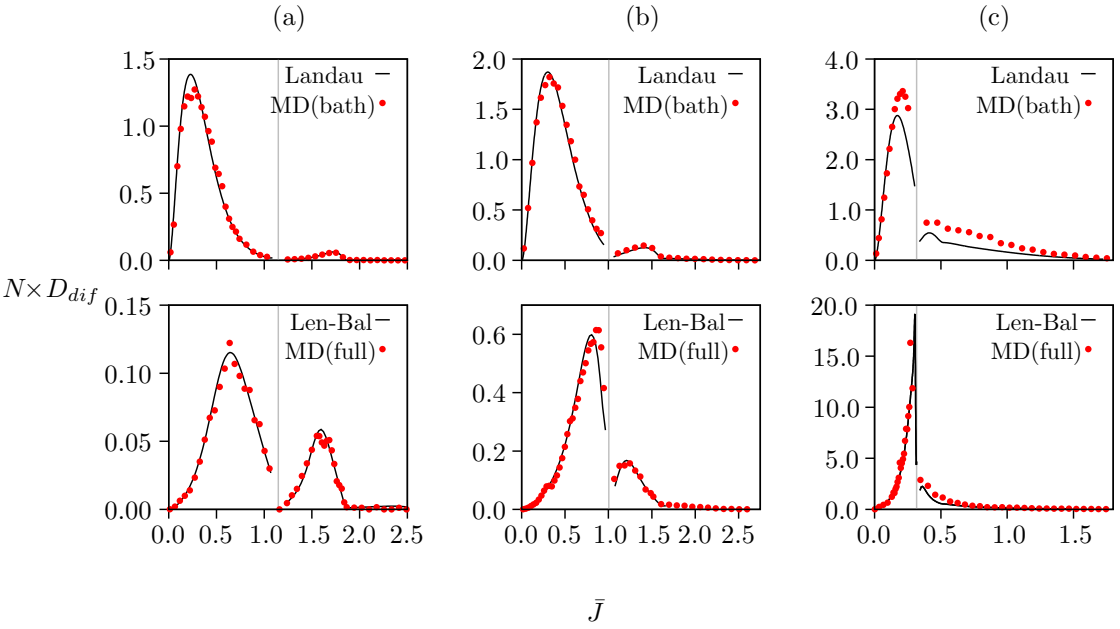

Figure 2.4 – Diffusion coefficients as a function of the averaged action in bins $\bar{J}$, calculated by molecular dynamics, red points, and the equation (2.38), black lines, for a thermal equilibrium distribution, with magnetization M_0 decreasing from left to right (left: high magnetization, very clustered system, right: low magnetization, close to homogeneous system). On the bottom, molecular dynamics simulations without collective effects with the prediction of the Landau equation. On the top, molecular dynamics simulations with collective effects with the theoretical curve predicted by the Lenard-Balescu (Len-Bal) equation and the molecular dynamics given by the regular HMF model – MD(full). The gray vertical line represents the separatrix.

the system at thermal equilibrium is supposed to be stationary. It is in fact related to a spontaneous breaking of the symmetry of the system. The Hamiltonian of the HMF (3.46) has rotational $U(1)$ invariance. Any inhomogenous QSS will break this symmetry by "choosing" a given phase θ_0 of the magnetization $M_0 = M_x + \mathrm{i}M_y$. In the limit $N \to \infty$, the system will remain trapped in this state: as we have seen in the previous chapters, the QSS cannot evolve, and M_x and M_y remain constant. Finite N fluctuations lead the system to explore, with zero cost in energy, all the degenerated space and consequently the magnetization M_0 move around the circle, keeping $|M_0|$ constant. This corresponds to a classical "Goldstone" mode [53, 54, 55]. In this work, we have explored in detail this mechanism for the HMF, for a particular QSS, the ground state, which corresponds to the thermodynamic equilibrium, and in a more qualitative manner for other systems.

In the case of the HMF, instead of looking to the magnetization $M(t)$, it is more

convenient to use as order parameter the center of mass of the particles, defined as

$$\phi(t) = \frac{1}{N}\sum_{i=1}^{N}\theta_i(t), \tag{2.41}$$

where $\theta_i(t)$ is the position of the $i-th$ particle. It is possible to relate the variance of the center of mass with the correlation function of the momentum

$$\begin{aligned}\sigma^2_\phi(t) &= \left\langle \frac{1}{N}\sum_{i=1}^{N}\theta_i(t) \times \frac{1}{N}\sum_{i=j}^{N}\theta_j(t) \right\rangle \\ &= \frac{1}{N^2}\sum_{i,j=1}^{N}\left\langle \int_0^t \mathrm{d}t' p_i(t') \int_0^t \mathrm{d}t'' p_j(t'') \right\rangle \\ &= \frac{t}{N}\int_0^t \mathrm{d}\tau\, \mathcal{C}_p(\tau),\end{aligned} \tag{2.42}$$

where we used the property $\mathcal{C}_p \equiv \langle p(0)p(\tau)\rangle = \langle p(t)p(t+\tau)\rangle$, valid for a stationary state, and $\langle\cdots\rangle$ stands for an average over different realizations for the same (macroscopic) initial state. In Fig. 2.5, left, we show the behavior of the momentum autocorrelation for times much smaller than the relaxation time $t \ll \tau_{coll} \sim N$. After a transient, it converges to the constant value $\tilde{\mathcal{C}}_p$. For times $t \gg \tau_{coll}$, Fig. 2.5, right, the momentum autocorrelation goes to zero. Then, two regimes appear in the problem, as a function

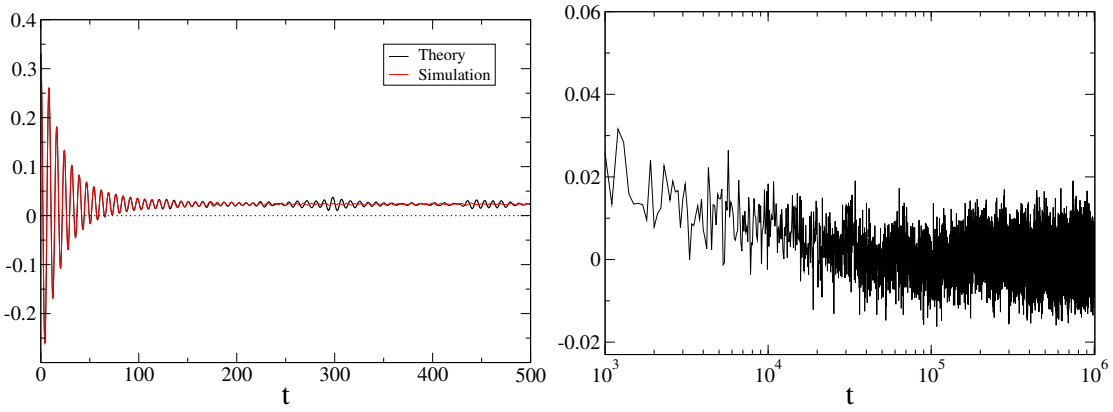

Figure 2.5 – Momentum auto-correlation function $\mathcal{C}_p(t)$. Left: small times. Right: large times. The units of time are $\tau_{dyn} = 1/\sqrt{|M_0|}$.

whether the last integral in Eq. (2.42) has converged or not. Its convergence properties are related to the time of collisional relaxation. Therefore, for $t \ll \tau_{coll}$ we have

$$\sigma^2_\phi(t) = \frac{t}{N}\int_0^t d\tau\, \tilde{\mathcal{C}}_p = \frac{\tilde{\mathcal{C}}_p}{N}t^2. \tag{2.43}$$

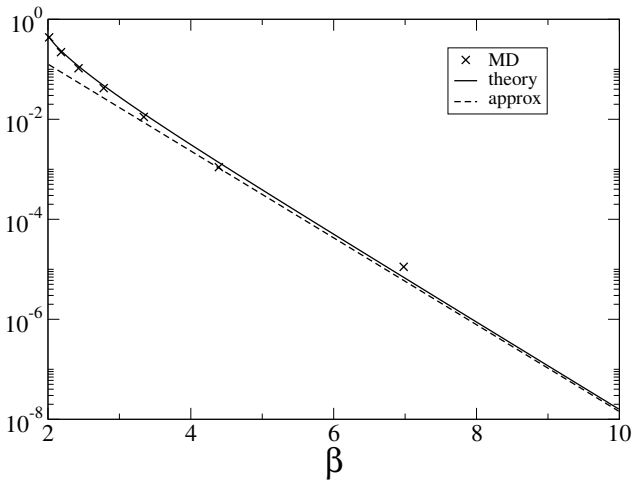

Figure 2.6 – Ballistic diffusion coefficient $\tilde{\mathcal{C}}_p$ from exact analytical calculation, molecular dynamics (MD) simulations, and analytical approximation (2.45).

The process is therefore *ballistic*. For times $t \gg \tau_{coll}$ we have

$$\sigma_\phi^2(t) = \frac{t}{N} \int_0^\infty d\tau \, \mathcal{C}(\tau). \tag{2.44}$$

In this last case the process is therefore *diffusive*. Equations (2.43) and (2.44) are valid for an *unfolded* representation of the system, i.e., when a particle makes a complete rotation its phase θ is increased by 2π.

The mechanism which leads to the ballistic diffusion is explained as follows. At the time the measurement of the diffusion starts to be performed, because of the finite number of the particle, the total momentum of the (librating) particles outside the separatrix is different of zero. As the total momentum of the system is chosen to be zero [5], this means that the total momentum of the (oscillating) particles inside the separatrix has exactly the same magnitude with opposite sign. Consequently, the value of the phase of the particles inside the separatrix is bounded in the unfolded system, whereas those outside the separatrix can increase their value indefinitely. With these ingredients, with a purely statistical calculation, it is possible to compute exactly the value of $\tilde{C}_p$. For sufficiently large β we get the simple expression:

$$\tilde{C}_p \simeq \frac{8N}{\pi} e^{1-2\beta}. \tag{2.45}$$

The variance of the ballistic diffusion decreases with β because the number of particles outside the separatrix also decreases. These results are shown in Fig. 2.6.

The *diffusive* dynamics is driven by particles *crossing* the separatrix. As we have seen in Sect. 2.5, there is still no theory to describe the separatrix crossing. We have

5. If not, a trivial additional global rotation of the system appears.

been then only able to obtain an approximate semi-analytic expression for the diffusion coefficient

$$\sigma_\phi^2(t) \simeq 730 \frac{\tilde{\mathcal{C}}_p}{N}. \tag{2.46}$$

2.7 Conclusions

One important conclusion of this chapter is that kinetic equations applied for inhomogeneous spatial configurations are technically tractable and give very accurate results when compared to numerical simulations, at least for the one-dimensional model we have studied. In addition, for the HMF model, it is possible to compute the diffusion coefficients analytically, for highly magnetized states.

We have seen that the Chandrasekhar approximation works remarkably well, at least qualitatively (i.e. scalings), for a wide range of interactions, for which the relaxation process can be dominated by close or distant encounters, depending of the value of γ. A priori, there are many reasons for which we would expect the Chandrasekhar approximation would give poor results:

1. Collisions are treated as statistically independent, i.e., the noise generated by the finite-N effects is treated as delta-correlated in time. If the noise is not delta-correlated, and treated as such, it is well known that the effect of the noise is over-evaluated [56]. In other words, in order the collisions to be described as independent, it should be a clear separation of the temporal scale between the duration of a collision and its periodicity. We have to focus then on the ratio between the duration of a collision (understood as the localization in space in time of the change in the velocity due to the fluctuations of the mean field) and the period of an orbit. We have shown in [V], that the duration of a collision is given by $t_c \sim b/v$, where b is the impact factor and v the velocity of the particle at the "moment" of the collision, which can be chosen as the time corresponding to the distance of closest approach. The ratio between the duration of the collision and the period of the orbit $\tau_{dyn} \sim R/v$ is then

$$\frac{t_c}{\tau_{dyn}} \sim \frac{b}{R}. \tag{2.47}$$

   We see therefore that for small impact factors compared with the size of the system $b \ll R$, then $t_c \ll \tau_{dyn}$, and the noise can be safely considered as delta-correlated. However, for large impact factors $b \sim R$, then $t_c \sim \tau_{dyn}$, and we expect that treating the noise as correlated is necessary.

2. In addition, when $b \sim R$, even if the noise could be treated as uncorrelated, the change in velocity would be systematically overestimated, because in the Chandrasekhar approximation, the change in the perpendicular velocity is estimated as if the system would be infinite, i.e., taking the limit $R/b \to \infty$ in the integral (see

[III], Appendix, and the discussion in [V]):

$$|\Delta \mathbf{V}_\perp| \propto \int_{-R/b}^{R/b} ds (1+s^2)^{-(\frac{\gamma}{2}+1)}. \tag{2.48}$$

For example, for gravity in $d = 2$ (i.e. $\gamma = 0$), taking $R/b \to \infty$ in Eq. (2.48) for a collision with $R/b \sim 1$ would give an error as much as $\sim 50\%$. For gravity in $d = 3$ (i.e. $\gamma = 1$), the error would be of $\sim 30\%$.

3. Another assumption of the Chandrasekhar approximation is that the impact factors are homogeneously distributed between the minimal impact factor b_{min} and the maximal impact factor b_{max}. This is a valid assumption for a homogeneous system, but it is much less clear in an inhomogenous one. The fact that the scalings (2.24) are verified by simulations indicates that the distribution of impact factors does not depart drastically from homogeneity, e.g., there are not of the form b^α with α some exponent, which would modify the scalings.

A simple argument that would explain, in light of the points listed above, why the Chandrasekhar approximation actually works well, may consist in the fact that most of collisions have a small impact factor compared with the size of the system. This is actually the case in the two-dimensional gravitational system studied in [V]: in Fig. 2.7 left, assuming that the orbits are approximately ellipses, we measure in simulations the ratio of the largest and smaller axis of relative orbit. We see that they are very eccentric, and hence most of collisions have a small impact factor. This is coherent with Fig. 2.7 right, in which we show the radial density of the QSS, and the vertical lines indicates the value of b_{max} taken in the theoretical calculations in order to match with the relaxation rate of the simulations. We observe that the values of b_{max} are smaller than the size of the system, in a manner coherent with the distribution of eccentricities of the relative orbits. In particular, observe how b_{max} is much smaller in the "core-halo" system than in the "compact" one (Fig. 2.7, left), even if the former system is the more spatially extended (Fig. 2.7, right), but with relative orbits with higher eccentricity.

To conclude this chapter, we may give an overview of recent advances and perspectives. The kinetic equations in angle-action variables have been solved for different systems, showing that it is numerically feasible even if it can be very costly numerically [57, 58, 59, 60, 61, 62]. On the other hand, recent studies arrived to the same kind of conclusions than the ones described above - most of collisions have a small impact factor - which may explain why the Chandrasekhar approximations describes more accurately than one might expect collisional relaxation [63]. It would be interesting to revisit, with the current perspective, relaxation in two-dimensional gravity, in which the effects of collisions with large impact factor are magnified compared with three-dimensional gravity, to refine the understanding of the accuracy of the Chandrasekhar approach.

Separatrix crossing in the HMF model is still an unsolved problem, with implications as we have seen in the description of the diffusive regime of Goldstone modes. In addition, a better understanding of the of collective effects would be interesting. For example, it is not understood why in the HMF they decrease the amplitude of the diffusion

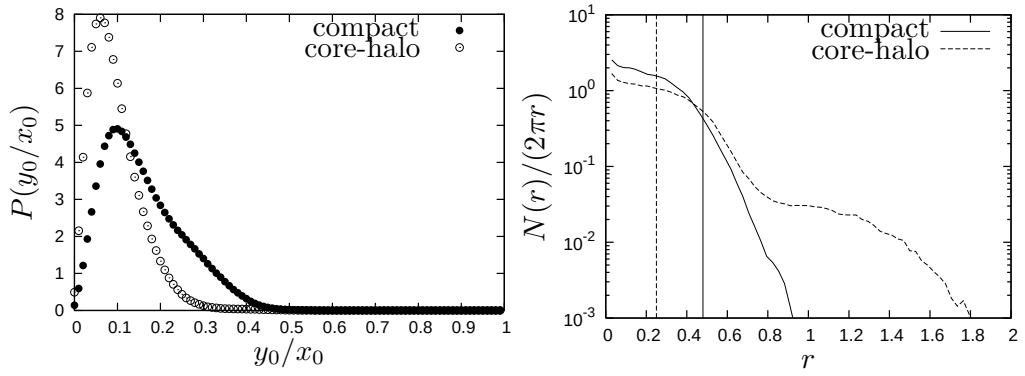

Figure 2.7 – Left: distribution of eccentricities of the relative orbits of the two simulated systems, which correspond to a "compact" and "core-halo" QSS. The eccentricity has been calculated assuming that the relative orbits are ellipses, and defined as the ratio of the axis x_0 and y_0 (with $x_0 \geq y_0$). Right: density profile for the same systems. The vertical lines correspond to the value of b_{max} taken in order the theoretical prediction and the numerical evolution of the system match.

coefficient in very spatially inhomogenous systems but they have the opposite effect in nearly homogeneous or homogeneous configurations (see Fig. 2.4 and [51, 52]). It is also intriguing that the studies of the value of the Coulomb logarithm (i.e. the value of the maximum impact factor b_{max}) using arguments similar to those presented in Sect. 2.2 concluded (like us) that the maximum impact parameter should be of the order of the size of the system, whereas studies based in the stochastic properties of the force (using techniques similar to those explained in Sect. 2.3, including the original paper of Chandrasekhar [64]), concluded that the maximum impact parameter should be of the order of the interparticle distance (e.g. [34, 65]).

3. Analogue long-range systems

This chapter is devoted to the study of analogue long-range systems, with special emphasis in analogue gravitational systems. In the next section we will give an introduction on cold (but classical) atomic systems and in non-linear optical systems. Then, we will describe our contributions using these systems.

3.1 Introduction

One of the difficulties studying self-gravitating systems is that their characteristic dynamical time is so large compared with the duration of human life that we are only able to observe *frozen* systems. Most of the phenomena described in this manuscript, e.g., violent relaxation and collisional relaxation, have been predicted by theory and simulated numerically, but never observed in nature. We can observe only their "consequence", for example that galaxies and globular clusters are not in thermal equilibrium, but in a non-equilibrium stationary state.

There are different systems which exhibit analogue long-range interactions. We can list Bose-Einstein condensates (e.g. [66, 67, 68, 69]), capillary interactions between colloids (e.g. [70]), thermally driven colloids [71], trapped electron plasma [72, 73, 74, 75, 76, 77, 78, 79], quasi-two-dimensional superfluids [80, 81], two-dimensional hydrodynamics [82], experiments using electron rings [83, 84], classical cold atoms [85, 86, 87, 88, 89, 90] and light propagating in thermally induced non-linear media [91, 92, 93, 94]. In this introduction we will describe classical cold atoms systems and light propagating in thermally induced non-linear media, systems we have used in our contributions.

3.1.1 Cold atoms systems

It is possible to create systems of neutral cold (but still classical) atoms using a atomic trap, in which it is induced an analogue coulomb and analogue gravitational-like interaction between the atoms. In the experiments we have collaborated, two kinds of traps have been used: magneto-optic and dipolar traps. We will describe first the basics of the former one, and then of the latter.

Magneto-optic traps (MOTs) are created using pairs of counter-propagating lasers, with frequency ω close to the frequency transition of the atom [95]. The probability that

the atom absorbs a photon depends on the detuning δ between the frequency of the laser and the atomic transition. The atoms are cooled using the Doppler effect: if the atom has a velocity v [1], the atoms "see" the photons with a frequency $\omega + k_L v$, where k_L is the wavenumber of the laser. The strategy of cooling consists in taking $\delta < 0$, which makes the probability of absorbing a photon in the opposite direction of v larger than the reciprocal. Therefore, the radiation pressure slows down the speed of the atom. In addition, a position-dependent magnetic field is applied to the atoms, which creates an effective detuning $\delta_{\text{eff}} = \delta \pm \mu x$. The force on a atom is given therefore by the formula [96]

$$F_{\pm} = \pm \frac{\hbar k \Gamma}{2m} \frac{1}{1 + 4\left(\frac{\delta \mp k v \mp \mu x}{\Gamma}\right)^2} \frac{I_{\pm}(x)}{I_s}, \tag{3.1}$$

where m is the mass of the atoms, $\hbar$ is the reduced Planck constant, I_s the saturation intensity, which measures how much intensity is needed to attain the maximum of the scattering rate, and $I_{\pm}$ is the actual intensity of the lasers at the position x of the cloud of atoms. The "+" sign stands for a laser propagating in the positive direction, the "−" one in the negative one. The total force which feels an atom is $F = \mathrm{F}_+ - F_-$. The attenuation of the laser intensity propagating inside the cloud is given by

$$I_+ = I_0 \exp\left(-\sigma \int_{-\infty}^{x} \mathrm{d}\, x'\, n(x')\right) \tag{3.2a}$$

$$I_- = I_0 \exp\left(-\sigma \int_{x}^{\infty} \mathrm{d}\, x'\, n(x')\right), \tag{3.2b}$$

where $n(x)$ is the normalized density of atoms, I_0 the intensity delivered by the lasers and σ is the absorption cross-section for a cloud of atoms The optical depth is defined as

$$b = \sigma \int_{-\infty}^{+\infty} \mathrm{d}\, x\, n(x). \tag{3.3}$$

The analogue long-range system appears in the $b \ll 1$ regime. In this case, it is possible to expand Eqs. (3.2) in Taylor series, obtaining

$$I_+(x) \simeq I_0 \left(1 - \sigma \int_{-\infty}^{x} \mathrm{d}\, x'\, n(x')\right) \tag{3.4a}$$

$$I_-(x) \simeq I_0 \left(1 - \sigma \int_{x}^{\infty} \mathrm{d}\, x'\, n(x')\right). \tag{3.4b}$$

In addition, the experiment is set in such a way in which velocities are small in the sense $kv/\delta \ll 1$, and the atoms are sufficiently close to the center of the system, following the condition $\mu x/\delta \ll 1$. It is then possible to expand in Taylor series Eq. (3.1) at first order in x and v, and using Eqs. (3.4), we get

$$F(x) = -\eta v - \omega_0^2 x + F_{\mathrm{g}}(x), \tag{3.5}$$

1. For simplicity we will describe the MOT in one spatial dimension.

where

$$\eta = \frac{8\hbar k\Gamma^3 I_0 k\delta}{m\left(\Gamma^2+4\delta^2\right)^2}\frac{I_0}{I_s} \tag{3.6a}$$

$$\omega_0^2 = \frac{8\hbar k\Gamma^3 I_0 \mu\delta}{m\left(\Gamma^2+4\delta^2\right)^2}\frac{I_0}{I_s} \tag{3.6b}$$

$$F_{\mathrm{g}}(x) = \frac{\hbar k\Gamma^3}{2m(\Gamma^2+4\delta^2)}\frac{1}{I_s}\left[I_+(x)-I_-(x)\right]. \tag{3.6c}$$

The first term of Eq. (3.5) corresponds to a friction and the second term to a harmonic confining potential, which functional forms can be computed from Eq. (3.4). The term $F_{\mathrm{g}}(x)$ corresponds to an effective self-gravitating interaction in one dimension:

$$\begin{aligned} I_+(x)-I_-(x) &= \sigma I_0\left[\int_x^\infty \mathrm{d}\,x'\,n(x') - \int_{-\infty}^x \mathrm{d}\,x'\,n(x')\right] \\ &= -\sigma I_0\int_{-\infty}^\infty \mathrm{d}\,x'\,n(x')\mathrm{sign}(x-x'). \end{aligned} \tag{3.7}$$

The last integral corresponds to the force which can be derived from the solution of the Poisson equation in one dimension, i.e.,

$$\frac{d^2\phi}{dx^2}(x) = 2\sigma I_0 n(x). \tag{3.8}$$

It is simple to check that $I_+(x)-I_-(x) = -\phi'(x)$.

Generally, a pair of counter-propagating lasers are used for each spatial dimension. Therefore, for each dimension, we have an expression for the force similar to Eq. (3.7), which does not correspond to a true analog self-gravitational interaction. For simplicity, in the literature (see. e.g. [97]), Eq. (3.8) it is often approximated to

$$\nabla^2\phi(\mathbf{x}) = 2\sigma I_0 n(\mathbf{x}), \tag{3.9}$$

where ∇^2 is the Laplacian in three dimensions. Equation (3.9) corresponds to a truly self-gravitational system, but it is an approximation in this context.

In addition to the self-gravitating like interaction, there is another effective force between the atoms. When an atom absorbs a photon, it will re-emit it by spontaneous emission. The photon will be eventually reabsorbed by another atom, producing an effective repulsive interaction between them. If the optical depth is small, very few photons are scattered more than twice, and this effect of can be approximated as an effective Coulomb repulsion. As the intensity decreases as $1/r^2$, an effective repulsive interaction appears between the atoms [97]

$$\mathbf{F}(\mathbf{r}) = \frac{\sigma\sigma_R}{4\pi c}\int d\mathbf{r}'\,n(\mathbf{r}')\frac{\mathbf{r}-\mathbf{r}'}{|\mathbf{r}-\mathbf{r}'|^3}, \tag{3.10}$$

where c is the speed of the light and σ_R the cross section of the scattered light. The force Eq. (3.10) corresponds *exactly* to an effective Coulomb force.

Dipole traps work in a very similar manner as MOTs. In this case no magnetic field is applied to the atoms, which are trapped using a laser, whose electromagnetic field induces an atomic dipole $\mathbf{d} \propto \mathbf{E}$, which generates an interacting potential

$$U_{dip} \propto \langle \mathbf{d} \cdot \mathbf{E} \rangle \propto I(\mathbf{r}), \tag{3.11}$$

where $I(\mathbf{r})$ is the intensity of the laser. The cooling strategy is the same as in the MOT, using counter-propagating lasers, and all the description above applies for the dipolar trap with the exception that $\mu = 0$ has to be set in Eq. (3.1) and $\eta = 0$ in Eq. (3.5).

3.1.2 Non-linear optical systems

A feature of the cold atomic systems presented above is that they present *noise* and *friction*. This is a problem when seeking to observe the formation of a quasi-stationary state (such as a galaxy), because mixing and violent relaxation are *fragile* processes that only occur in Hamiltonian systems, or at least systems which are sufficiently close to be Hamiltonian.

A very good candidate of a system which is close to be Hamiltonian is laser propagating in a thermo-optical refractive medium [93]. If we consider the coordinate z as the direction of propagation of the laser, the evolution of the amplitude of the beam $\mathcal{E}(x, y, z; t)$ can be written, using the paraxial approximation (see e.g. [98]), as [94]

$$i\partial_z \mathcal{E} + \frac{1}{2k}\nabla_\perp^2 \mathcal{E} + k_0 \Delta n \mathcal{E} + i\frac{\alpha}{2}\mathcal{E} = 0 \tag{3.12a}$$

$$\frac{\rho_0 C}{\kappa}\frac{\partial \Delta n}{\partial t} = \nabla_\perp^2 \Delta n + \frac{\alpha\beta}{\kappa}|\mathcal{E}|^2, \tag{3.12b}$$

where $\nabla_\perp^2$ is the Laplacian in the transverse direction of propagation, k_0 is the wave-vector of the laser, $\rho_0 C$ is the heat capacity per volume, β is the medium thermo-optic coefficient, κ is the thermal conductivity, α the absorption coefficient, $k = n_b k_0$, n_b the background refractive index and Δn the change in refractive index due to the heating of the medium. The paraxial approximation consists in approximating $\nabla_\perp^2 \mathcal{E} \gg \partial^2 \mathcal{E}/\partial z^2$, which is always the case in our setup, as the typical transversal size is of order of the hundred of μm and the typical longitudinal scale of the order of cm. For the same reason, it is possible to approximate safely the Laplacian in Eq. (3.12b) by the transversal Laplacian $\nabla_\perp^2$. For a more detailed discussion, see [99].

For sufficiently long time (of the order of the second for our system), the system described by Eqs. (3.12) attains a stationary state, and therefore $\partial \Delta n/\partial t = 0$. Equations (3.12) become then

$$i\partial_z \mathcal{E} + \frac{1}{2k}\nabla_\perp^2 \mathcal{E} + k_0 \Delta n \mathcal{E} + i\frac{\alpha}{2}\mathcal{E} = 0 \tag{3.13a}$$

$$\nabla_\perp^2 \Delta n = -\frac{\alpha\beta}{\kappa}|\mathcal{E}|^2. \tag{3.13b}$$

It is remarkable that Eqs. (3.13) are formally the same as the ones which describe the evolution of quantum self-gravitating particles:

$$i\hbar\partial_t\Psi + \frac{\hbar^2}{2m}\Delta\Psi + V\Psi = 0 \tag{3.14a}$$

$$\nabla^2 V = -4\pi G m|\Psi|^2, \tag{3.14b}$$

when making the correspondence

$$\begin{aligned} 2d &\longrightarrow 3d \\ \mathcal{E} &\longrightarrow \Psi \\ z &\longrightarrow t \\ \frac{1}{2k} &\longrightarrow \frac{\hbar^2}{2m} \\ \frac{\alpha\beta k_0}{\kappa}\Delta n &\longrightarrow 4\pi G m V \\ \alpha &\longrightarrow 0 \\ P = \int d\mathbf{r}_\perp |\mathcal{E}|^2 &\longrightarrow M = \int d\mathbf{r}|\Psi|^2, \end{aligned} \tag{3.15}$$

where $\hbar$ is the reduced Planck constant, G the gravitational constant, Δ is the Laplace operator, m the mass of a particle, M the total mass of the system and P the power of the laser. The only differences between the two systems is the dimensionality of the system, and the presence of absorption in the optical system. For the former difference, if we are interested in the violent relaxation process, it is well known that it appears in a very similar fashion in $d = 1$, $d = 2$ and $d = 3$ [45, 100]. The absorption term would correspond to a global loss of mass with time. This can be see by performing the Madelung transformation $\Psi(\mathbf{r}, t) = \sqrt{\rho(\mathbf{r}, t)}e^{iS(\mathbf{r},t)/\hbar}$ of Eq. (3.14a), having previously inserted the absorption term of Eq. (3.13a). We get

$$\frac{\partial\rho}{\partial t} + \nabla(\rho\mathbf{u}) + \alpha\rho = 0 \tag{3.16a}$$

$$\frac{\partial\mathbf{u}}{\partial t} + (\mathbf{u}\cdot\nabla)\mathbf{u} = -\frac{1}{m}\nabla(Q - V), \tag{3.16b}$$

where Q is the quantum pressure

$$Q = -\frac{\hbar^2}{2m}\frac{\nabla^2\sqrt{\rho}}{\sqrt{\rho}} \tag{3.17}$$

and $\mathbf{u} = \nabla S/m$. Integrating Eq. (3.16a) over space, and integrating over time, we get

$$\int d\mathbf{r}\rho(\mathbf{r}, t) = M(t) = M_0 e^{-\alpha t}. \tag{3.18}$$

It is worth noting that a very serious model of dark matter in cosmology consists in particles modeled by Eq. (3.14). The reason of the introduction of such quantum particles

is that discrepancies were observed between observations and numerical simulations in the small-scale structure of the universe (e.g. density in excess in the center of the galaxies, what is called the "cuspy halo problem"), discrepancies that can be solved assuming that dark matter particles are bosons with an extremely small mass [101, 102, 103, 104, 105]. This is the so-called "Fuzzy dark matter" model, in which particles are expected to have extremely small masses of the order of $m \sim [10^{-19}, 10^{-22}]$eV [106]. A consequence that particles would have a so small mass is that the thermal De Broglie wavelength would be of the order of galactic scales (and hence orders of magnitude larger than the mean interparticle distance), and therefore the system would be well below the temperature of transition of a Bose - Einstein condensate, very well described by the Schrödinger - Poisson system of equations (3.14) (see e.g. [103, 107] for recent reviews).

3.2 Approximate solutions of the dynamics of long-range systems

Papers [VIII, IX, X].

Finding an exact solution of the Vlasov-Poisson or Schrödinger-Poisson system is almost an impossible task, because the equations are highly non-linear and, in addition, usually in a non-perturbative regime. In this section we will present different simple approximate solutions of these systems, which can be useful to study some problems. These kinds of solutions give a global evolution of the system, using an appropriate ansatz, which is generically some rescaling of the initial condition using a single parameter $\lambda(t)$. From the exact equations of motion, the goal is to obtain an equation for $\lambda(t)$ that will describe the evolution of the original system as accurately as possible.

In the context of MOTs, breathing oscillations, i.e., the lowest mode of oscillations, are an important tool to characterize and understand collective effects. In the literature there were many descriptions of the breathing dynamics, in different contexts and different regimes, see e.g. [108, 109, 110, 111, 112, 113, 114, 115, 116, 117, 118]. The goal of [VIII, IX] was to construct a global framework for different regimes, and test the results using extensive numerical simulations. We will describe here the simplest case without diffusion and friction, the generalization is straightforward (see [IX]). We will focus here on MOTs, i.e. on systems with a confining potential. The system is modeled by the Vlasov equation

$$\frac{\partial f}{\partial t} + \mathbf{v} \cdot \nabla_{\mathbf{r}} f + (\mathbf{F}_{trap} + \mathbf{F}_{int}) \cdot \nabla_{\mathbf{v}} f = 0 \tag{3.19a}$$

$$\mathbf{F}_{trap} = -\omega_0^2 \mathbf{r} \tag{3.19b}$$

$$\mathbf{F}_{int}(\mathbf{r}) = \frac{g}{r^{k+1}} \mathbf{r}, \tag{3.19c}$$

in which we have separated the force into two contributions, an (external) harmonic force due to the trapping mechanism of the MOT and the binary force between the particles, which we will assume to a power-law (g is the coupling constant). In order

to simplify the very complicate dynamics of (3.19a) we will assume that the density $\rho(\mathbf{r},t) = \int d\mathbf{v} f(\mathbf{r},\mathbf{v},t)$ is rescaled, but keeps its shape as time evolves, i.e.

$$\rho(\mathbf{r},t) = \frac{1}{\lambda^d}\rho(\mathbf{r}/\lambda(t), t=0). \tag{3.20}$$

The continuity equation for ρ, which follows from integrating Eq. (3.19a) with respect to $\mathbf{r}$ and $\mathbf{v}$, gives the following constraint over the phase space density f:

$$f(\mathbf{r},\mathbf{v},t) = f(\mathbf{r}/\lambda, \lambda\mathbf{v} - \dot{\lambda}\mathbf{r}, t=0) := f_0(\mathbf{r}/\lambda, \lambda\mathbf{v} - \dot{\lambda}\mathbf{r}). \tag{3.21}$$

We are going to follow a different, more pedagogical, derivation than in the paper. The energy E is a conserved quantity of Vlasov equation, with

$$E = \frac{1}{2}\int d\mathbf{r}d\mathbf{v}\, v^2 f(\mathbf{r},\mathbf{v},t) + \frac{1}{2}\omega_0^2 \int d\mathbf{r}d\mathbf{v}\, r^2 f(\mathbf{r},\mathbf{v},t) + \frac{g}{2}\int d\mathbf{r}d\mathbf{r}'d\mathbf{v}d\mathbf{v}' \frac{f(\mathbf{r},\mathbf{v},t)f(\mathbf{r}',\mathbf{v}',t)}{|\mathbf{r}-\mathbf{r}'|^{k-1}}, \tag{3.22}$$

where we have used the explicit expressions (3.19b) and (3.19c). Using the scaling (3.21) we get the equation for the time derivative of the energy

$$\frac{1}{\dot{\lambda}}\frac{dE}{dt} = -\frac{\langle v^2\rangle_{f_0}}{\lambda^3} + (\ddot{\lambda} + \omega_0^2\lambda)\langle r^2\rangle_{f_0} - \frac{k-1}{\lambda^k}V_{int}(t=0) = 0 \tag{3.23}$$

where $\langle\rangle_{f_0}$ means average over the distribution function f_0, and we have assumed statistical independence between position and velocities, i.e., $\langle \mathbf{r}\cdot\mathbf{v}\rangle_{f_0} = 0$. At this point we can make a further simplification if f_0 is a stationary state of the system, which is of interest in the context of breathing oscillations. This implies that $\lambda = 1$ is a stationary solution of Eq. (3.23), which permits to express V_{int} as a function of $\langle v^2\rangle_{f_0}$ and $\langle r^2\rangle_{f_0}$. Defining

$$p = \frac{\langle v^2\rangle_{f_0}}{\omega_0^2\langle r^2\rangle_{f_0}}, \tag{3.24}$$

we get

$$\ddot{\lambda} + \phi'(\lambda) = 0 \tag{3.25a}$$

$$\phi(\lambda) = \omega_0^2\left(\frac{1}{2}\lambda^2 + \frac{1}{2}\frac{p}{\lambda^2} + \frac{p-1}{1-k}\lambda^{1-k}\right). \tag{3.25b}$$

Equations (3.25) give a very simple, one dimensional, description of the system. The first term of the r.h.s. of Eq. (3.25b) corresponds to a kinetic energy, the second one to a pressure, and the last one to the interaction. It is simple to include a dissipation and a friction (which can depend on the radial position as in MOTs, see [IX]). Comparing the predictions of Eqs. (3.25) with simulations, there is a good overall agreement when the interaction is repulsive, and a good agreement only in the frequency when the interaction is attractive. This is because in the latter case there is violent relaxation in the system,

a phenomenon the ansatz (3.20) is not able to tackle. To illustrate this phenomenon, we show the evolution of different shells of a gaussian initial density

$$\rho(r, t = 0) = \frac{1}{\sqrt{2\pi}} e^{-r^2/2}, \tag{3.26}$$

with no initial velocities, with the interaction (3.19c) with $k = 1$, $\omega_0 = 0$ (no trap) and $g = 1$. We observe (this is a consequence of Gauss theorem) that the different shells do not collapse at the same rate, and at some point they cross each other. This phenomenon will lead to the violent relaxation mechanism, which in spherical systems can be seen as the crossing of different shells of the distribution of matter. The interested reader can find a detailed description of this mechanism in [119], in which we studied the energy ejection during the violent relaxation process of initially spherically homogeneous distributions of matter.

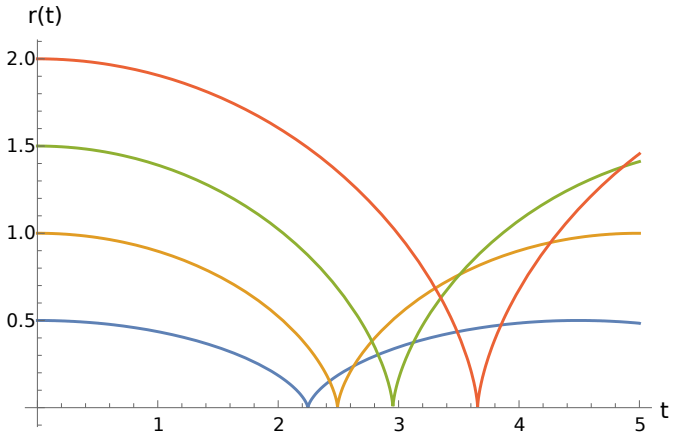

Figure 3.1 – Plot of the distance towards the center of different shells of the initial density distribution (3.26). Observe how shells initially at a larger distance towards the center collapse slower than ones initially closer to the center. If the density would be perfectly homogeneous all the shells would arrive at $r = 0$ exactly at the same time.

It is possible to use the same approach in the framework of the Schrödinger - Poisson equation, with the same scaling ansatz Eq. (3.20) for the density $\rho(\mathbf{r}, t) = |\Psi(\mathbf{r}, t)|^2$. Results in $d = 3$ can be found in [120], which has been generalized to the $d = 2$ case in [99]. In this case the system is not confined in a harmonic potential (introducing it would be straightforward), and only the self-gravity acts on the system. Starting from a spatially Gaussian initial condition, and assuming the ansatz

$$\rho(\mathbf{r}, t) = M \frac{e^{-r^2/\lambda(t)^2}}{\pi \lambda(t)^2}, \tag{3.27}$$

we get the potential

$$\phi(\lambda) = \frac{\hbar^2}{2m^2\lambda^2} + GM \ln \lambda. \tag{3.28}$$

In this case, as the system is supported by the quantum pressure (3.17), it is possible to obtain a closed equation (in this case the quantum system is somewhat simpler than its semi-classical limit). When approaching the semi-classical limit, the difficulties described above in closing the hierarchy of equations appear.

It is possible to generalize these results for ellipsoidal systems and obtain analytical results in two dimensions. In a different context, but it is worth citing here because it shares the same ideas, in [X] we studied the symmetry breaking in the collapse of initially homogeneous systems. In d dimensions the gravitational force inside an homogeneous ellipsoid (see [121]) can be written as

$$F_i(x_1, x_2, \ldots, x_d) = -\frac{d}{2} x_i \int_0^\infty \frac{ds}{(x_i^2 + s)\prod_{j=1}^d \sqrt{x_j^2 + s}}. \tag{3.29}$$

In $d = 2$, Eq. (3.29) has an analytical solution, which permits to write an explicit equation for the "envelope" of the $i - th$ coordinate of the position of the particle distribution $X_i(t) = 2\sqrt{\langle x_i^2 \rangle}$

$$\ddot{X}_i = \frac{\epsilon_i}{X_i^3} - \frac{2}{X_1 + X_2}, \tag{3.30}$$

where the *emmitances* ϵ_i are conserved quantities during the dynamics. In $d \neq 2$ the integral (3.29) has to be performed numerically. Starting from a slightly asymmetric initial conditions, the study of the bifurcations of Eq. (3.30) permitted us to predict the presence or absence of symmetry breaking in the collapse of homogeneous self-gravitating systems as a function of the initial temperature.

3.3 Systems with non-potential forces

Paper [XI].

When forces derive from a potential, this has many consequences, as the conservation of the energy. There are models in which an effective force does not derive from a potential. This is e.g. the case in the MOT system described in Sect. 3.1. For systems in $d = 2$ spatial dimensions the force reads:

$$F_x[\rho](x, y) = -C \int \mathrm{sgn}(x - x')\rho(x', y)\, dx' \tag{3.31a}$$

$$F_y[\rho](x, y) = -C \int \mathrm{sgn}(y - y')\rho(x, y')\, dy', \tag{3.31b}$$

where C are constants. Although the forces (3.31) would derive from a potential if the system would be in $d = 1$ (i.e. considering solely Eq. (3.31a) or Eq. (3.31b)), the forces defined by Eqs. (3.31) do not derive from a potential. These kind of forces are shared in other systems, such as active matter (see e.g. [71]).

The existence of an equilibrium is an interesting theoretical problem. In our context, the system is over-damped; it is then described by the Smoluchowski equation, which in adimensional units reads (see [XI] for the details):

$$\frac{\partial \rho}{\partial t} = \nabla \cdot \mathbf{J} \tag{3.32a}$$

$$\mathbf{J} = \mathbf{r}\rho - \mathbf{F}[\rho]\rho + \Theta \nabla \rho. \tag{3.32b}$$

If the interparticle force derive from a potential, then automatically $\mathbf{F}[\rho]$ would derive also from a potential, i.e., $\mathbf{F} = -\nabla U$. It is straightforward to see that a solution of Eq. (3.32) is $\mathbf{J} = \mathbf{0}$ and $\rho = e^{-U_T/\Theta}$, with $U_T = (U + r^2/2)$. If $\mathbf{F}$ does not derive from a potential, the situation is much more complex, and it is impossible to find a simple solution of (3.32). In addition, a flux $\mathbf{J} \neq \mathbf{0}$ must appear in the system: if $\mathbf{F}$ does not derive from a potential, its general expression is $\mathbf{F} = -\nabla U + \nabla \times \mathbf{A}$, where $\mathbf{A}$ is a potential vector. Then, the only term of the r.h.s. of (3.32) which is not curl-free is $\nabla \times \mathbf{A}$, and it cannot be compensated by any other term of the r.h.s., which are curl-free. Then, automatically $\mathbf{J} \neq \mathbf{0}$.

The questions we addressed in this work, is *(i)* the existence of an equilibrium configuration, *(ii)* in the affirmative case, how are the fluxes and *iii)* if it exists a non-equilibrium phase transition to a collapse state. In the case of two dimensional gravity (i.e. the same divergence in the interaction but no curl component of the force), there is a phase transition at $\Theta = 4$ when the system is not in presence of a harmonic potential [45].

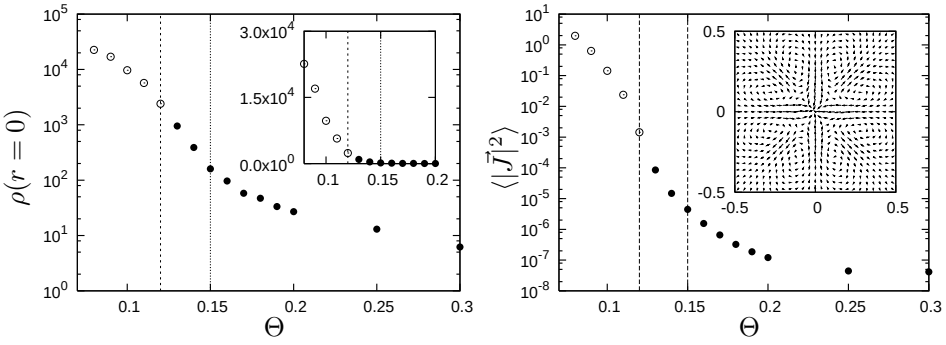

Figure 3.2 – Left: density ρ at the center of the trap, as a function of the reduced temperature Θ. Filled (empty) points correspond to simulations which (do not) have numerically converged with respect to the time step, which indicates a catastrophic collapse. *Inset*: Same quantity plotted in linear-linear scale. Right: Spatially averaged square intensity of the currents as a function of Θ. The vertical dashed lines indicates the numerically estimated location of the transition region *Inset*: Spatial distribution of current $\mathbf{J}$ in the stationary state; $\Theta = 0.2$. The laser beams are along the axes of the figure.

From a theoretical point of view, it is possible to show that the entropy $S(t) = -\int \rho \ln \rho$ can decrease without bound only if $\Theta < 0.17$, which gives a hint of the existence

and the temperature of transition. Studying numerically the system, we have found, as shown in Fig. 3.2 a transition in the range of temperatures $\Theta \in [0.12, 015]$ (indicated between the vertical lines), and the presence of fluxes in the system.

An experimental realization of this work was performed subsequently [122]. Unfortunately, the non-equilibrium phase transition was "smeared" by the particles escaping in the third dimension. This work remains, in our opinion, interesting from the theoretical point of view, and can potentially be applied to other non-potential systems.

3.4 Experimental realization of long-range systems with cold atoms

In this section we will describe the experimental realization of two analogue long-range systems: the first one, an analogue one-dimensional self-gravitating system at thermal equilibrium, and the second one, an analogue one-component plasma.

3.4.1 Analogue one-dimensional system at thermal equilibrium

Paper [XII].

We have seen in Sect. 3.1 that in a system of cold atoms, when some conditions on the experimental parameters are met (in particular sufficiently small velocity of the atoms and small optical depth b), there are two analogue forces in the system: an analogue one-dimensional self-gravitating force per pair of lasers (which we have seen in Sect. 3.3 it does not derive from a potential), and an analogue Coulomb force. If the system is very elongated (i.e. quasi-one-dimensional), then *(i)* the analogue self-gravitating force derives from a potential and *(ii)* the analogue Coulomb force (which in $d = 3$ dimensions dominates [97]) becomes negligible because photons escape in the perpendicular directions of the one-dimensional cloud.

The experiment was performed using a dipole trap, described in Sect. 3.1. We observed different indications compatible with the presence of a self-gravitating analogue system of particles at thermal equilibrium:

— The longitudinal size of the cloud decreases as $1/N$ as the number of particles is increased, which indicates a long-range interaction (not necessarily gravity, however).

— The density profile was measured, obtaining profiles that were compatible with interacting forces $|\mathbf{f}(r)| = 1/r^{\alpha}$, with $\alpha \in [0, 1]$ ($\alpha = 0$ corresponds to gravity in $d = 1$).

— The frequency of breathing oscillations was studied using Eqs. (3.25), obtaining results compatible with the range $\alpha \in [0, 1]$.

These results are encouraging, even though do not demonstrate that the system is truly self-gravitating. A careful analysis of the experimental parameters shows that the small velocity regime is not fulfilled, which implies that the friction coefficient would depend

on the velocity (see Eqs. (3.1), (3.4)), as well as the small optical depth requirement (we have indeed $b \sim 0.5$). In practice, we do not completely control the model we are "simulating" experimentally. For a detailed analysis see [123].

3.4.2 Attempt to measure the Debye length in an analogue one-component plasma

Paper [XIII].

In three-dimensional cold atoms clouds, the repulsive Coulomb-like interaction dominates over the self-gravitating-like one, which makes it analogous to a *one component plasma* (OCP) [124]. The OCP consists in an idealized spatially infinite homogeneous configuration of charged particles, embedded in a negative neutralizing background. In the experiment, the trap takes the role of this background. The OCP is characterized to be a super-homogeneous distribution of particles, i.e., the variance of the number of particles in a sphere of radius R grows as R^4, instead of R^3 in a poissonian distribution (see e.g. [125]). It is convenient to define the structure factor $S(\mathbf{k})$, as the Fourier transform of the density as

$$S(\mathbf{k}) = \frac{1}{N} \left\langle |\hat{\rho}(\mathbf{k})|^2 \right\rangle . \tag{3.33}$$

The intensity of the light in diffracted experiments is proportional to $S(k)$ (see e.g. [124]). In the case of the OCP, at sufficiently high temperature, $S(k)$ can be calculated very simply with the Debye-Hückel theory, obtaining

$$S(k) = N\delta(k) + \frac{k^2}{k^2 + \kappa_D^2}, \tag{3.34}$$

where κ_D is the inverse of the Debye length $\lambda_D = 1/\kappa_D$. Except the peak at the origin, (which corresponds to the auto-correlation of the particles), the structure factor goes to zero as $k \to 0$: this is a manifestation of super-homogeneity [125].

The goal to this experimental work is to observe the Debye length, i.e., two-point correlations, in an atomic Coulomb-like system. We will see however that, despite measuring the $S(k)$ in the OCP is relatively simple (the first measurement were done back in the 70's [126]), the difficulty here is that the cloud of atoms is not spatially homogeneous, and the leading contribution of the structure factor would be the density of the cloud itself (hence a one-point correlation), instead of two-point correlations. In other words, the peak localized at $k = 0$ in Eq. (3.34) (corresponding to a homogeneous distribution) would be "smeared out" up to a wavenumber $k \sim 2\pi/L$, where L is the size of the cloud. In the experiment we expect theoretically $\lambda_D/L \sim 0.05$ (for an expected value of $\lambda_D \approx 100\mu$m), which does not give a sufficient separation of scales to be observable experimentally, taking into account the signal-noise ratio in the experiment.

A different approach was taken, consisting in detecting the signature of the correlations in the cloud in the response to an external potential with modulation wavelength k_e:

$$\phi_{ext} = A \sin(k_e x). \tag{3.35}$$

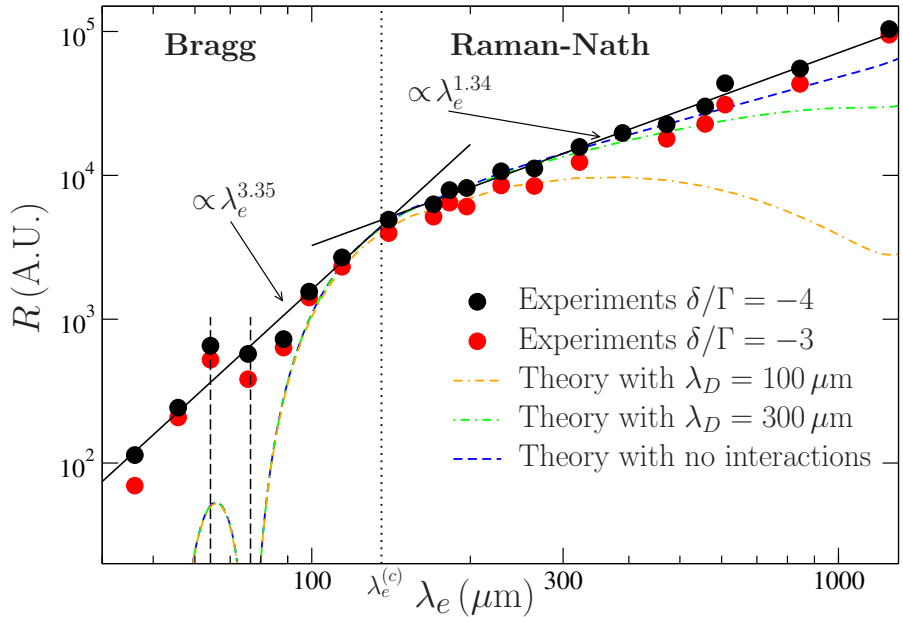

Figure 3.3 – Comparison of the total diffracted power $R(\lambda_e)$ in the experiment (for two different detunings) and theory (lines). The vertical line indicated the crossover between the two diffraction regimes.

At linear order, fluctuations generated in the potential are

$$\delta\rho \simeq \frac{A}{k_B T}\frac{k_e^2}{k_e^2+\kappa_D^2}\sin(k_e x)\rho_0, \tag{3.36}$$

where ρ_0 is the unperturbed potential. The diffraction of a plane wave $e^{ik_z z}$ through the distribution (3.36) presents two different regimes. The density fluctuations (3.36) indicates that the incident beam diffracts over fluctuations of size $\sim \lambda_e = 2\pi/k_e$ separated by a distance λ_e. After being diffracted by the individual atoms, the beam spreads, and if there is no enough cloud in the z direction, they will not be a subsequent interference before the beam exits the cloud. In this case the condition $k_z L \ll 1$ is satisfied, and it corresponds to the Raman-Nath regime [127]. In this regime, there is no effects of the density ρ_0, as all the diffraction process are driven by the fluctuations of size $\sim \pi/k_e$. If $k_z L \gg 1$, the diffracted beam can interact before finishing to cross the cloud, and there would be density effects. This is the Bragg regime [127]. These two regimes can be seen in Fig. 3.3, in which we plot the theoretical curves (for different possible values of λ_D, and experimental points). Unfortunately, the signature of λ_D does not appear in the experimental points, and therefore no Debye length can be identified in the system.

A last attempt to determine the presence of a Debye length taking advantage that an indirect signature of the Debye length is present in the tails of the density profile. This is however very model-dependent. Comparing numerical simulations and experiment, we

found tails compatible with $\lambda_D \sim 1$mm, much larger than the estimates, and that would explain that it was impossible to detect it in Fig. 3.3.

To conclude, we note that, once again in this experiment the optical depth is not small but $b \sim 1$. This can be a possible explanation of our results.

3.5 Observation of violent relaxation

Paper [XIV].

As we have seen in Chapter 1, violent relaxation is the essential mechanism which leads to the formation of Quasi-Stationary states, such as galaxies. However, this phenomenon has never been observed. The reason for this is that *(i)* in astrophysical systems, the typical dynamical time is of the order of millions of years, and obviously the dynamics is frozen at the human timescale, and *(ii)* in analogue systems, such as the ones we have described in this chapter, noise prevents their formations.

In this section we will describe the observation of violent relaxation in a non-linear self-focusing medium, system described in Sect. 3.1.2. We are going first to describe precisely the regime in which the experiment has been performed, then some theoretical and experimental details, and finally the experiment. At the end of the chapter we will discuss some aspects on numerical methods.

3.5.1 Different regimes

Let us discuss the different regimes of a system described by Eqs. (3.13) or (3.14), as a function of the "quantumness" of the system. In the deep quantum regime, the system tends to form a "soliton" (see e.g. [128]), defined as a stationary structure which forms as a result of the balance of the self-focusing (the analogue of the self-gravity) and the quantum pressure. Solitons are solutions of the stationary Schrödinger - Poisson equation. In this case the density ρ can be schematized by the picture of Fig. 3.4, left. There is a single scale in the system, the size of the soliton ξ. Close to the semi-classical limit, the stationary structure is not a soliton anymore but a QSS, which is not a solution of the stationary Schrödinger-Poisson equation, but a "weak" stationary solution of the Schrödinger - Poisson system in the semi-classical limit. It is schematized in Fig. 3.4, right. Now there are two spatial scales in the system: the minimal wavelength, the De Broglie wavelength in the quantum mechanical context, and the size s of the QSS.

We stress that the experiment described in the manuscript is in this latter regime, very differently from previous experiments involving analogue "boson stars" [93, 94], which are in the former regime. In the experimental system described by Eqs.(3.13) it is possible to control the degree of "quantumness" by varying the size of the initial condition, or the power of the laser. We define the parameter χ, which measures the distance to the semi-classical limit (which is attained for $\chi \to 0$):

$$\chi \propto \frac{1}{s\sqrt{P}}, \tag{3.37}$$

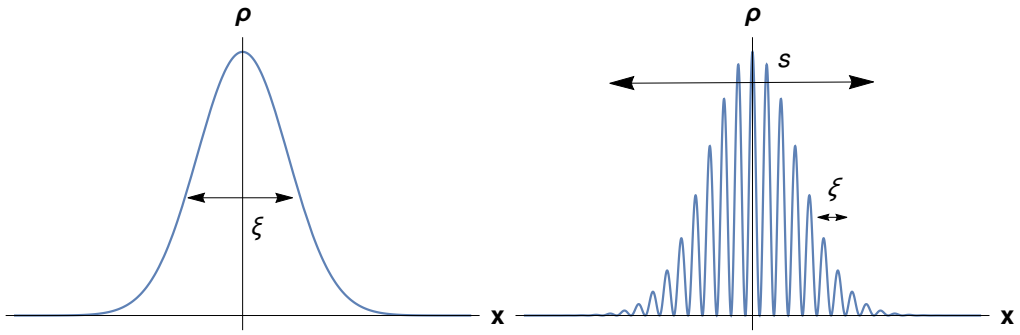

Figure 3.4 – Left: modulus of the wavefunction in the deep quantum regime. Right: the same quantity close to the semi-classical limit.

where P is the power of the laser and s the waist (transversal size) of the beam. Therefore varying s or P we can vary the degree of 'quantumness". It is then possible to "simulate" systems from the deep quantum regime to close to the semi-classical one.

3.5.2 Some points about the experiment

— The astrophysical system is three dimensional and the optical one bi-dimensional. This is the main difference between them. However, we have seen in this manuscript that gravitational systems, in different dimensions, have the same behavior. In particular violent relaxation will be present in all dimensions, with a very similar manifestation (see e.g. [45, 100]).

— There are losses in the system because the laser is attenuated during its propagation (see Eq. (3.18)) [2]. In our setup, we loose a total of 50% of the power because of losses. Even though the absorption modify the dynamics of the system, violent relaxation will continue to be present in it.

— There is a practical difficulty: how to measure the *evolution* of the amplitude of the beam as a function of the longitudinal coordinate z (analogue of the time t) *inside* the medium? Experimentally, we are able to measure the intensity and phase only at the end of the medium. One possibility would be to make a measurement, then saw the medium to shorten its longitudinal size, make another measurement and so on. This is obviously not practical experimentally. A different solution consists in using an invariance of the Schrödinger - Newton equation in the *semi-classical regime*. In this regime, in Eq. (3.14), with initial conditions the Gaussian

$$\mathcal{E}(\mathbf{r}_\perp, z=0) \;=\; A\, e^{-\frac{r_\perp^2}{2s^2}}\, e^{-ik_0 \frac{r_\perp^2}{2f}}, \tag{3.38}$$

2. In our experiment setup, there is in addition reflections at the interfaces air-crystal, as the medium is composed of three aligned pieces of glass. At the end of the last crystal there is a loss of $\sim 25\%$ of the initial power because of the reflections alone. These reflections could be mitigated filling the gap between the crystals with a liquid with a index of refraction close to the one of the crystal.

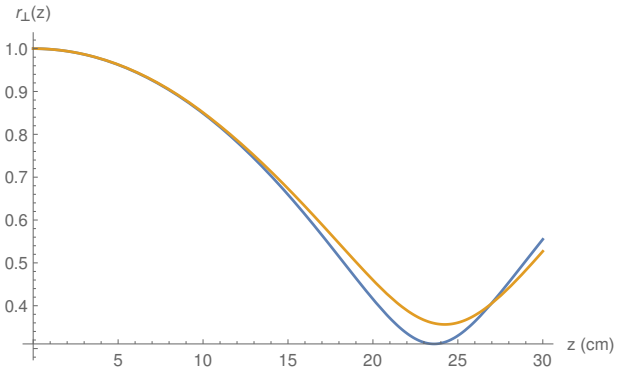

Figure 3.5 – Evolution of the transversal size of the beam normalized to the initial size, with and without losses (yellow and blue curve respectively).

there are three characteristic scales in the system, which we will take as s, k_0/f, and the typical scale in the longitudinal direction $z_{dyn} \propto s/\sqrt{P}$ (quantum effects would give a fourth scale). In the experiment we have chosen to keep s constant and to take $k_0/f \to 0$. We denote by $\mathcal{E}(\mathbf{r}_\perp, z; P)$ the amplitude in the transversal plane $\mathbf{r}_\perp$ of the laser at a distance z, when the incident laser has a power P. Then, we have the exact relation in the semi-classical limit for the evolution of the beam written in polar form $\mathcal{E}(\vec{r}_\perp, z; P) = \sqrt{I(\mathbf{r}, z; P)} e^{\mathrm{i}S(\vec{r}_\perp, z; P)}$

$$I(\vec{r}_\perp, z = L; \lambda^2 P_{max}) = \lambda^2 I(\vec{r}_\perp, z = \lambda L; P_{max}) \tag{3.39a}$$

$$S(\vec{r}_\perp, z = L; \lambda^2 P_{max}) = \lambda S(\vec{r}_\perp, z = \lambda L; P_{max}), \tag{3.39b}$$

where $z = L$ is the end of the medium, P_{max} the maximum available power and $\lambda \in [0, 1]$. The r.h.s. of Eq. (3.39) is what we want to measure, and the l.h.s what we can measure easily.

— Because there are losses in the system, the scalings (3.39) are only approximately verified. In Fig. 3.5 we plot the average size of the system, calculated with the variational method described in Sect. 3.2, with all the losses present in the experiment: three aligned pieces of medium of length 10cm, with reflection transmission coefficient of 0.92 between each interface medium/air, an absorption coefficient $\alpha = 1\mathrm{m}^{-1}$, and the power set up in order to have the maximum collapse close to the end of the medium. We see that losses do not modify drastically the dynamics of the system.

— One can define a local energy density of the optical system as

$$\mathcal{U}(\mathbf{r}_\perp, z) = \frac{|\nabla_\perp \mathcal{E}(\mathbf{r}_\perp, z)|^2}{2k\,|\mathcal{E}(\mathbf{r}_\perp, z)|^2} - k_0 \Delta n(\mathbf{r}_\perp, z). \tag{3.40}$$

The first contribution corresponds to the kinetic (linear) energy density $\mathcal{K}(\mathbf{r}_\perp, z)$, the second one to the potential (nonlinear) energy density $\mathcal{V}(\mathbf{r}_\perp, z)$. Note that this

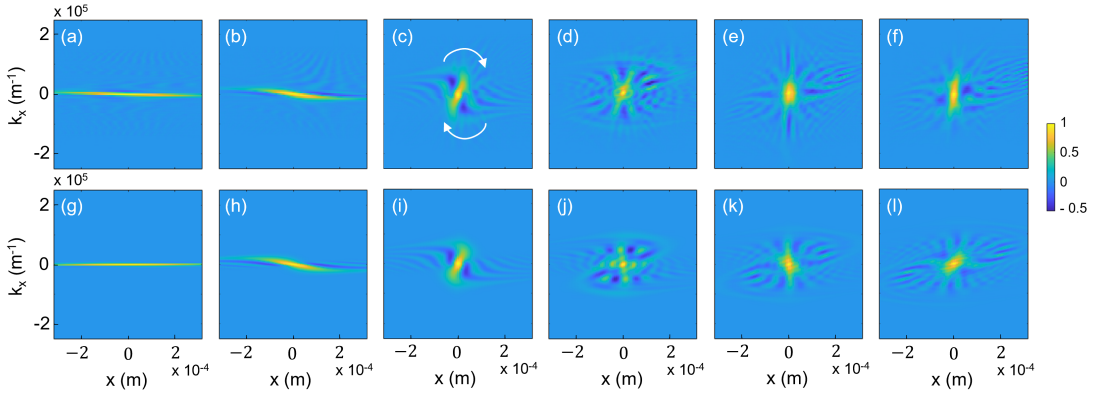

Figure 3.6 – Results of experiment / numerics (top / bottom) for the $y = 0, k_y = 0$ profiles of the Wigner distribution at different input powers: (a) $P = 0.2$W, (b) $P = 1$W, (c) $P = 2$W, (d) $P = 3$W, (e) $P = 4$W, (f) $P = 5$W.

energy is not the physical one (e.g. the energy carried by the photons), it is the energy associated to Eqs. (3.13).

— The total energy

$$E = \int d\mathbf{r}_\perp \mathcal{E}^*(\mathbf{r}_\perp, z) \left[-\frac{\nabla_\perp^2}{2k} - \frac{k_0}{2} \Delta n(\mathbf{r}_\perp, z) \right] \mathcal{E}(\mathbf{r}_\perp, z) \tag{3.41}$$

is a conserved quantity (if losses are neglected).

— We define a phase space representation $F(\boldsymbol{r}_\perp, \boldsymbol{k}_\perp, z)$ of the optical field $\mathcal{E}$ via the Wigner transform [129], i.e., the density of probability to find a portion of the optical beam at the position $\boldsymbol{r}_\perp$ with wave-vector $\boldsymbol{k}_\perp$. It is analogous to the semi-classical phase-space $(\mathbf{r}, \mathbf{v})$.

3.5.3 Observation of mixing and violent relaxation

Paper [XIV].

Mixing can be observed visually with the evolution of phase space increasing P (remember the mapping $z \propto \sqrt{P}$). The experimental results, appear in Fig. 3.6, observing a good agreement between experience and simulation. Filamentation is well visible up to $P = 2$W, for larger powers, because of the interference in the Wigner transform [3], it is not visible anymore in the figure.

To observe violent relaxation, its natural signature (and even for some authors its definition [2]) is the evolution (and subsequent stabilization) of the energy distribution, defined from Eq. (3.40). The change of the energy distribution can have three origins: *(i)*

3. Using other kind of transform such as Husimi gives the same kind of interference.

violent relaxation *(ii)* quantum (non-zero χ effects) and *(iii)* losses. Because the system is sufficient close to the semi-classical regime (i.e. χ sufficiently small), the change of energy because of finite-χ effects is negligible (see [XIV], Appendix). The effect of the losses is non negligible, but they only modify the details of the violent relaxation process (see [XIV], Appendix). To characterize the presence of violent relaxation in the system is therefore sufficient to compare experience with simulations. We can see in Fig. 3.7 a reasonable agreement, in [XIV] can be found details of slices of the energy distribution for different values of P. We observe that most of the energy density changes between $P = 0$ and $P \approx 2$W, which corresponds to the moment in which most of the violent relaxation process occurs. We stress that there is no causality relation between the intensity $\mathcal{E}$ at different P because they correspond to different experiments. Therefore, experimental fluctuation observed at some P cannot be causally propagated at a larger P, showing the robustness of the experiment.

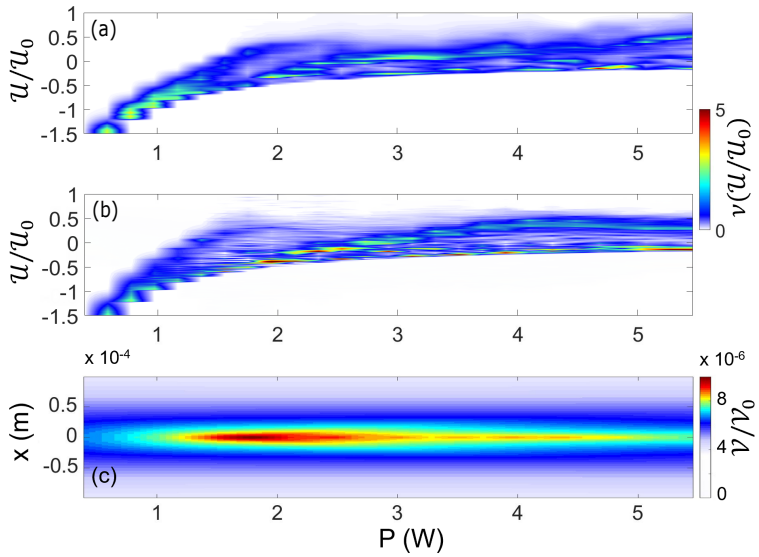

Figure 3.7 – Distribution of energy density map $\nu(\mathcal{U}/\mathcal{U}_0)$ for the experiment (a) and simulation (b). The energy density units are $\mathcal{U}_0 = (\alpha\beta k_0 P) / (2\pi\kappa)$. (c) Numerical $y = 0$ slice of the normalized potential $\mathcal{V}/\mathcal{V}_0$, computed at $z = L$, as a function of transverse coordinate x and power P, ($\mathcal{V}_0 = k_0 P$).

3.6 Numerical methods

Paper [XV, XVI].

There are two important classes of time integrators of Schrödinger-like equations: integrating factor and split-steps algorithms.

The first one is based in integrating exactly the linear part of the equation. First, we write the Schrödinger equation in Fourier space:

$$\mathrm{i}\,\partial_t\,\widehat{\psi} \;-\; \frac{1}{2}\,k^2\,\widehat{\psi} \;-\; \widehat{V\psi} \;=\; 0. \tag{3.42}$$

Then, performing the change of variable $\phi(\boldsymbol{k},t) = \widehat{\psi}(\boldsymbol{k},t)\,\mathrm{e}^{\mathrm{i}k^2(t-t_0)/2}$, which is equivalent to integrate exactly the (linear) kinetic operator, one obtains

$$\partial_t\,\phi \;=\; -\mathrm{i}\,\mathrm{e}^{\mathrm{i}k^2(t-t_0)/2}\;\widehat{V\psi}\,. \tag{3.43}$$

Equation (3.43) is integrated with a Runge-Kutta method. Even if this method is non symplectic, energy conservation can be achieved up to machine precision integrating with sufficient accuracy.

The split-step class of integrators are based on separating the linear terms from the nonlinear ones, in a different manner compared with the integrating factor [130]. The formal solution of the Schrödinger equation can be written as

$$\psi(\boldsymbol{r},t) \;=\; \exp\!\left[-\mathrm{i}\int_{t_0}^{t}(K+V)\;\mathrm{d}t\right]\psi(\boldsymbol{r},t_0), \tag{3.44}$$

where $K = -\frac{1}{2}\nabla^2$. The Split-Step algorithm consists, using the Baker–Campbell–Hausdorff formula, in writing the exponential of (3.45) as a product of exponentials (the Laplacian ∇^2 and the potential V do not commute in general). For example, the approximation corresponding to the Split-Step method of order 2 is

$$\mathrm{e}^{-\mathrm{i}\int_{t_0}^{t}H\,\mathrm{d}t} \;=\; \mathrm{e}^{-\mathrm{i}K(t-t_0)/2}\,\mathrm{e}^{-\mathrm{i}\int_{t_0}^{t}V\,\mathrm{d}t}\,\mathrm{e}^{-\mathrm{i}K(t-t_0)/2} \;+\; O\left((t-t_0)^2\right). \tag{3.45}$$

The integrating factor method has proven to be extremely performing for different systems, such as the non-linear Schrödinger equation [131], but there was no literature on their performance when long-range interactions are present in the system. Motivated by this lack in the literature, we performed in [XV] a systematic study of a comparison of the performance of both integrators, for the Non-Linear Schrödinger Equation (local interaction, $V = |\psi|^2$) and Schrödinger- Poisson (non-local interaction), in one and two spatial dimensions, open or periodic boundary conditions. In the latter case, when Poisson equation is integrated, the $k = 0$ is removed to ensure convergence of the potential. This is physically justified in the case of neutral systems (see Sect. 3.4), or in an expanding universe in cosmology (see e.g. [44]).

The conclusion is that in short-ranged systems (i.e. Non-Linear Schrödinger), the integrating factor technique performs always better (by a factor 1.5–3). For long-range systems (i.e. Schrödinger - Poisson), split-step methods perform slightly better, except for periodical systems in which the integrating factor performs better. This latter result may be explained by the fact that the $k = 0$ is removed in the calculation of the potential, and therefore the system becomes actually less long-range. In addition, we emphasize that using at least a fourth-order split-step method speed-ups simulations by a factor 10 to 100 compared with the very used split-step order of order two.

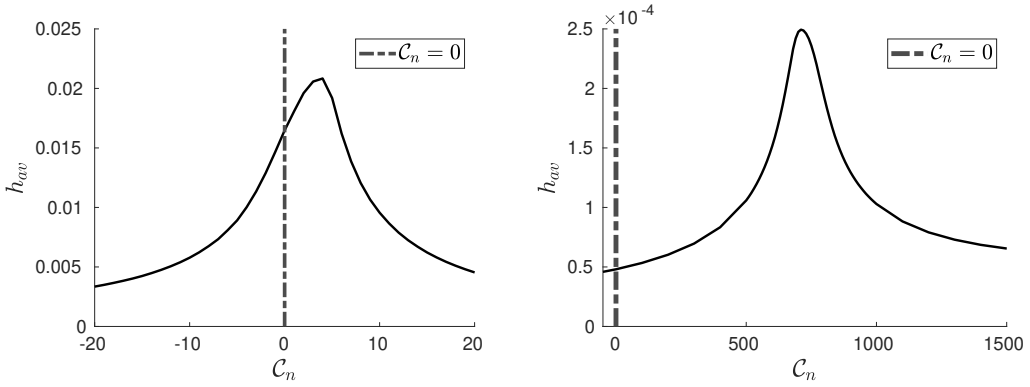

Figure 3.8 – Average time-step $h_{av} = \frac{1}{N_h}\sum_{n=1}^{N_h} h_n$ with a constant $\mathcal{C}_n$ for the IF method applied to the one dimensional Non-Linear Schrödinger (left) and Schrödinger - Newton (right) equations.

In addition, it was observed performing the numerical tests that, in the case of the integrating factor, the choice of the gauge (the constant) of the potential has great impact in the performance of the algorithm. In [XVI] we have seen that it is possible to exploit the gauge invariance of the Schrödinger equation to speed-up the numerical time-integration. The idea is to use the fact that the function $\Psi = \psi\, \mathrm{e}^{-\mathrm{i}\mathcal{C}t}$ is a solution of

$$\mathrm{i}\,\partial_t\,\Psi \;+\; \frac{1}{2}\,\nabla^2\Psi \;-\; (V+\mathcal{C})\;\Psi \;=\; 0, \tag{3.46}$$

if ψ is a solution of (3.46) with $\mathcal{C} = 0$. Thus, if at each time-step a constant $\mathcal{C}_n$ to V is added in (3.42), it modifies the final solution in the trivial manner

$$\psi(t_n) \;\rightarrow\; \psi(t_n)\,\mathrm{e}^{-\mathrm{i}\varphi}, \qquad \varphi \;=\; \sum_{j=1}^{n} \mathcal{C}_j\, h_j, \tag{3.47}$$

where $h_j = t_{j+1} - t_j$ is the j-th time-step. It is therefore possible to look for an optimal value of $\mathcal{C}_n$ which speeds up the computation without modifying the final result. We have calculated analytically the optimal value of $\mathcal{C}_n$ which maximizes the size of the time-step imposing the error between the solution of the order considered and the error of the solution of one order higher to be minimal, which is exactly the procedure in adaptive time-stepping algorithms to determine the size of time steps. In Fig. 3.8 we show an example of the average size of the time-step as a function of the choice of $\mathcal{C}_n$. Note that the value of $\mathcal{C} = 0$ is given by the boundary conditions, and then a simulation with $\mathcal{C} = 0$ can be faster or slower "by chance". Finding the optimal value of $\mathcal{C}_n$ can be computationally expensive. We have shown that choosing a value of $\mathcal{C}_n$ which minimizes the L_2-norm of the r.h.s. of Eq. (3.43) (having replaced V by $V + \mathcal{C}_n$), gives an approximate optimal value of $\mathcal{C}_n$, which is computationally very inexpensive.

3.7 Conclusions

We have seen in this chapter that experiments which mimic long-range interacting systems, and in particular non-relativistic gravity, are possible to be realized. They can be a tool to demonstrate that phenomena that have been only theorized (by calculations and/or simulations) have a real existence, such as violent relaxation. In addition, such experiments can be a vector to share ideas and methods between fields that are usually not connected, for instance between astrophysics, cold atoms, and non-linear optics. One can also think in such systems to perform "hardware" simulations, i.e., to simulate the system with an experiment instead of performing numerical simulations. For example, preliminary simulations have shown that it is possible to reproduce the formation of the large scale structure in a Fuzzy Dark Matter model with an experiment very similar to the one presented in Sect. 3.5, the expansion of the universe being mimicked with the phase of the laser. Simulations of such systems are computationally very expensive, current state-of-the-art simulations use a ratio between the largest and smaller scales simulated of the order $\sim 10^{-6}$ [132]. Hardware simulations do not have limitations on resolution as a telescope can be used to explore smaller and smaller parts of the systems. The resolution in the hardware simulations is limited by the ratio of the size of the system and the soliton size. In the case of the simulations presented in [132], this ratio is of the order $\sim 10^{-3}$, to be compared with the ratio $\sim 10^{-2}$ in the experiment presented in Sect. 3.5. With high power lasers of $\sim$ 100W, it would be possible to attain currently the same ratio. These "simulations" could permit in future the study of high resolution phenomena difficult to attain in numerical simulations.

A. Publications

The papers discussed in this manuscript are indicated with an asterisk.

Research articles published in international journals with refeering process:

1. *"Causality constraints on fluctuations in cosmology: a study with exactly solvable one dimensional models"*, A. Gabrielli, M. Joyce, B. Marcos and P.Viot, Europhys. Lett., **66**, 1 (2004).
2. *"A method of generating initial conditions for cosmological N body simulations"*, M. Joyce, D. Levesque and B. Marcos, Phys. Rev. D, **72**, 103509 (2005).
3. *"Gravitational evolution of a perturbed lattice and its fluid limit"*, M. Joyce, B. Marcos, A. Gabrielli, T. Baertschiger, F. Sylos Labini, Phys. Rev. Lett. **95**, 011304 (2005).
4. *"Linear perturbative theory of the discrete cosmological N-body problem"*, B. Marcos, T. Baertschiger, M. Joyce, A. Gabrielli, F. Sylos Labini, Phys. Rev. D **73**, 103507 (2006).
5. *"Force distribution in a randomly perturbed lattice of identical particles with* $1/r^2$ *pair interaction"*, A. Gabrielli, T. Baertschiger, M. Joyce, B. Marcos, F. Sylos Labini, Phys. Rev. E, 74, 021110 (2006).
6. *"Quantification of discreteness effects in cosmological N-body simulations: I. Initial Conditions"*, M. Joyce and B. Marcos, Phys. Rev. D **75**, 063516 (2007).
7. *"Quantification of discreteness effects in cosmological N-body simulations: II. Evolution up to shell crossing."*, M. Joyce and B. Marcos, Phys. Rev. D **76**, 103505 (2007).
8. *"Gravitational dynamics of an infinite shuffled lattice: early time evolution and universality of non-linear correlations"*, T. Baertschiger, M. Joyce, F. Sylos Labini and B. Marcos, Phys. Rev. E**77**, 051114 (2008).
9. *"Particle linear theory on a self-gravitating perturbed cubic Bravais lattice."*, B. Marcos, Phys. Rev. D043536, (2008).

10. *"Towards quantitative control on discreteness error in the non-linear regime of cosmological N-body simulations"* , M. Joyce, B. Marcos and T. Baertschiger, Mon. Not. R. Astron. Soc. 394, 791 (2009).
11. *"Energy ejection in the collapse of a cold spherical self-gravitating cloud"*, M. Joyce, B. Marcos and F. Sylos Labini, Mon. Not. R. Astron. Soc. 397, 775 (2009)
12. * *"Breathing mode for systems of interacting particles"*, A. Olivetti, J. Barré, B. Marcos, F. Bouchet, R. Kaiser, Phys. Rev. Lett. 103, 224301 (2009) .
13. * *"Breathing Dynamics for Systems of Interacting Particles in the Microcanonical and Canonical Descriptions"*, A. Olivetti, J. Barré, B. Marcos, F. Bouchet and R. Kaiser, Transp. Theo. and Stat. Phys. 39, 524 (2010).
14. * *"A dynamical classification of the range of pair interactions"*, A. Gabrielli, M. Joyce, B. Marcos, F. Sicard, J. Stat. Phys., **141**, 970 (2010).
15. * *"Quasi-stationary states and the range of pair interactions"*, A. Gabrielli, M. Joyce, B. Marcos, Phys. Rev. Lett, 105, 210602 (2010).
16. * *"Symmetry Breaking in d-Dimensional Self-Gravitating Systems"*, R. Pakter, B. Marcos, Y. Levin, Physical Review Letters **111**, 230603 (2013).
17. * *"Collisional relaxation of two-dimensional self-gravitating systems"*, B. Marcos, Physical Review. E, **88**, 032112 (2013).
18. * *"Long-range one-dimensional gravitational-like interaction in a neutral atomic cold gas"*, M. Chalony, J. Barré, B. Marcos A. Olivetti,D. Wilkowski, **87**, 013401 (2013).
19. * *"Nonequilibrium Phase Transition with Gravitational-like Interaction in a Cloud of Cold Atoms"*, J. Barré, B. Marcos D. Wilkowski, Physical Review Letters, **112**, 133001 (2014).
20. *"Self-similarity and stable clustering in a family of scale-free cosmologie"* , D. Benhaiem, M. Joyce, B. Marcos, Monthly Notices of the Royal Astronomical Society , **443**, 2126 (2014).
21. * *"Collisional relaxation in the inhomogeneous Hamiltonian-Mean-Field model: diffusion coefficients"*, F. Benetti et B. Marcos, Phys. Rev. E **95**, 022111 (2017).
22. * *"Formation and relaxation of quasi-stationary states in particle systems with power law interactions"*, B. Marcos, A. Gabrielli and M. Joyce, Phys. Rev. E **96**, 032102 (2017).
23. *"Two-temperature Brownian dynamics of a particle in a confining potential"*, V. Mancois, B. Marcos, P. Viot, and D. Wilkowski, Phys. Rev. E **97**, 052121 (2018).
24. * *"Series expansions of the deflection angle in the scattering problem for power-law potentials"*, D. Chiron and B. Marcos, J. Math. Phys. **60**, 052901 (2019).
25. * *"Towards a measurement of the Debye length in very large Magneto-Optical traps"*, J. Barré, R. Kaiser, G. Labeyrie, B. Marcos and D. Metivier, Phys. Rev. A **100**, 013624 (2019).

26. * *"Classical Goldstone modes in Long-Range Interacting Systems"*, T. M. Rocha Filho and B. Marcos, Phys. Rev. E **102**, 032122 (2020).
27. * *"Optimized integrating factor technique for Schrödinger-like equations"*, M. Lovisetto, D. Clamond, B. Marcos, Applied Numerical Mathematics, **178**, 329 (2022).

Proceedings published in international journals with refeering process:

1. *"Vlasov limit and discreteness effects in cosmological N-body simulations"*, Bruno Marcos, Journal of Computational Physics, **13**, 119 (2008).
2. B. Marcos, A. Gabrielli, M. Joyce, *"Relaxation of quasi-stationary states in long-range interacting systems and a classification of the range of pair interactions"*, Central European Journal of Physics, **10**, 676 (2012).

Proceedings published in books:

1. *"Perturbative treatment of the cosmological N-body problem"*, B. Marcos, Proceedings of the Albert Einstein Century International Conference, AIP Conference Proceedings Volume **861** (2006).
2. *"Cold spherical collapse revisited"*, M. Joyce, B. Marcos and F. Sylos Labini, proceedings of "The Invisible Universe", international conference in Paris, July 2009.
3. *"Mass Ejection and Vlasov-Poisson Limit in the Collapse of a Cold Spherical Self-Gravitating Cloud"*, M. Joyce, B. Marcos, F. Sylos-Labini, Proceedings of the Twelfth Marcel Grossmann Meeting on General Relativity, World Scientific, Singapore, 2011.
4. *"Quasi-stationary states and a classification of the range of pair interactions"*, A. Gabrielli, M. Joyce and B. Marcos, Proceedings of Non-Equilibrium Statistical Physics Today, AIP Conference Proceedings, American Institute of Physics, 2011.

Preprints :

1. * *"Experimental observation of violent relaxation and the formation of out-of-equilibrium quasi-stationary states"*, M. Lovisetto, M.C. Braidotti, R. Prizia, C. Michel, D. Clamond, M. Bellec, E.M. Wright, B. Marcos and D. Faccio, `arXiv:2205.10948`.
2. * *"Integrating factor techniques applied to the Schrödinger-like quations. Comparison with Split-Step methods"*, M. Lovisetto, D. Clamond, B. Marcos, `hal-03483942`.

Bibliography

[1] A. Campa, T. Dauxois, and S. Ruffo, "Statistical mechanics and dynamics of solvable models with long-range interactions," *Physics Reports*, vol. 480, no. 3, pp. 57–159, 2009.

[2] J. Binney, "Discreteness effects in cosmological n-body simulations," *Mon. Not. Roy. Astron. Soc.*, vol. 350, no. 3, p. 939, 2004.

[3] D. Lynden-Bell, "Statistical mechanics of violent relaxation in stellar systems," *Monthly Notices of the Royal Astronomical Society*, vol. 136, p. 101, 1967.

[4] J. Tanekusa, "Statistical theory of violent relaxation," PASJ, vol. 39, pp. 425–436, Jan. 1987.

[5] P. de Buyl, D. Mukamel, and S. Ruffo, "Statistical mechanics of collisionless relaxation in a non-interacting system.," *Philos. Trans. R. Soc. London, Ser. A*, vol. 369, no. 1935, pp. 439–52, 2011.

[6] M. Assllani, D. Fanelli, A. Turchi, T. Carletti, and X. Leoncini, "Statistical theory of quasistationary states beyond the single water-bag case study," *Phys. Rev. E*, vol. 85, no. 2, p. 021148, 2012.

[7] T. Teles, Y. Levin, and R. Pakter, "Statistical mechanics of 1D self-gravitating systems: the core-halo distribution," *Mon. Not. R. Astron. Soc.*, vol. 417, pp. L21–L25, 2011.

[8] R. Pakter and Y. Levin, "Core-Halo Distribution in the Hamiltonian Mean-Field Model," *Phys. Rev. Lett.*, vol. 106, p. 200603, 2011.

[9] G. Giachetti and L. Casetti, "Violent relaxation in the Hamiltonian mean field model: I. Cold collapse and effective dissipation," *Journal of Statistical Mechanics: Theory and Experiment*, vol. 4, p. 043201, Apr. 2019.

[10] A. Santini, G. Giachetti, and L. Casetti, "Violent relaxation in the Hamiltonian mean field model: II. Non-equilibrium phase diagrams," *Journal of Statistical Mechanics: Theory and Experiment*, vol. 2022, p. 013210, Jan. 2022.

[11] R. Balescu, *Statistical Mechanics. Matter out of equilibrium.* London: Imperial College Press, 1997.

[12] S. Chandrasekhar, "The time relaxation of stellar systems," *Astrophy. J.*, vol. 93, p. 285, 1941.

[13] L. D. Landau and E. M. Lifshitz, *Mechanics*. Oxford: Butterworth-Heinemann, 1976.

[14] I. V. Sideris and H. E. Kandrup, "Noise-enhanced parametric resonance in perturbed galaxies," *The Astrophysical Journal*, vol. 602, p. 678, feb 2004.

[15] A. A. Vedenov, E. P. Velikhov, and R. Z. Sagdeev, "Stability of plasma," *Soviet Physics Uspekhi*, vol. 4, pp. 332–369, feb 1961.

[16] W. E. Drummond and D. Pines, "Non-linear stability of plasma oscillations," *Nucl. Fusion Suppl.*, vol. 3, p. 1049, 1962.

[17] P. H. Chavanis, "Kinetic theory of spatially homogeneous systems with long-range interactions: I. General results," *European Physical Journal Plus*, vol. 127, p. 19, Feb. 2012.

[18] J. Marsden and M. Hoffman, *Basic Complex Analysis*. W. H. Freeman, 1999.

[19] L. D. Landau, "On the vibrations of the electronic plasma," *J. Phys. (USSR)*, vol. 10, pp. 25–34, 1946.

[20] L. Landau, E. Lifshitz, and L. Pitaevskij, *Course of theoretical physics. vol. 10: Physical kinetics*. Oxford, 1981.

[21] E. M. Lifshitz and L. P. Pitaevskii, *Physical Kinetics*. Oxford: Pergamon Press, 1981.

[22] P.-H. Chavanis, "Kinetic theory of spatially homogeneous systems with long-range interactions: II. Historic and basic equations," *European Physical Journal Plus*, vol. 128, p. 126, Oct. 2013.

[23] J. Binney and S. Tremaine, *Galactic Dynamics*. Princeton University Press, 2008.

[24] A. Lichtenberg and A. Lieberman, *Regular and Chaotic Dynamics*. Applied Mathematical Sciences, Springer, 2010.

[25] B. V. Chirikov, "A universal instability of many-dimensional oscillator systems," *Physics Reports*, vol. 52, no. 5, pp. 263–379, 1979.

[26] A. J. Kalnajs, "Dynamics of Flat Galaxies. II. Biorthonormal Surface Density-Potential Pairs for Finite Disks," ApJ, vol. 205, pp. 745–750, May 1976.

[27] J. Heyvaerts, "A Balescu-Lenard-type kinetic equation for the collisional evolution of stable self-gravitating systems," *Mon. Not. R. Astr. Soc.*, vol. 407, pp. 355–372, Sept. 2010.

[28] P.-H. Chavanis, "Kinetic theory of long-range interacting systems with angle-action variables and collective effects," *Physica A Statistical Mechanics and its Applications*, vol. 391, pp. 3680–3701, July 2012.

[29] J. Barré, D. Mukamel, and S. Ruffo, "Inequivalence of ensembles in a system with long-range interactions," *Phys. Rev. Lett.*, vol. 87, p. 030601, Jun 2001.

[30] H. M. Mott-Smith, "Collision Trajectories for Inverse Power Intermolecular Potentials," *Physics of Fluids*, vol. 3, pp. 721–724, Sept. 1960.

[31] H. Friedrich, *Scattering Theory*. 872, Springer-Verlag Berlin Heidelberg, 2013.

[32] V. Springel, "The cosmological simulation code gadget-2," *Monthly Notices of the Royal Astronomical Society*, vol. 364, pp. 1105–1134, Dec. 2005.

[33] S. Chandrasekhar, *Principles of stellar dynamics*. Chicago: University of Chicago Press, 1942.

[34] H. E. Kandrup, "Stochastic gravitational fluctuations in a self-consistent mean field theory," Phys. Rep., vol. 63, pp. 1–59, July 1980.

[35] H. Smith, Jr., "Mass segregation, relaxation, and the Coulomb logarithm in N-body systems," ApJ, vol. 398, pp. 519–524, Oct. 1992.

[36] L. Spitzer, Jr. and M. H. Hart, "Random Gravitational Encounters and the Evolution of Spherical Systems. I. Method," ApJ, vol. 164, pp. 399–+, Mar. 1971.

[37] R. T. Farouki and E. E. Salpeter, "Mass segregation, relaxation, and the Coulomb logarithm in N-body systems," ApJ, vol. 253, pp. 512–519, Feb. 1982.

[38] R. T. Farouki and E. E. Salpeter, "Mass segregation, relaxation, and the Couloumb logarithm in N-body systems (again)," ApJ, vol. 427, pp. 676–683, June 1994.

[39] C. Theis, "Two-body relaxation in softened potentials," *Astron. Astrophys.*, vol. 330, pp. 1180–1189, Feb. 1998.

[40] S. Chandrasekhar, "Stochastic problems in physics and astronomy," *Rev. Mod. Phys.*, vol. 15, p. 1, 1943.

[41] P. H. Chavanis, "Statistics of the gravitational force in various dimensions of space: from gaussian to lévy laws," *The European Physical Journal B*, vol. 70, pp. 413–433, jul 2009.

[42] M. K.-H. Kiessling, "The Jeans swindle; A true story — mathematically speaking," *Adv. Appl. Math.*, vol. 31, pp. 132–149, 2003.

[43] J. A. Peacock, *Cosmological Physics*. Cambridge: Cambridge University Press, 1999.

[44] P. Peebles, *The Large-Scale structure of the Universe*. Princeton: Princeton University Press, 1980.

[45] T. N. Teles, Y. Levin, R. Pakter, and F. B. Rizzato, "Statistical mechanics of unbound two-dimensional self-gravitating systems," *Journal of Statistical Mechanics: Theory and Experiment*, vol. 5, p. 7, May 2010.

[46] M. N. Rosenbluth, W. M. MacDonald, and D. L. Judd, "Fokker-planck equation for an inverse-square force," *Phys. Rev.*, vol. 107, pp. 1–6, Jul 1957.

[47] Y. Levin, R. Pakter, F. B. Rizzato, T. N. Teles, and F. P. d. C. Benetti, "Nonequilibrium Statistical Mechanics of Systems with Long-Range Interactions: Ubiquity of Core-Halo Distributions," *Phys. Reports*, vol. 535, p. 1, Oct. 2014.

[48] C. N. C. Pichon, *Dynamics of self-gravitating disks*. PhD thesis, University of Cambridge, UK, Jan. 1994.

[49] M. Antoni and S. Ruffo, "Clustering and relaxation in hamiltonian long-range dynamics," *Phys. Rev. E*, vol. 52, pp. 2361–2374, Sep 1995.

[50] T. Dauxois, S. Ruffo, E. Arimondo, and M. Wilkens, *Dynamics and Thermodynamics of Systems with Long Range Interactions*. Berlin: Springer, 2002.

[51] F. Bouchet, "Stochastic process of equilibrium fluctuations of a system with long-range interactions," *Phys. Rev. E*, vol. 70, p. 036113, Sep 2004.

[52] F. Bouchet and T. Dauxois, "Prediction of anomalous diffusion and algebraic relaxations for long-range interacting systems, using classical statistical mechanics," *Phys. Rev. E*, vol. 72, p. 045103, Oct 2005.

[53] J. Goldstone, "Field Theories with Superconductor Solutions," *Nuovo Cim.*, vol. 19, pp. 154–164, 1961.

[54] J. Goldstone, A. Salam, and S. Weinberg, "Broken symmetries," *Phys. Rev.*, vol. 127, pp. 965–970, Aug 1962.

[55] C. Gruber and P. A. Martin, *Goldstone theorem in Statistical mechanics*. Springer, 1981.

[56] H. E. Kandrup, I. V. Pogorelov, and I. V. Sideris, "Chaotic mixing in noisy Hamiltonian systems," MNRAS, vol. 311, pp. 719–732, Feb. 2000.

[57] J.-B. Fouvry, C. Pichon, and S. Prunet, "Secular resonant dressed orbital diffusion – i. method and wkb limit for tepid discs," *Monthly Notices of the Royal Astronomical Society*, vol. 449, no. 2, pp. 1967–1981, 2015.

[58] J.-B. Fouvry and C. Pichon, "Secular resonant dressed orbital diffusion – ii. application to an isolated self-similar tepid galactic disc," *Monthly Notices of the Royal Astronomical Society*, vol. 449, no. 2, pp. 1982–1995, 2015.

[59] J. B. Fouvry, C. Pichon, and P. H. Chavanis, "Secular diffusion in discrete self-gravitating tepid discs. I. Analytic solution in the tightly wound limit," A&A, vol. 581, p. A139, Sept. 2015.

[60] J. B. Fouvry, C. Pichon, J. Magorrian, and P. H. Chavanis, "Secular diffusion in discrete self-gravitating tepid discs II. Accounting for swing amplification via the matrix method," A&A, vol. 584, p. A129, Dec. 2015.

[61] J.-B. Fouvry, C. Pichon, and P.-H. Chavanis, "Secular diffusion in discrete self-gravitating tepid discs III. Resonant thickening in the tightly wound limit," *arXiv e-prints*, p. arXiv:1605.03384, May 2016.

[62] M. Roule, J.-B. Fouvry, C. Pichon, and P.-H. Chavanis, "Long-term relaxation of one-dimensional self-gravitating systems," Phys. Rev. E, vol. 106, p. 044118, Oct. 2022.

[63] J.-B. Fouvry, C. Hamilton, S. Rozier, and C. Pichon, "Resonant and non-resonant relaxation of globular clusters," MNRAS, vol. 508, pp. 2210–2225, Dec. 2021.

[64] I. S. Chandrasekhar, "The time of relaxation of stellar systems," *Astr. J.*, vol. 93, p. 285, 1941.

[65] J. Peñarrubia, "Stochastic tidal heating by random interactions with extended substructures," *Monthly Notices of the Royal Astronomical Society*, vol. 484, pp. 5409–5436, 02 2019.

[66] D. O'dell, S. Giovanazzi, G. Kurizki, and V. Akulin, "Bose–Einstein condensates with $1/r$ interatomic attraction: Electromagnetically induced "gravity"," *Physical Review Letters*, vol. 84, no. 25, p. 5687, 2000.

[67] T. Kinoshita, T. Wenger, and D. S. Weiss, "A quantum newton's cradle," *Nature*, vol. 440, no. 7086, pp. 900–903, 2006.

[68] S. Hofferberth, I. Lesanovsky, B. Fischer, T. Schumm, and J. Schmiedmayer, "Non-equilibrium coherence dynamics in one-dimensional bose gases," *Nature*, vol. 449, no. 7160, pp. 324–327, 2007.

[69] P. Makotyn, C. E. Klauss, D. L. Goldberger, E. Cornell, and D. S. Jin, "Universal dynamics of a degenerate unitary bose gas," *Nature Physics*, vol. 10, no. 2, pp. 116–119, 2014.

[70] A. Domínguez, M. Oettel, and S. Dietrich, "Dynamics of colloidal particles with capillary interactions," *Phys. Rev. E*, vol. 82, p. 011402, Jul 2010.

[71] R. Golestanian, "Collective behavior of thermally active colloids," *Phys. Rev. Lett.*, vol. 108, p. 038303, Jan 2012.

[72] R. Kawahara and H. Nakanishi, "Quasi-stationary states of two-dimensional electron plasma trapped in magnetic field," *Journal of the Physical Society of Japan*, vol. 75, no. 5, p. 054001, 2006.

[73] X.-P. Huang and C. Driscoll, "Relaxation of 2d turbulence to a metaequilibrium near the minimum enstrophy state," *Physical review letters*, vol. 72, no. 14, p. 2187, 1994.

[74] J. Danielson, F. Anderegg, and C. Driscoll, "Measurement of landau damping and the evolution to a bgk equilibrium," *Physical review letters*, vol. 92, no. 24, p. 245003, 2004.

[75] C. Damm, J. Foote, A. Futch Jr, A. Hunt, K. Moses, R. Post, and J. Taylor, "Evidence for collisionless damping of unstable waves in a mirror-confined plasma," *Physical Review Letters*, vol. 24, no. 10, p. 495, 1970.

[76] K. Gentle and A. Malein, "Observations of nonlinear landau damping," *Physical Review Letters*, vol. 26, no. 11, p. 625, 1971.

[77] M. Sugawa, "Observation of self-interaction of bernstein waves by nonlinear landau damping," *Physical review letters*, vol. 61, no. 5, p. 543, 1988.

[78] C. Chen, K. Klein, and G. G. Howes, "Evidence for electron landau damping in space plasma turbulence," *Nature communications*, vol. 10, no. 1, pp. 1–8, 2019.

[79] J. E. Borovsky and M. H. Denton, "A survey of the anisotropy of the outer electron radiation belt during high-speed-stream-driven storms," *Journal of Geophysical Research: Space Physics*, vol. 116, no. A5, p. 1, 2011.

[80] T. Simula, M. J. Davis, and K. Helmerson, "Emergence of order from turbulence in an isolated planar superfluid," *Physical review letters*, vol. 113, no. 16, p. 165302, 2014.

[81] R. Pakter and Y. Levin, "Nonequilibrium statistical mechanics of two-dimensional vortices," *Physical review letters*, vol. 121, no. 2, p. 020602, 2018.

[82] L. Onsager, "Statistical hydrodynamics," *Il Nuovo Cimento (1943-1954)*, vol. 6, pp. 279–287, Mar. 1949.

[83] R. A. Kishek, P. O'Shea, S. Bernal, I. Haber, J. R. Harris, Y. Huo, H. Li, and M. Reiser, "The university of maryland electron ring: A platform for study of galactic dynamics on a laboratory scale," *Annals of the New York Academy of Sciences*, vol. 1045, no. 1, pp. 45–54, 2005.

[84] D. Comparat, T. Vogt, N. Zahzam, M. Mudrich, and P. Pillet, "Star cluster dynamics in a laboratory: electrons in an ultracold plasma," *Monthly Notices of the Royal Astronomical Society*, vol. 361, no. 4, pp. 1227–1242, 2005.

[85] L. Pruvost, I. Serre, H. T. Duong, and J. Jortner, "Expansion and cooling of a bright rubidium three-dimensional optical molasses," *Physical Review A*, vol. 61, no. 5, p. 053408, 2000.

[86] G. Labeyrie, F. Michaud, and R. Kaiser, "Self-Sustained Oscillations in a Large Magneto-Optical Trap," *Physical Review Letters*, vol. 96, p. 023003, Jan. 2006.

[87] T. Pohl, G. Labeyrie, and R. Kaiser, "Self-driven nonlinear dynamics in magneto-optical traps," *Physical Review A*, vol. 74, no. 2, p. 023409, 2006.

[88] J. Mendonça, R. Kaiser, H. Terças, and J. Loureiro, "Collective oscillations in ultracold atomic gas," *Physical Review A*, vol. 78, no. 1, p. 013408, 2008.

[89] J. Mendonça and H. Terças, "Laser scattering by density fluctuations of ultra-cold atoms in a magneto-optical trap," *Journal of Physics B: Atomic, Molecular and Optical Physics*, vol. 44, no. 9, p. 095301, 2011.

[90] H. Terças, J. T. Mendonça, and R. Kaiser, "Driven collective instabilities in magneto-optical traps: A fluid-dynamical approach," *EPL (Europhysics Letters)*, vol. 89, no. 5, p. 53001, 2010.

[91] C. Rotschild, O. Cohen, O. Manela, M. Segev, and T. Carmon, "Solitons in nonlinear media with an infinite range of nonlocality: first observation of coherent elliptic solitons and of vortex-ring solitons," *Physical review letters*, vol. 95, no. 21, p. 213904, 2005.

[92] C. Rotschild, B. Alfassi, O. Cohen, and M. Segev, "Long-range interactions between optical solitons," *Nature Physics*, vol. 2, no. 11, pp. 769–774, 2006.

[93] R. Bekenstein, R. Schley, M. Mutzafi, C. Rotschild, and M. Segev, "Optical simulations of gravitational effects in the newton–schrödinger system," *Nature Physics*, vol. 11, no. 10, pp. 872–878, 2015.

[94] T. Roger, C. Maitland, K. Wilson, N. Westerberg, D. Vocke, E. M. Wright, and D. Faccio, "Optical analogues of the newton–schrödinger equation and boson star evolution," *Nature communications*, vol. 7, no. 1, pp. 1–8, 2016.

[95] E. L. Raab, M. Prentiss, A. Cable, S. Chu, and D. E. Pritchard, "Trapping of Neutral Sodium Atoms with Radiation Pressure," *Physical Review Letters*, vol. 59, pp. 2631–2634, Dec. 1987.

[96] J. Dalibard, "Laser cooling of an optically thick gas: The simplest radiation pressure trap?," *Optics Communications*, vol. 68, pp. 203–208, Oct. 1988.

[97] T. Walker, D. Sesko, and C. Wieman, "Collective behavior of optically trapped neutral atoms," *Physical Review Letters*, vol. 64, pp. 408–411, Jan. 1990.

[98] B. E. A. Saleh and M. C. Teich, *Fundamentals of photonics; 2nd ed.* Wiley series in pure and applied optics, New York, NY: Wiley, 2007.

[99] M. Lovisetto, *Modeling and experimental observation of mixing and vilent relaxation in an analogue gravitational system.* PhD thesis, Université Côte d'Azur, France, May 2022.

[100] M. Joyce and T. Worrakitpoonpon, "Quasi-stationary states in the self-gravitating sheet model," *Phys. Rev. E*, vol. 84, no. 1, p. 011139, 2011.

[101] W. Hu, R. Barkana, and A. Gruzinov, "Fuzzy cold dark matter: the wave properties of ultralight particles," *Physical Review Letters*, vol. 85, no. 6, p. 1158, 2000.

[102] H.-Y. Schive, T. Chiueh, and T. Broadhurst, "Cosmic structure as the quantum interference of a coherent dark wave," *Nature Physics*, vol. 10, no. 7, pp. 496–499, 2014.

[103] L. Hui, J. P. Ostriker, S. Tremaine, and E. Witten, "Ultralight scalars as cosmological dark matter," *Physical Review D*, vol. 95, no. 4, p. 043541, 2017.

[104] D. J. Marsh and J. C. Niemeyer, "Strong constraints on fuzzy dark matter from ultrafaint dwarf galaxy Eridanus ii," *Physical review letters*, vol. 123, no. 5, p. 051103, 2019.

[105] S. Alexander, J. J. Bramburger, and E. McDonough, "Dark disk substructure and superfluid dark matter," *Physics Letters B*, vol. 797, p. 134871, 2019.

[106] K. Hayashi, E. G. M. Ferreira, and H. Y. J. Chan, "Narrowing the Mass Range of Fuzzy Dark Matter with Ultrafaint Dwarfs," ApJ, vol. 912, p. L3, May 2021.

[107] E. G. M. Ferreira, "Ultra-light dark matter," A&A Rev., vol. 29, p. 7, Dec. 2021.

[108] D. Guéry-Odelin, "Mean-field effects in a trapped gas," *Phys. Rev. A*, vol. 66, p. 033613, Sep 2002.

[109] Y. Castin and R. Dum, "Bose-einstein condensates in time dependent traps," *Phys. Rev. Lett.*, vol. 77, pp. 5315–5319, Dec 1996.

[110] Y. Kagan, E. L. Surkov, and G. V. Shlyapnikov, "Evolution of a bose gas in anisotropic time-dependent traps," *Phys. Rev. A*, vol. 55, pp. R18–R21, Jan 1997.

[111] D. H. E. Dubin, "Theory of electrostatic fluid modes in a cold spheroidal non-neutral plasma," *Phys. Rev. Lett.*, vol. 66, pp. 2076–2079, Apr 1991.

[112] S. Amiranashvili, M. Y. Yu, and L. Stenflo, "Nonuniform non-neutral plasma in a trap," *Phys. Rev. E*, vol. 67, p. 016408, Jan 2003.

[113] T. Sheridan, C. Buckey, D. Cox, R. Merrill, and W. Theisen, "Breathing-mode resonance of a complex plasma disk," *Physics Letters A*, vol. 329, no. 1, pp. 88–93, 2004.

[114] S. A. Tatarkova, A. E. Carruthers, and K. Dholakia, "One-dimensional optically bound arrays of microscopic particles," *Phys. Rev. Lett.*, vol. 89, p. 283901, Dec 2002.

[115] V. A. Schweigert and F. m. c. M. Peeters, "Spectral properties of classical two-dimensional clusters," *Phys. Rev. B*, vol. 51, pp. 7700–7713, Mar 1995.

[116] B. Partoens and F. M. Peeters, "Classical artificial two-dimensional atoms: the thomson model," *Journal of Physics: Condensed Matter*, vol. 9, p. 5383, jun 1997.

[117] S. W. S. Apolinario, B. Partoens, and F. M. Peeters, "Structural and dynamical aspects of small three-dimensional spherical coulomb clusters," *New Journal of Physics*, vol. 9, p. 283, aug 2007.

[118] S. Chandrasekhar and D. D. Elbert, "Some elementary applications of thevirial theorem to stellar dynamics," MNRAS, vol. 155, p. 435, Jan. 1972.

[119] M. Joyce, B. Marcos, and F. Sylos Labini, "Energy ejection in the collapse of a cold spherical self-gravitating cloud," *Mon. Not. R. Astron. Soc.*, vol. 397, no. 2, pp. 775–792, 2009.

[120] G. Manfredi, P.-A. Hervieux, and F. Haas, "Variational approach to the time-dependent schrödinger–newton equations," *Classical and Quantum Gravity*, vol. 30, p. 075006, mar 2013.

[121] O. D. Kellogg, *Foundations of potential theory.* Berlin: Springer, 1967.

[122] V. Mancois, J. Barré, C. C. Kwong, A. Olivetti, P. Viot, and D. Wilkowski, "Anisotropic long-range interaction investigated with cold atoms," *Phys. Rev. A*, vol. 102, p. 013311, Jul 2020.

[123] A. Olivetti, *Effets collectifs et particules en interaction : Des systèmes à longue portée aux atomes froids.* Theses, Université Nice Sophia Antipolis, Dec. 2011.

[124] J.-P. Hansen and I. R. McDonald, *Theory of simple liquids (Third Edition).* Elsevier, 2006.

[125] A. Gabrielli, F. Sylos Labini, M. Joyce, and L. Pietronero, *Statistical Physics for Cosmic Structures.* Berlin: Springer, 2004.

[126] A. J. Greenfield and N. Wiser, "The low- q region of the structure factor for liquid metals," *Physics Letters A*, vol. 34, pp. 123–124, Feb. 1971.

[127] A. K. Ghatak and K. Thyagarajan, *Optical Electronics.* Cambridge: Cambridge University Press, 1989.

[128] I. M. Moroz, R. Penrose, and P. Tod, "Spherically-symmetric solutions of the Schrödinger-Newton equations," *Classical and Quantum Gravity*, vol. 15, pp. 2733–2742, Sept. 1998.

[129] E. P. Wigner, "On the quantum correction for thermodynamic equilibrium," in *Part I: Physical Chemistry. Part II: Solid State Physics*, pp. 110–120, Springer, 1997.

[130] P. Bader, S. Blanes, F. Casas, and M. Thalhammer, "Efficient time integration methods for gross-pitaevskii equations with rotation term," *Journal of Computational Dynamics*, vol. 6, no. 2, pp. 147–169, 2019.

[131] C. Besse, G. Dujardin, and I. Lacroix-Violet, "High order exponential integrators for nonlinear schrödinger equations with application to rotating bose–einstein condensates," *SIAM Journal on Numerical Analysis*, vol. 55, no. 3, pp. 1387–1411, 2017.

[132] M. Mina, D. F. Mota, and H. A. Winther, "Solitons in the dark: First approach to non-linear structure formation with fuzzy dark matter," A&A, vol. 662, p. A29, June 2022.